IMPROVED ESTIMATION OF CATCHMENT RAINFALL FOR CONTINUOUS SIMULATION MODELLING

Mehari Suim Frezghi

BScEng (Agric), University of Natal

Submitted in fulfilment of the requirement for the degree of

MScEng

School of Bioresources Engineering and Environmental Hydrology

University of KwaZulu-Natal

Pietermaritzburg

South Africa

2005

DECLARATION

The research described in this dissertation was carried out within the school of Bioresorces Engineering and Environmental Hydrology, University of Kwazulu-Natal, Pietermatitzburg, under the supervision of Professor of J C Smithers (School of Bioresources Engineering and Environmental Hydrology, University of Kwazulu-Natal).

I hereby certify that the research reported in this dissertation is my own original and unaided work except where specific acknowledgement is made.

Signed_____

Mehari S Frezghi

Signed_____

Jeff C Smithers

Professor of Agricultural Engineering

(Supervisor)

TABLE OF CONTENTS

ABSTRACT

Long sequences of rainfall at fine spatial and temporal details are increasingly required, not only for hydrological studies, but also to provide inputs for models of crop growth, land fills, tailing dams, disposal of liquid waste on land and other environmentally-sensitive projects. However, rainfall records from raingauges frequently fail to meet the requirements of the above studies. Therefore, it is important to improve the estimation of the depth and spatial distribution of rainfall falling over a catchment.

A number of techniques have been developed to improve the estimation of the spatial distribution of rainfall from sparsely distributed raingauges. These techniques range from simple interpolation techniques developed to estimate areal rainfall from point rainfall measurements, to statistical and deterministic models, which generate rainfall values and downscale the rainfall values based on the physical properties of the clouds or rain cells. Furthermore, these techniques include different statistical methods, which combine the rainfall information gathered from radar, raingauges and satellites. Although merging the radar and raingauge rainfall fields gives a best estimate of the "true rainfall field", the length of the radar record and spatial coverage of the radar in a country such as South Africa is relatively short and hence is of limited use in hydrological studies.

Therefore, the relationship between the average merged rainfall value for a catchment and a "driver" station, which is selected to represent rainfall in the catchment, is developed and assessed in this study. Rainfall data from the Liebenbergsvlei Catchment near Bethlehem in the Free State Province and a six-month record of radar data are used to develop relationships between the average merged subcatchment rainfall for each of the Liebenbergsvlei subcatchments and a representative raingauge selected to represent the rainfall in each of the subcatchments. The relationships between daily raingauges and the average rainfall depth of the subcatchments are generally good and in most of the subcatchments the correlation coefficient is greater than 0.5. It was also noted that, in most of the subcatchments, the daily raingauges overestimate the average areal rainfall depth of the subcatchments.

In addition, the String of Beads Model (SBM) developed by Clothier and Pegram (2002) was used to generate synthetic rainfall series for the Liebenbergsvlei catchments. The SBM is able to produce rainfall values at a spatial resolution of 1x1 km with a 5 minute temporal

resolution. The SBM is a high-resolution space-time model of radar rainfall images, which takes advantage of the detailed spatial and temporal information captured by weather radar and combines it with the long-term seasonal variation captured by a network of daily raingauges. Statistics from a 50 year period of generated rainfall values were compared with the statistics computed from a 50 year raingauge data series, and it was found that the generated rainfall values mimic the rainfall data from the raingauges reasonably well.

The relationship developed between the merged catchment rainfall values and driver rainfall station values, which are selected to represent the mean areal rainfall of the subcatchment, was used to adjust the Conventional Driver rainfall Station (CDS) into Modified Driver Station (MDS) values. Streamflow was simulated using both the CDS and MDS rainfall compared against the observed streamflow from the Liebenbergsvlei catchment. In general, the streamflow simulated by the ACRU model do not correlate well with the observed streamflow, which is attributed to unrealistic observed flow and inter-catchments transfers of water. However, it is noted that the volume of streamflow simulated with the MDS rainfall is only 71 % of that simulated with the CDS rainfall, thus highlighting the limitation of using the CDS rainfall approach for modelling and the need to apply the methodology to improve the estimation of catchment rainfall developed in this study to other catchments in South Africa.

ACKNOWDEGEMENT

Professor J C Smithers, Professor of Agricultural Engineering and Head of the School of Bioresources Engineering and Environmental Hydrology, University of Kwazulu-Natal for his encouragement, support, inspired Supervision throughout this research and being receptive to different ideas.

Mr G S Sinclair, PhD Student, Department of Civil Engineering, University of Kwazulu-Natal, for his continuous support and providing raingauge- radar merging softwares, radar rainfall data and tipping bucket rainfall data.

Dr A N Clothier, London, United Kingdom, for providing us a String of Beads Stochastic Rainfall model and his support.

Mr M Horan, GIS programmer, School of Bioresources Engineering and Environmental Hydrology, University of Kwazulu-Natal for his continuous support in GIS and providing necessary resources.

Mrs S Kunz, Secretarial staff, School of Bioresources Engineering and Environmental Hydrology, University of Kwazulu-Natal, for her continuous support in providing the school services.

Mr H Minassie and Mr Ikechukwu Achilonu, University of Kwazulu-Natal, for being very good friends and their continuous encouragement and support.

Water Resource Commission (WRC), South Africa, for sponsoring the research.

Bioresources Engineering and Environmental Hydrology students and staff, for being friendly and for providing support when I need their support.

My Family, Friends and Colleagues, for their continuous moral support and believing on me.

Finally, my heartfelt thanks to God for being there in every aspect of my life.

I DEDICATE THIS DISSERTATION TO MY LATE MOTHER,
NIGSTI TEKLE

LIST OF FIGURES

LIST OF TABLES

LIST OF ABBREVATIONS AND DEFINITIONS

Abbreviations

ACRU	Agricultural Catchment Research Unit
CAPPI	Constant Altitude Plan Position Indicators
CDS	Conventional Driver Station
CSM	Continuous Simulation Models
MDS	Modified Driver Station
MDV	Meteorological Data Volume
R^2	Coefficient of Correlation
SAWS	South Africa Weather Services
SBM	String of Beads Model

1. INTRODUCTION

In the application of information derived from rainfall data in the fields of hydrology, engineering and agriculture, it is becoming increasingly important to know, or at least have a reasonable estimate of, rainfall in space as well as time, and in more detail than it is possible to deduce from the data collected at raingauges in a sparse network (Pegram and Seed, 1998). In addition to raingauge measured data, radar information is now available as a means of rainfall measurement. Radar measurement has some drawbacks with respect to the performance of the instrument and the availability of long records of continuous data. However, radar measurements represent an important source of information that allows the continuous spatial distribution of rainfall to be studied.

Traditionally, mathematical interpolation techniques have been used to interpolate rainfall data from a raingauge network to estimate rainfall at ungauged sites. However, a rain field which is estimated using mathematical interpolation does not accurately represent the "true rainfall" field. Therefore, other techniques have been developed to improve the rainfall input as required by most hydrological analyses as well as agricultural and ecological studies. Some of these methods generate synthetic rainfall values using statistical models (Pegram and Seed, 1998; Pegram and Clothier, 2001), or are models based on the physical properties of a rain cell or cloud (Gupta and Waymire, 1993), or are techniques that merge the radar fields and raingauge data (Todini, 2001; Ehret 2002). The merged rainfall fields are the "best" estimation of the "true" rainfall field.

Storm events may vary considerably in space, and the use of data from a single raingauge to represent the rainfall over the entire catchment might not realistically represent the spatial distribution of storms. Rainfall intensity is important in determining the characteristics of streamflow hydrographs and the intensity often varies significantly over distances of less than one km. The spatial detail of rainfall required for flood estimation or generation of steamflow hydrographs will vary with the spatial scale of the catchment. According to Dawdy and Bergmann (1969), errors in rainfall volume and intensity over a catchment are likely to limit the accuracy of runoff simulation. Michaud and Sorooshian (1994) examined the effect of rainfall sampling errors on the simulation of flash floods using a distributed model on a 150 km^2 semi-arid catchment. Their results indicate that the accurate estimation of the spatial

resolution of rainfall is essential to simulate flood peaks, as coarse resolution data led to the underestimation of flood peaks by as much as 50 %.

The accurate estimation of design floods quantifies risk in the design of hydraulic structure and in the risk assessment for water management in dams. Design floods may be estimated from long records of observed streamflow data. However, the density and record length of flow records are generally less than required for design flood estimation in most parts of the world, including South Africa. Design floods are frequently estimated from rainfall data using event-based approaches (Cameron *et al.*, 1999). Recently, continuous simulation models (CSM) have been successfully used to improve the accuracy of design flood estimates (Cameron *et al.*, 1999). Rainfall is the most important input into CSM and, therefore, CSM requires accurate rainfall input, both in space and time.

It can be concluded that the shape and volume of flood hydrographs are highly dependent on the spatial and temporal variability of rainfall, but the importance of rainfall will vary greatly as a function of catchment and rainfall properties. Therefore, accurate estimation of rainfall at fine spatial and temporal scales is fundamental to rainfall-runoff modelling or the success of hydrological modelling, crop growth models and for land fills, tailing dams, disposal of liquid waste on land and other environmentally sensitive projects.

The objectives of this research are to:

(i) Develop and assess a methodology to improve the estimation of the average depth and spatial distribution of rainfall over a catchment using radar images and point rainfall data.
(ii) Assess the influence of the improved catchment rainfall on the simulated streamflow.
(iii) Evaluate a detailed space-time stochastic rainfall model to generate long sequences of rainfall over a catchment for use in continuous simulation models.

Three different techniques for measuring rainfall are reviewed in Chapter 2 and the advantages and disadvantages of each technique are compared and their accuracy in estimating the "true" rainfall is assessed.

Chapter 3 contains a review of a number of different techniques to estimate the spatial distribution of rainfall. These techniques include different interpolation techniques, rainfall

models and techniques that merge rainfall information from raingauges, radar and satellites. Interpolation techniques are deterministic or stochastic in nature and serve to estimate areal rainfall only from point rainfall data, while rainfall models are classified as empirical statistical models, dynamic meteorological and intermediate stochastic models. Bayesian and Conditional merging techniques is also discussed in Chapter 3.

The Liebenbergsvlei catchment, which is used as a study area for this research, and the spatial distribution of rainfall in Liebenbergsvlei catchment is presented in Chapter 4. Chapter 5 focuses on the development of the merging technique used by Sinclair (2004) which utilises a conditional merging technique (Ehret, 2002). The validation of the merging technique and the development of relationships between a mean merged subcatchment rainfall values and gauged point rainfall data are presented.

Chapter 6 contains the results of using the String of Beads Model (SBM) developed by Clothier and Pegram (2002) to generate stochastic rainfall series for the Liebenbergsvlei catchment. The relationships developed in Chapter 5 are used to adjust the Conventional Driver rainfall Station (CDS) into Modified Driver Station (MDS) values and streamflow simulated using the two methods are compared against each other and against observed streamflow of Liebenbergsvlei catchment. Finally, the discussion of the results, conclusions drawn and recommendation for future work are contained in Chapter 8.

2. RAINFALL MEASUREMENT

Rainfall is the fundamental driving force and pulsar input behind most hydrological processes (Schulze *et al.*, 1995). The rainfall-runoff process is non-linear and a larger proportion of rainfall is converted to runoff as a catchment becomes wetter. Rainfall-runoff models are thus particularly sensitive to the rainfall input and any errors in the estimated rainfall are amplified in streamflow simulations. This implies that the success of hydrological simulation studies depends to a large extent on the accuracy with which the rainfall data are observed temporally and spatially and processed in the model (Schulze, 1995).

The most common rainfall-measuring instrument is the raingauge and, more recently, radar and satellites have also been used to estimate rainfall.

2.1. Raingauges

Raingauge measurements represent a simple, inexpensive method for point or areal rainfall estimation and they are therefore used extensively as a land surface precipitation-measuring device. These instruments are good at measuring the temporal distribution of the rainfall process at a specific location. However, they fail to give reliable information about the spatial distribution of the rainfall and are not representative of the true areal precipitation of a catchment (Schäfer, 1991; Balascio, 2001).

The degree to which a raingauge sample represents the true rainfall on a catchment has a major influence on the accuracy with which the areal rainfall may be estimated. Inherent sampling errors of raingauges are caused by adhesion or gauge funnel wetting, inclination of the gauge, splash into and out of gauge funnel, evaporation of water from inside the gauge and airflow around the gauge (Deyzel *et al.*, 2004). Turbulence and increased wind speed in the vicinity of the gauge orifice contributes to the airflow-induced sampling errors. As air rises to pass over the gauge the precipitation particles that should have been sampled by the gauge may be deflected and carried further downwind. These characteristic sampling errors of raingauges, and random sampling errors in areas where there is a substantial variation in the spatial distribution of rainfall, contribute to the inherent error in gauge estimates of areal

rainfall. These errors depend on the gauge's orifice, the area of the gauge, the length of the measurement period and the spatial variability of the rainfall event (Deyzel *et al.*, 2004).

2.2. Radar

Radar estimates of rainfall over a given area are made by transmitting an electromagnetic wave with a wavelength of between 1 mm to 150 mm. This wave propagates through the atmosphere to interact with the droplets and reflects back from the droplets. All weather radars consist of a transmitter which produces electromagnetic radiation of a known power and at a given frequency. The radiation is concentrated into a beam, usually 1 or 2 degree wide, by an antenna which also receives that part of the beam which is scattered back by the water droplets. A receiver detects the back-scattered radiation, amplifies it and converts the microwave signal to a low frequency signal, which is related to the properties of the droplets. Therefore, weather radars do not measure rainfall or rain rate directly; rather, they measure reflectivity. There is no simple correspondence between rain rate (R) and reflectivity (Z), so numerous different Z-R relationships are to be found in the literature. However, the most popular and frequently used method is the Marshal-Palmer relationship developed in 1948, shown in Equation 1 (Mittermaier and Terblanche, 1997).

$$Z = aR^{b} \qquad (1)$$

where

Z	=	reflectivity (dB),
R	=	rainfall rate in $mm.h^{-1}$, and
a and b	=	are constants and values of 200 and 1.6 respectively are used in South Africa (Mittermaier and Terblanche, 1997)

A major disadvantage of weather radars is the need for constant calibration of parameters used to convert reflectivity into rainfall rates. This generally requires the installation of a conventional ground-based raingauge network. However, the advantages of radar estimated rainfall outweigh its disadvantages. The advantages of radar derived rainfall compared raingauge networks are listed by Deyzel *et al.* (2004) as:

(i) spatial continuity of observation,

(ii) improved information regarding the spatial and temporal variability of the precipitation,

(iii) the three dimensional structure of the system generating the precipitation is apparent,
(iv) real-time surveillance is possible over a wide area from a single observation point, and
(v) the facility exists for in-situ data acquisition, storage and processing.

Weather radars are highly sensitive to certain properties of precipitation and hence are a valuable tool in precipitation observation. However, technical problems and limitations may seriously hamper their performance (Deyzel *et al.*, 2004). These problems include:

(i) attenuation of the radar signal by precipitation elements, clouds, gases or radome,
(ii) non-uniform beam filling causing loss of data accuracy,
(iii) side lobes detecting storms erroneously,
(iv) presence of melting layer or ground clutter causing outliers,
(v) the formation or evaporation of precipitation below the radar beam,
(vi) violation of the assumption that all reflective power are from droplets,
(vii) calibration difficulties, and
(viii) limitations in the assumption and implementation of the standard between reflectivity and rainfall rate, power law relationship.

2.3. Satellites

Satellites, i.e. spacecraft which orbits the earth and return images of the earth and atmosphere back to a receiving station on the ground, are used to estimate rainfall by using observed radiation signals reflected or emitted from the ground and atmosphere. The objective of satellite-based rainfall estimation is to address issues such as rainfall occurrence, amount and distribution at all temporal scales for a range of applications. Satellite rainfall information is invaluable where there is no radar coverage (Levizzani *et al.*, 2000) or where the conventional rainfall monitoring network is sparse.

In meteorological satellites the radiation emitted by the earth and the atmosphere, may be either reflected solar radiation, e.g. by clouds, water vapour or aerosols, or it may be terrestrial radiation emitted by the Earth. The Earth's atmospheric gases are affected differently by different wavelengths of radiation. Meteorological satellites have been designed to take advantage of these responses to observe different aspects of the Earth and its atmosphere (Grimes, 1999). A radiometer measures the intensity of the radiant energy coming from the Earth's surface and atmosphere in a specific wavelength band (channel). When a

radiometer collects a certain amount of energy it registers a count, which is proportional to the intensity of the radiation received. The relationship between radiation and count is established by the radiometer's calibration. The radiometer's footprint, i.e. its viewing area, has its total radiation assigned to a pixel cantered at the middle of the footprint. A complete image is built up when all the pixels in the image have been assigned a value by the radiometer (Grimes, 1999).

Satellite fills the gap in information from radar and raingauge rainfall fields, to produce large scale (e.g. national) rainfall maps. The advantages of utilising satellites for rainfall estimation include (Deyzel *et al.*, 2004):

(i) acquisition data for any point on Earth, irrespective of countries or surface conditions,
(ii) the cost-effectiveness, since many countries can share the cost of single instrument, and that
(iii) the radiometer on board the satellite has a fixed calibration irrespective of point measurement position.

The limitations of estimating of rainfall from satellites include (Deyzel *et al.*, 2004):

(i) the effect of warm, orographic cloud development on rainfall fields, which are then not always correctly quantified, and
(ii) the complex nature and variation of cloud top structure under varying dynamic conditions, which are processed at an average level and thus produce limitations for non-climatological outlier storms.

Raingauge and radar rainfall information alone are not adequate for large scale rainfall mapping. The lack of information over the oceans, in areas where there is a sparse raingauge network and no radar coverage justifies the use of satellites to derive rainfall information. Whether for national rainfall mapping or rainfall-runoff modelling to estimate design floods, the rainfall information gathered by these instruments needs to be improved. The ideal information required is a long series of areal rainfall estimated with a high spatial and temporal resolution.

* * *

Three rainfall measuring techniques and their advantage and disadvantages have been discussed in this chapter. The three techniques do not individually provide detailed spatial and long temporal rainfall information required by hydrological models. Therefore, different

techniques to estimate the spatial distribution of rainfall from the information gathered by raingauges, radar and satellites is discussed in Chapter 3.

3. TECHNIQUES FOR ESTIMATING THE SPATIAL DISTRIBUTION OF RAINFALL

For flood estimation or risk assessment, an accurate estimation of rainfall with detailed spatial and temporal rainfall information is required. In South Africa, daily time step rainfall data have been collected and quality controlled from various raingauge networks (Lynch, 2003). However, in many cases rainfall data are required at sub-daily level and the rainfall needs to be representative of the "true spatial rain field", and not only for of a point rainfall location.

Different techniques have evolved to meet the requirements of hydrological models with reference to the availability of rainfall data. In cases where only raingauge data are available and areal rainfall is required, numerical surface interpolation techniques can be applied to estimate the areal rainfall (Schäfer, 1991). However, if the historical data are not long enough to meet the requirement of the hydrological model, stochastic rainfall models may be applied to generate synthetic rainfall series.

Areal rainfall estimated from a raingauge network may not be sufficient to represent the true spatial variability of the rain field. In such cases radar fields can be merged with the raingauge fields to provide a better representation of the spatial variability of the true rain field (Todini, 2001). However, over- lapping periods and spatial coverage between these two fields in South Africa are currently limited. Therefore, multi-site rainfall models or stochastic downscaling models may be applied to generate synthetic rainfall values at gauged and ungauged sites (Wilks, 1998; Clothier and Pegram, 2002). These different approaches are discussed in the following sections.

3.1. Numerical Surface Fitting Techniques

Ideally raingauge networks should be adequate to represent the spatial variability of the rainfall within a region. Network design must thus account for the systematic variation in rainfall over an area and the random errors incurred when extrapolating from gauged to ungauged sites. Despite the design recommendations, most raingauge networks are poorly developed. According to Hutchinson (1974), the error in estimating areal rainfall at an

ungauged location, using only raingauge observations, increases as the distance between the location and the nearest gauged site increases.

Different methods maybe applied to determine areal rainfall from raingauge networks. Classical methods such as the arithmetic mean, Thiessen polygon technique and the manual isohyetal approach are simple and well tried (Schäfer, 1991). However, they do not always give spatially accurate and representative rainfall values, especially in catchments with a marked variability in relief and a sparse gauge network. Hence, more sophisticated methods have evolved to interpolate areal rainfall (Schäfer, 1991). According to Schulze (1976), the complex pattern of rainfall distribution seldom permits a simple approach in the determination of the areal rainfall.

Interpolation is a mathematical operation which strives to preserve the functional continuity as well as the slope and curvature continuity of a surface. Interpolation procedures may be used fit rainfall surfaces to the observed raingauge values, connecting adjacent points by mathematical functions or by the superpositioning of individual surfaces. Interpolation can be deterministic or stochastic, based on the function used to interpolate (Schäfer, 1991):

3.1.1. Deterministic Interpolation

The simplest spatial interpolation methods are mostly based on deterministic concepts. Deterministic methods do not use probability theory, and assume that the measurement error or mean-square error of prediction is zero. Deterministic interpolation methods are based directly on the surrounding measured values or on a specified mathematical formula that determines the smoothness of the resulting surface (Lynch, 2003). They include methods such as inverse distance weighted averages, splines or polynomial interpolation, multiquadratic analysis, Delauney triangulation and others.

Inverse distance weighting is a function of the inverse of the distance to each gauge point; hence nearby gauges carry a higher weight than points further away from the point of interest (Simonton and Osborn, 1980). Spline or polynomial interpolation is achieved by connecting each pair of adjacent points by either an algebraic or trigonometric polynomial function (Tabios and Salas, 1985). Trend surface analysis (TSA) is a smoothing function, which rarely fits the original data points, unless there are a relatively small number of data points and the

order of the surface function is large. TSA employs the location of the rainfall stations to determine the order of the surfaces and uses a least square criterion to fit surfaces of increasing orders to spatially distributed rainfall data. A high order surface allows flexibility on the computed three-dimensional surface to have a satisfactory goodness of fit results (Burrough, 1986). Schulze (1979) used TSA in the Natal Drakensberg and incorporated physiographic factors to improve the results. TSA is generally associated with impressive goodness of fit statistics. However, it requires cautious application in mountainous areas, especially when the rainfall patterns have to be extrapolated and when short-duration data are being utilised (Schulze, 1979).

However, the most important and more accurate deterministic interpolation method is multiquadratic analysis (Balascio, 2001), which is a technique by which the areal rainfall surface is estimated by fitting individual polynomial or quadratic surfaces placed at each gauge point. Balascio (2001) examined the weighting coefficients associated with unbiased forms of conic multiquadric surfaces and showed that the unbiased conic multiquadric surface yields optimal gauge weighting coefficients for rainfall data correlated by a linear covariance function. Borga and Vizzaccaro (1997) showed that the conic multiquadratic surfaces associated with a linear covariance structure are equivalent to kriging with a linear variogram. This explains why multiquadric equations have been employed so successfully to fit spatial data. The method of kriging (Borga an Vizzaccaro, 1997) results in optimal fitting (in a least-square sense) of a surface to spatial data for the particular type of variogram function that describes the data.

3.1.2. Stochastic Interpolation

Stochastic interpolation attempts to obtain unbiased, minimum variance estimates of precipitation at points where measurements are not available, as a function of measurements available at a number of gauged sites. These methods consider rainfall as a two-dimensional random process. The early work on stochastic interpolation was by Gandini (1970), cited by Lanza *et al.* (2001), who developed an objective analysis of meteorological fields. Objective analysis defines an unbiased, minimum variance estimator, based on the assumption that the covariance structure of the variable to be interpolated is known. Stochastic interpolation has since been expanded to different methods which encompass trend surface analysis, kriging, Fourier analysis, multiple regression and others. Among all these methods, kriging is widely

used in spatial interpolation of rainfall. This method was developed by a South African engineer, Krige, in 1971 when he introduced kriging into the field of mining engineering to determine the spatial distribution of ores. Lanza *et al.* (2001) explain that kriging, or the optimal linear interpolation technique derived by Krige, but formalised into more appropriate mathematical terms, led to the development of kriging as geostatistical tool. Kriging requires that the spatial structure of the rainfall process, defined by a semivariogram, be derived from the rainfall data. When the data are inadequate for empirical definition of the semivariogram, as is often the case, then deterministic methods can be employed.

Spatial regression analysis uses multiple regression and trend surface techniques to determine the spatial distribution of rainfall. Multiple regression analysis uses a set of independent variables related to rainfall, such as location, slope, aspect and altitude and minimises the sum of the squared errors (Lynch, 2003). The areal rainfall estimated from these interpolation techniques are highly dependent on the spatial density of the rain gauges. Therefore, where there is a low density of raingauges with short record lengths, the raster surface obtained from above interpolation techniques are smooth and less detailed. However, rainfall-runoff models or any other hydrological models may require a long series with detailed spatial information of rainfall as input. In such situations, it is important to acquire a rainfall model which can generate rainfall values at gauged and ungauged sites.

3.2. Rainfall Models

There are different approaches to modelling of rainfall. Cox and Isham (1994) presented three broad categories of precipitation models, namely empirical statistical, dynamic meteorological and intermediate stochastic models. Empirical statistical models are based on empirical analysis of raingauge data and do not model rainfall structure or processes explicitly. In these models statistical functions are fitted to the available data. They generally consider a single time scale, for example, daily or hourly (Foufoula-Georgiou and Lettenmaier, 1987), and have most frequently been used to represent single site rainfall. However, they are also applied as multi-site models to represent the distribution of rainfall over an area.

Dynamic meteorological models explicitly represent the physical processes of mass, momentum and energy transport in the atmosphere, in contrast to the empirical statistical

models which do not (Chandler *et al.*, 2002). They are generally used for weather forecasting and general circulation models (GCMs) rather than for rainfall value generation. For continuous simulation modelling, in the context of flood design estimation, computational constraints preclude the use of dynamic meteorological models. Scaling and multi-scaling models have difficulty with the accurate reproduction of the wet/dry field (Gupta and Waymire, 1993). Intermediate stochastic models simulate a continuous space and time and hence can be aggregated to any required spatial or temporal scale. Few parameters are used to represent the rainfall process and these parameters relate to simplified conceptual rainfall process representations such as rain cells, rain bands and cell clusters. The approach is based on single-site models developed by Rodriguez-Itrube *et al.* (1987), in which storm arrivals are modelled using a Poisson process and associated with each storm arrival is a random number of cells, of random duration and intensity, which are dependent on the model process. Further discussion is limited to a review of empirical stochastic and intermediate stochastic models, as dynamic meteorological models are seldom used for generation of data (Chandler *et al.*, 2002).

3.2.1. Empirical Stochastic Models

Stochastic series are random numbers, which have the same statistical characteristics (e.g. mean, variance and auto-correlation structure) as the data set on which they are based. Even though there are a number of stochastic rainfall models documented in the literature, most of them have not been adequately applied with regard to the characteristics at different time scales or at locations with different climates (Zhou *et al.*, 2002). Daily rainfall stochastic models, which adequately preserve not only the daily, but also monthly and annual characteristics, are discussed below. These models are generally classified into two categories: models for stochastic generation of rainfall series and stochastic models for spatial and temporal rainfall downscaling.

3.2.1.1. Stochastic Rainfall Generation Models

Models for the stochastic generation of rainfall mimic a sequence of wet and dry days at a site and assign synthetic rainfall values for wet days. These models are based purely on probabilistic functions developed from the characteristics of the observed rainfall data at a

site. The models can be designed to generate synthetic rainfall values at a single site, or at several sites.

Single Site Daily Rainfall Generation Model

Daily rainfall models at a single site have a temporal structure which consists of two parts: a model for the occurrence of wet and dry days and a model for the generation of rainfall amounts on wet days (Zhou *et al.*, 2002). Models for rainfall occurrence are commonly based on Markov chains, which specify the state of each day as wet or dry and develop a relationship between the state of the current day and the states of preceding days. Models used for rainfall amounts on wet days include the exponential, the gamma and skewed normal distributions. Two sequences of random variables fit into the description of the temporal structure of rainfall. The first sequence controls the number of 'rainfall events' within various intervals of time. The second sequence associates a rainfall depth with each rainfall event (Zhou *et al.*, 2002).

Single site daily rainfall models are important for providing long sequences of rainfall data for hydrological and other environmental projects, and for in-filling the missing data in observed rainfall records (Rajagopalan *et al.*, 1996). They are broadly classified into four groups, namely two part models, transition probability matrix models, re-sampling models and time series models of the Auto Regressive Moving Average (ARMA) type.

Two Part Models

As explained above, two part models consist of rainfall occurrence models and rainfall amount models. The definition of rainfall occurrence or events depends on the time scale over which the rainfall process is to be described. For daily time scales, two main types of stochastic structures are used, namely a Markov chain process and a Wet-Dry spell approach (Rajagopalan *et al.*, 1996).

Markov chain processes specify the state of each day as "wet" or "dry" and develop a relationship between the state of the current day and the states of the preceding days. The order of the Markov chain is the number of preceding days taken into account. Most Markov chain models referred to in the literature are first order, i.e. utilises the state of one preceding

day, although models of second and higher order have been utilised by some researchers (Rajagopalan *et al.*, 1996). Jimon and Webster (1999) investigated the intra-annual variation of the Markov chain parameters for seven sites in Nigeria. They concluded that a first order model is adequate for many locations, but a second or higher model may be required at other locations or during certain periods of the year.

A wet-dry spell approach is also called the alternating renewal processes (Srikanthan and McMahon, 2001). The term renewal stems from the independence between the dry and wet period length, while the term alternating refers to the fact that wet and dry states alternate. In alternating renewal process, the daily rainfall data are considered as a sequence of alternating wet and dry spells of varying length and no transition to the same state is possible. The wet and dry spells are assumed to be independent and the distribution may be different for wet and dry spells (Srikanthan and McMahon, 2001).

Models used to generate daily rainfall amounts include the two parameter Gamma distribution, mixed exponential distribution, a skewed normal distribution and a truncated power of normal distribution. Cole and Sherriff (1972) applied separate models to rainfalls for a solitary wet day, the first day of a wet spell and to the other days of a wet spell, while Buishand (1978), cited by Srikanthan and McMahon (2001), related the mean rainfall amount on a wet day to its position in a wet spell i.e. such as a solitary wet day, a wet day bounded on one side by a wet day, and a wet day bounded on each side by a wet day.

Chin and Miller (1980) examined the possible conditional dependence of the distribution of daily rainfall amounts on the occurrence of rainfall of the day under consideration and on the preceding day using 25 years of daily rainfall data at 30 stations in the contiguous USA. They concluded that, except for the winter season in the Pacific Northwest, the distribution of daily rainfall did not depend on whether the preceding day was wet or dry.

Chapman (1994), cited by Srikanthan and McMahon (2001), compared five different rainfall amount models based on the Akaike Information Criterion (AIC), which is used to determine the order of Markov chains. A skewed normal distribution was found to be the best, followed by the mixed exponential, the kappa, the gamma distribution and the one parameter exponential distribution. The rank was uniform when the model selected for different groups of data (e.g. solitary, wet days, first day of wet spell etc) were consistent.

Wang and Nathan (2000) developed a Daily and Monthly Mixed (DMM) algorithm for the generation of daily rainfall. Daily rainfall values were generated month-by-month using the two part model with two sets of parameters for the gamma distribution: one estimated from the daily rainfall data and the other from monthly rainfall data. The generated daily rainfalls from the daily gamma parameters are scaled linearly to match the serially correlated monthly rainfalls. The algorithm was tested for seven sites in Australia and it was found to work well in reproducing the mean, coefficient of variation and skewness of maximum daily rainfall for individual months, but not as well for the annual maximum daily rainfall.

Transition Probability Matrix Models

Srikanthan and McMahon (1985), in a study covering the main climatic regions of Australia, combined the modelling of rainfall occurrences and rainfall amounts by extending the Markov chain concepts to a multi-state model, or Transition Probability Matrix (TPM). The daily rainfalls were grouped into states (maximum of seven) of specified sizes as shown in Table 3.1, and the probabilities were calculated for transition from each state to any other.

Table 3.1 State boundaries for TPM models (after Srikanthan and McMahon 1985)

State Number	State boundary in (mm)	
	Lower	Upper
1	0.0	0.0
2	0.1	0.9
3	1.0	2.9
4	3.0	6.9
5	7.0	14.9
6	15.0	30.9
7	30.9	∞

Transition to the lowest state specifies the occurrences of dry days, to the other states gives the occurrences of wet days. The state of the largest magnitude was modelled by a power transformation and intermediate states were modelled by a linear distribution. Boughton (1999) observed that the TPM models underestimate the standard deviation of annual rainfall and proposed an empirical adjustment (F) to match the observed standard deviation. The adjustment factor is obtained by trial and error until the frequency distribution of the observed and generated annual rainfalls agrees. Zhou *et al.* (2002) presented the application of two

stochastic rainfall data generation models (TPM and DMM) at 21 stations in Australia and evaluated the models accordingly. They found that both the models preserved the key statistical characteristics of the historical rainfall at the annual, monthly and daily levels so long as the Boughton adjustment was applied to the TPM model. However, the DMM model did not preserve the rainfall depth for solitary wet days while the TPM did. This factor is considered important for estimating runoff using generated daily rainfall in a rainfall-runoff model.

Re-Sampling Models

Re-sampling models generate rainfall values by re-sampling data from historical records. These methods compare a vector of weather (rainfall) variables for day t against a vector of the same variables from similar dates in the historical record. The k most similar days are taken as k-nearest neighbours. One of these neighbours is selected randomly, and the day following the selected neighbour is taken as the next simulated day (day $t+1$). Lall *et al.* (1996) developed a non-parametric wet/dry spell model for re-sampling daily precipitation at a site. The model considers alternating sequences of wet and dry days in a given season of the year, and the values of the dry spell length, wet spell length and the rainfall amount on wet days are estimated non-parametrically using at-site and kernel probability density estimators. Kernel density estimation is a non-parametric method of estimating a probability density function from a given data set. The model was applied to daily rainfall data at Silver Lake meteorological station in Utah (USA) and the model satisfactorily reproduced the amount of rainfall on the wet days and the spell length of both wet and dry periods.

Rajagopalan *et al.* (1996) and Lall and Sharma (1996) developed re-sampling models and used a Kernel estimator and nearest-neighbour conditional bootstrap for re-sampling daily rainfall respectively. Both the models performed well for reproducing the daily rainfall data on wet days and predicting the wet and dry spell lengths. The limitation of the non-parametric density estimation is the inability to extrapolate daily rainfall values beyond the largest value recorded. The simulations from the k-nearest-neighbour method do not produce values that have not been observed in the historical data (Rajagopalan and Lall, 1999).

Time Series Models

In time series approaches, time series models, similar to streamflow data generation, are used to generate synthetic daily rainfall data. Adamowski and Smith (1972) used a first order Markov Model to generate standardised daily rainfall data. The major problem with this procedure is the cyclical standardisation that occurs if there are a large number of zero daily values. A truncated power of the normal distribution has been suggested to model daily rainfall (Hutchinson, 1995). Hutchinson (1995) examined two point stochastic rainfall models, alternating renewal and truncated power of normal models, for occurrence of rainfall on the basis of computing requirements and economic parameterisation. Hutchinson (1995) concluded that both the stochastic point models describe point rainfall well, but both have significant problems in being extended to space-time settings.

Conditional Models

In the stochastic rainfall process, when model parameters have been estimated using all the historical data for a given time period (e.g. daily periods), the process is called unconditional. However, when the parameters are estimated independently for a subset of climatologically classified data (e.g., dry, scattered, wet) the process is called conditional. Conditional stochastic models of daily rainfall with annual varying parameters usually do not preserve the variance of monthly and annual precipitation (Zucchini and Adamson, 1984; Woolhiser et al., 1993). Wilks (1989), Hay *et al.* (1991) and Woolhiser (1993) developed conditional models which all underestimated the monthly and annual variances.

Synthesis of Single Site Models

According to Srikanthan and McMahon (2001), models for generating daily rainfall are well developed and a great deal of progress has been made in recent years in developing techniques for parameter estimation. The transitional probability method appears to preserve most of the characteristics of daily, monthly and annual characteristics and has been shown to be the best performing model (Chapman, 1994). The main drawback with this model is the large number of parameters, which makes it almost impossible to regionalise the parameters. The two part model has been shown to perform well in some parts of the world by many

researchers (Srikanthan and McMahon, 2001). However, a shortcoming of the current formulation is the consistent underestimation of the variances of the simulated monthly and annual totals. Wang and Nathan (2000) constrained a two part model within a monthly model which performed well.

Multisite Daily Rainfall Generation Model

In hydrological models, when hydrological and land management changes are to be simulated at gridded points or at a number of subcatchments, then the spatial dependence between the climatic inputs at different sites has to be accommodated. This is particularly important in the simulation of rainfall fields, which display the largest variability among the meteorological variables, both in time and space. The models used to generate daily rainfall at a number of sites can be grouped broadly into three categories: Conditional models, extensions of the Markov chain models and random cascade models. Random cascade models are discussed under the stochastic models for spatial and temporal rainfall downscaling.

Conditional models

Pegram and Seed (1998) developed a space-time model for the generation of daily rainfall over a 256 km^2 region near Bethlehem, South Africa. The model has two components:

(i) a climate generator in the form of a three-state Markov chain with periodically varying parameters, and

(ii) bins of rainfall data which are a collection of historical rainfall dates on which the various types of rain occurred.

The daily rainfall was classified by Seed (1992) into three types, based on the number of rain gauges reporting rainfall as shown in Table 3.2.

Table 3.2 Daily rainfall classification (after Seed, 1992)

Dry	< 3% gauges report rain
Scattered	> 3% gauges report rain, but < 50% report > 5mm rain
General	> 50% gauges report rain

The model starts from a known current state and determines the state of the following days using Markov chain transition probabilities. Then, if the state is dry, zero rainfall is assigned

to all gauges. If the state is scattered or general rain days, a rainfall value is assigned conditionally based on the historical record. The model will thus produce a sequence of rainfall values based on the historical data. Srikanthan and McMahon (2001) described the model as a form of extended bootstrap. Models by Zucchini and Guttorp (1991), Bardossy and Plate (1991) and Wilson *et al.* (1992) are also classified under this category of models.

Extension of Single Site Markov Chain Models

Wilks (1998) extended the chain–dependent process stochastic model, which consists of a two-state model. The two states are a first order Markov chain for rainfall occurrence and a mixed distribution for rainfall amounts. The model was developed to generate rainfall simultaneously at multiple locations by driving a collection of individual models with serially independent but spatially correlated random numbers.

The model was applied to a network of 25 rainfall stations in the State of New York, (USA) with inter-station distances ranging from 10 to 500 km. The model reproduced the various aspects of the joint distribution of daily rainfall at the modelled stations reasonably well. The mixed exponential distribution provided a substantially better fit than the more conventional Gamma distribution and was convenient for representing the tendency for smaller amounts at locations near the edge of wet areas. The mean values, variances and inter-station correlation of monthly rainfalls were also reproduced well. In addition, the use of the mixed Exponential rather than Gamma distribution resulted in the inter-annual variability being closer to the observed values (Wilks, 1998).

3.2.1.2. Stochastic Downscaling Models

Stochastic downscaling aims to reconstruct the small scale structure of rainfall in either the spatial or temporal domain, or both, by assuming that rainfall can be suitably interpreted as a random process with specified conditions applied to some statistics that are relevant to the application of concern (Mackay *et al.*, 2001). The models used for rainfall downscaling range from approaches based on the random positioning of a given number of rainfall cells, to autoregressive time series processes, to the more recent approaches based on fractal cascades.

In this section rainfall downscaling in space and time, using autoregressive time series process (Pegram and Clothier, 2001), will be discussed, as will multifractal theory (multiplicative random cascade theory). In recent years, multifractals have been increasingly used in rainfall modelling (Foufoula-Georgiou and Vuruputur, 2000). The main reason for the increased use of the multifractal formalism lies in the capability to achieve, over a wide range of spatial and/or temporal scales, strong control on the statistical moments for a given distribution of measures.

Much of the research dealing with multifractal analysis and simulation of rainfall addresses mainly two objectives:

(i) "Time modelling", that is, analysis of time series of precipitation and simulation of synthetic series with one-dimensional multifractal models preserving scaling laws observed in real rainfall; and

(ii) "Space modelling", that is, analysis and simulation of the rainfall distribution in space with two dimensional multifractal models.

"In the multifractal cascade models, the basic idea is to construct a multiplicative hierarchy of random numbers, where each level in the cascade represents variability of the rain field at some scale" (Seed *et al.*, 2000). There are two kinds of assumptions on the scaling of the multiplicative hierarchy of the rainfall (Gupta and Waymire, 1993): The first assumption is that space-time rainfall displays self-similarity, while the second assumption regards space-time rainfall as being self-affine process. The choice between self-similar and self-affine multifractal frameworks has important implications for the behaviour of the scaling parameter. The self-similarity assumption characterises velocity fluctuations in space from a time series of velocity measurements taken at a fixed point; in other words, it interprets the temporal variations at a fixed locations as being spatial variations. In a similar way, the self-similarity hypothesis can be employed to characterise the space-time statistical properties of rainfall as being a three-dimensional homogeneous and isotropic process. The second assumption relates to the self-affine process, where a scale dependent velocity parameter is used to rescale the time variables (Gupta and Waymire, 1993).

Jothityangkoon *et al.* (2000) constructed a daily time step space-time model to generate synthetic fields of space-time daily rainfall. The model has two components, a temporal model based on a first order, four-state Markov chain which generates a daily time series of

the regionally averaged rainfall, and a spatial model based on non-homogeneous multiplicative random cascade process which disaggregates the above regionally averaged rainfall to produce spatial patterns of daily rainfall. The cascade used to disaggregate the rainfall spatially is a product of stochastic and deterministic factors.

The synthetic rainfall generated by the model compares favourably in most respects with rainfall fields estimated from the raingauge data. In particular, the model is able to mimic well (i) the spatial patterns of long term means of daily, monthly and annual rainfall, (ii) spatial patchiness characteristics of daily rainfall, estimated in terms of a wet fraction, (iii) statistical characteristics relating to storm arrival and inter-arrival times at a selected number of stations, and (iv) the probability distribution and exceedance probabilities of rainfall for selected months. However, the model under-predicted the mean number of wet days and the mean wet spells lengths, especially during winter months. Jothityangkoon *et al.* (2000) concluded that the model they developed was a significant further step towards the development of space-time rainfall models for large regions, which have strong temporal and spatial non-homogeneities. However, theoretical advances are required before random cascades can be used to simulate rainfall across any large regions.

The second approach to downscaling of rainfall fields is the use of autoregressive time series. Pegram and Clothier (2001) developed the String of Beads model (SBM) which is a space-time model of rain fields measured by weather radar. The SBM is driven by two autoregressive time series model, one at image scale and the other at the pixel scale, to model the temporal correlation structure of the wet period series. The marginal distribution of the pixel scale intensities on a given radar-rainfall image is described by a log-normal distribution. The spatial dependence structure of each image is defined by a power spectrum approximated by a power law function with a negative exponent. Pegram and Clothier (2001) argue that an autoregressive time series downscaling model gives the correct temporal correlation structure rather than a random cascade or a modified power law, as proposed by Menabde *et al.* (1999).

Synthesis of Multisite and Stochastic Downscaling Models

The method developed by Bardossy and Plate (1991) uses a censored power normal distribution and requires a procedure to resolve the problem of correlation based on rainfall

occurrence and intensity. The model developed by Pegram and Seed (1998) generates only rainfall values which are already present in the historical record. While the extension of single-site Markov chain models to multiple sites appears to be cumbersome in terms of the number of model parameters and in the way parameters are estimated, this approach was found to perform well (Wilks, 1998). Srikanthan and McMahon (2001) claim that, based on limited work done in generating daily rainfall at multiple sites, the approach of Jothityangkoon *et al.* (2000) appears to be promising. However, further research is required before it can be used to simulate rainfall over a large area.

The model developed by Clothier and Pegram (2002) performed well in the simulation of high-resolution space-time rainfall and shows great potential for generating long sequences of rainfall and improved detailed rainfall information, both in space and time. However, a reliable calibration technique is required before the model can be used successfully in the simulation of long sequences of rainfall values at gridded sites.

3.2.2. Intermediate Stochastic Models

Intermediate stochastic approaches are based on single-site models developed by Rodriquez-Itrube *et al.* (1987), in which storm arrivals are modelled using a Poisson cluster point process. Associated with each storm arrival are a random number of cells, each with a random duration and intensity. Poisson models are attractive as the model parameters have physical significance. However, at their present stage of development, these models represent rainfall as being stochastically stationary in space and time (Chandler *et al.*, 2002). Hence systematic effects, such as topographic variation in rainfall, cannot be represented. This means that they require adequate spatial data to allow for identification of model parameters representing spatial structure.

Northrop (1998) developed a clustered spatial-temporal rainfall model which is a spatial analogue of the point-process based model that have been used to represent the temporal process of rainfall at single site (Rodriguez-Itrube *et al.,* 1987) and which generalises the simpler spatial-temporal models of Cox and Isham (1998). Chandler *et al.* (2002) examined two spatial and temporal rainfall models using continuous simulation models for flood estimation. These models are the General Linear Models (GLM) of Chandler and Wheater (2002) and the Poissson process-based spatial-temporal models of Northrop (1998). The

spatial and temporal models of Northrop were tested using both radar and raingauge network rainfall data in the UK. The performance of the model using radar was "excellent" and according to Chandler *et al.* (2002) the model of Northrop has the flexibility to allow application to event-based or continuous simulation modelling at any required space and time step. However, the model utilises radar data and the length of the radar record, spatial coverage and quality of the data are mentioned as limitations of the model to fully describe the spatial and temporal distribution of the rainfall. Moreover, Chandler *et al.* (2002) examined the model using limited rainfall data from the Brue raingauge network (United of Kingdom), and the major limitation was insufficient information available to identify the spatial structure of the rain field.

There are two major concerns reflected in the use of a point process approaches to simulate rainfall fields. The first, and most difficult, is related to parameter estimation, because the characteristic of rainfall at each scale in the hierarchy needs to be modelled separately, each with its own set of parameters which may be quite large and difficult to estimate unambiguously (Sivapalan and Wood, 1987). The second problem is that most models based on point process approach have suffered from the inability to fully describe the statistical structure of rainfall over a large range of scales.

3.3. Combining of Radar and Raingauge Fields

Weather radar provides high-resolution rainfall fields. However, their quantitative use is restricted by errors and uncertainty in derived rainfall estimates. The sources of the errors and their relative influence are discussed in Section 2.2. Calibrating the radar-derived rainfall values to raingauge gauge measurements can reduce these errors. The merging of a radar image and point measurements from raingauges reduces the bias and uncertainty in estimates of rainfall from radar and provides spatial information of the rain field, which the raingauge data lacks (Pegram and Sinclair, 2003).

Significant research effort is currently directed towards developing merging techniques for combining the radar field and observed rainfall from raingauges. Some of these efforts use a Bayesian merging technique (Todini, 2001), geo-statistical merging of radar and raingauge data (Ehret, 2002), and the use of regression models to estimate rainfall fields from radar and

raingauge data (Sokol, 2003). The Bayesian merging technique is discussed below as an example to describe the merging process.

Bayesian merging technique

In order to consistently combine the point measurements provided by the gauges to the spatial estimates provided by the radar, a block kriging Bayesian merging technique, which is an extension of geostatistical kriging, interpolates the raingauge measurement spatially onto the same scale/pixels at which the radar derived values are given. The rainfall estimates provided by the radar and block kriging of the gauges are comparable and can be considered as independent estimates of the same unknown field, i.e. the true rainfall field. A Kalman filtering approach is applied to find the combination of the radar and raingauge measurement, which is called a posterior estimate, by combining the priori estimates which are estimates of the rainfall from the radar and the block kriging of the raingauge data. The block kriging technique is illustrated in Figure 3.1.

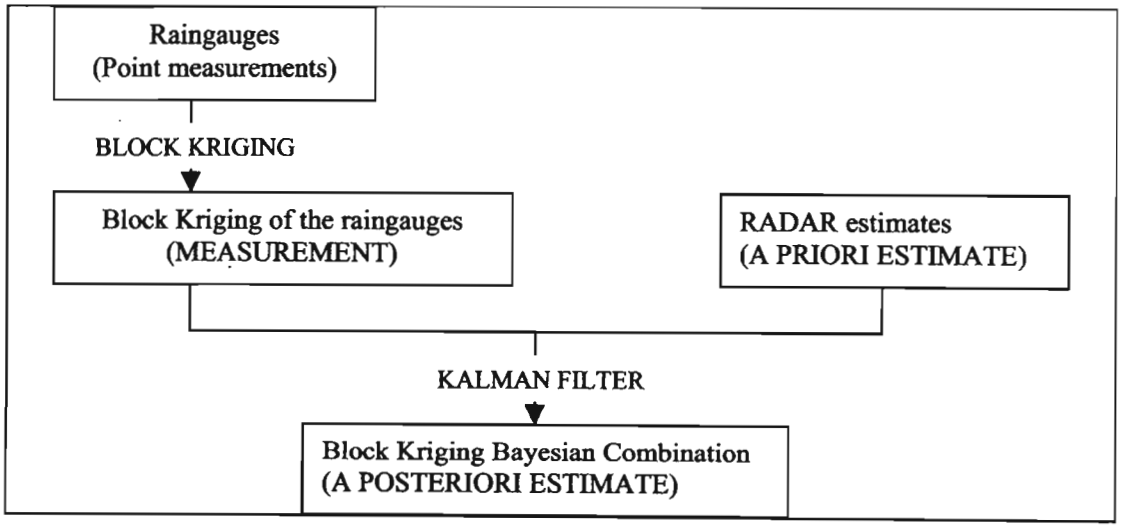

Figure 3.1 Block kriging Bayesian merging (after Todini, 2001)

Since the introduction of weather radar, merged rain fields have been used in real-time flood forecasting and have been successful in short-term forecasting (nowcasting). However, there have been no studies which have used merged rainfields for the simulation of long series of rainfall values. A statistical rainfall model, the String of Beads model developed by Clothier and Pegram (2002), can be used to predict high temporal resolution rainfall fields based on radar images. The short-duration predicted rainfall values and observed historical rainfall data

are then set as an input to flood forecasting. The operational system for flood forecasting is shown in Figure 3.2.

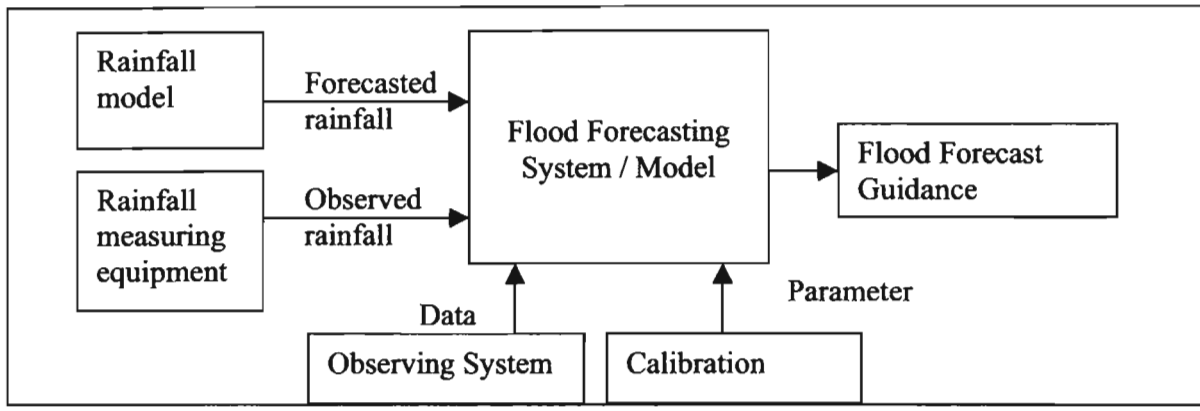

Figure 3.2 An example of the flood forecasting process (Pegram and Sinclair, 2004)

* * *

In Chapter 3 the different techniques documented in literatures to improve the estimation of the spatial distribution of rainfall are discussed. Among these techniques, merging rainfall values from radar and raingauges using the conditional merging technique developed by Ehret (2002) and the String of Beads stochastic rainfall model developed by Clothier and Pegram (2002) are discussed in Chapter 5 and Chapter 6 respectively. These two techniques will be assessed in Liebenbergsvlei catchment. The next chapter describes the Liebenbergsvlei catchment and the spatial distribution of rainfall in the catchment and the sources and representation of the data used in both techniques are presented.

4. LIEBENBERGSVLEI CATCHMENT

The Liebenbergsvlei catchment is a subcatchment of the Vaal River catchment and is located near Bethlehem in the Free State Province of South Africa as shown in Figure 4.1. The Liebenbergsvlei catchment is in a relatively dry region of South Africa and has an area of 4694 km^2 which receives an average annual rainfall total of 650 mm (Pegram and Sinclair, 2002). Most of this precipitation falls during the summer season, which ranges from October to February. The mean annual runoff depth from the catchment for the twenty-one year period from 1978 up to and including 1998 was 38mm (Midgley *et al.*, 1994).

Rainfall has been intensively monitored in the Liebenbergsvlei catchment both by raingauges (daily and continuously recorded) and by radar. Therefore the Liebenbergsvlei catchment was selected a test site for this study.

4.1. Spatial Distribution of Rainfall

A nearly rectangular network of 45 tipping bucket raingauges is distributed in the Liebenbergsvlei catchment, as shown in Figure 4.2. The gauges are on a grid spacing of approximately 10 km by 10 km. A data logger is attached to each gauge and records time, event count and various flags for each tip event. The gauges have a resolution of 0.2 mm of rain per tip and the logger's memory can record 510 mm of rain given that the storage capacity of the loggers is 2550 events (Pegram and Sinclair, 2002). Thirty-four active daily rainfall South Africa Weather Stations (SAWS) are in, and in close proximity, to the Liebenbergsvlei catchment, as shown in Figure 4.2.

The SAWS's MRL5 weather radar is located to the Northwest of Bethlehem and provides full coverage of the Liebenbergsvlei catchment. The radar is capable of recording real-time rain rates at a spatial resolution of 1 km^2 and with a temporal resolution of approximately 5 minutes. Figure 4.1 shows the location of the Liebenbergsvlei catchment in South Africa while the layout of the catchment, distribution of raingauges, the position of the MRL5 radar and the river network are shown in Figure 4.2.

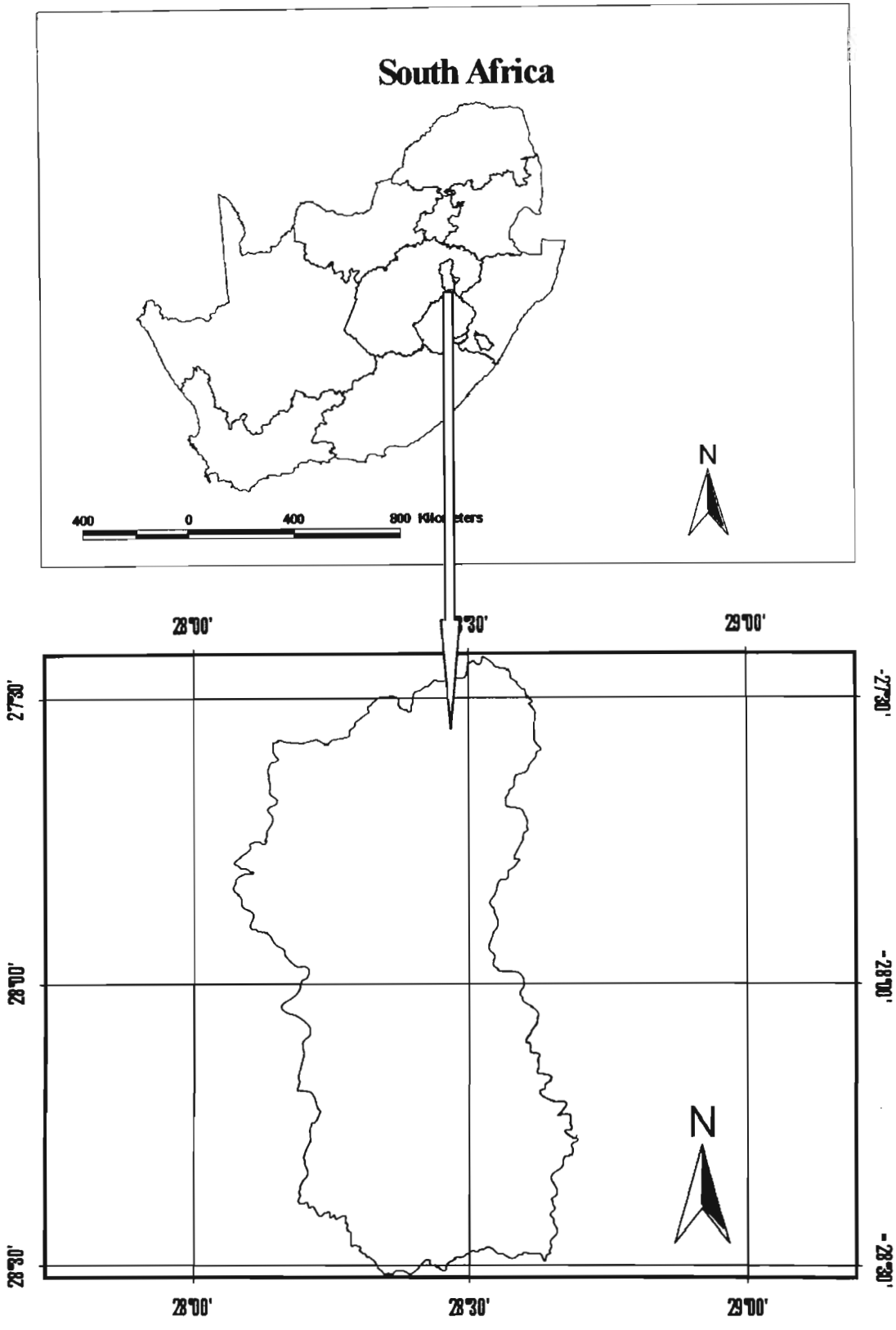

Figure 4.1 Location of the Liebenbergsvlei catchment

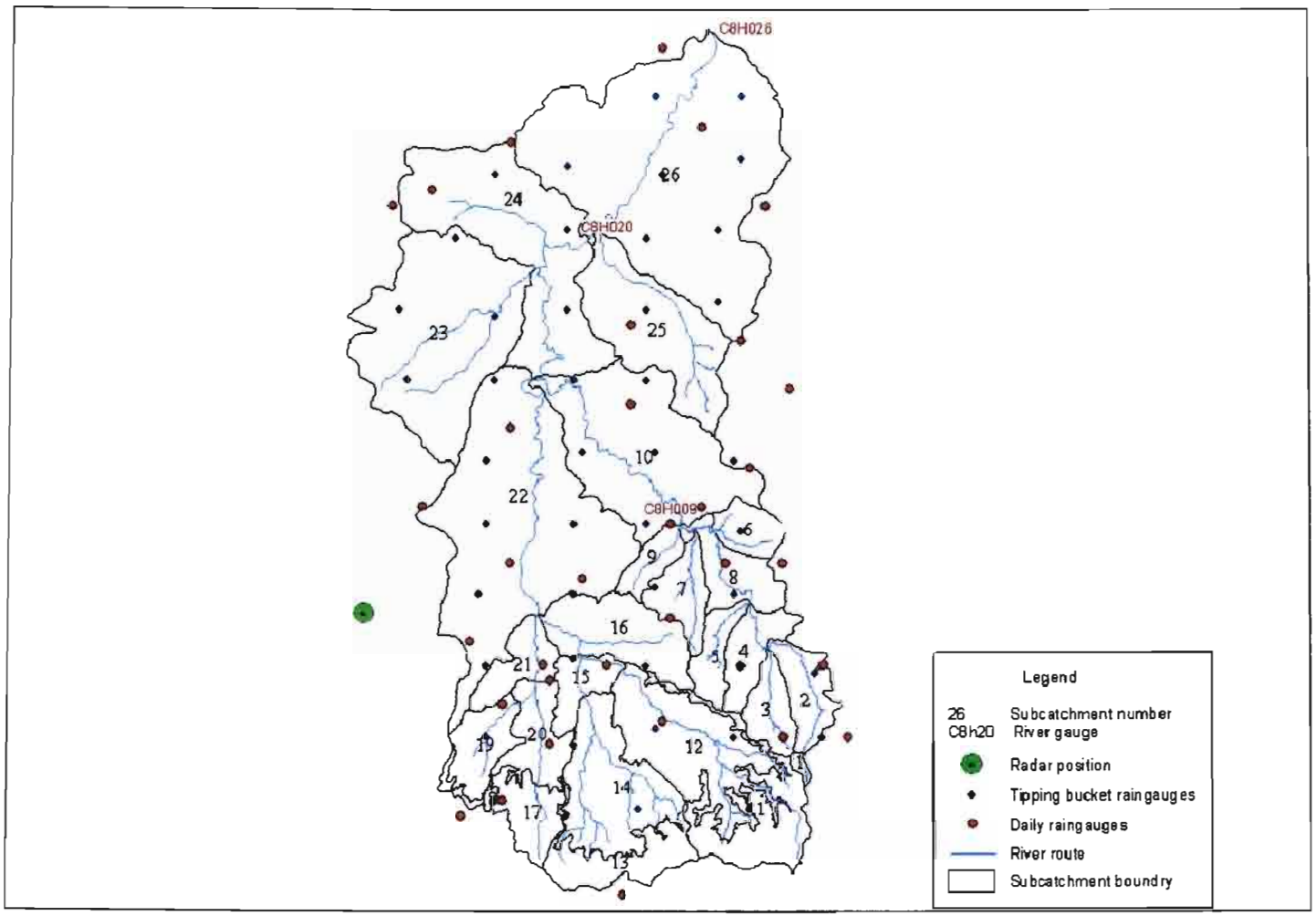

Figure 4.2 Liebenbergsvlei catchment and raingauge network

4.2. Estimation of the Spatial Distribution of Rainfall

The spatial distribution of rainfall is affected by the prevailing weather condition as well as by local geographical factors, such us topography and latitude. The Liebenbergsvlei catchment is a relatively flat area with a mountainous peripheral (Figure 4.3), and as a consequence the spatial distribution of rainfall, derived from the radar images, is highly variable in the areas of higher altitude. The catchment was delineated into 26 subcatchment by Jewitt *et al.* (1997) to represent relatively homogenous area of hydrological response, which includes soil type, land cover and spatial variation of rainfall. As a consequence, the areas of the subcatchments are relatively smaller in regions where the spatial distribution of rainfall is highly variable. The same subcatchment delineation was adopted in this study and the areas of the subcatchments are contained in Table 4.1.

Table 4.1 Size of the subcatchments

Subcatchment Number	Area (km^2)
1	6.26
2	71.65
3	60.31
4	70.65
5	70.11
6	52.65
7	71.52
8	84.86
9	42.04
10	387.14
11	153.36
12	230.75
13	100.41
14	203.31
15	55.86
16	151.84
17	73.41
18	14.91
19	77.84
20	86.38
21	68.42
22	621.46
23	453.08
24	409.63
25	249.10
26	827.34
Total	4694.32

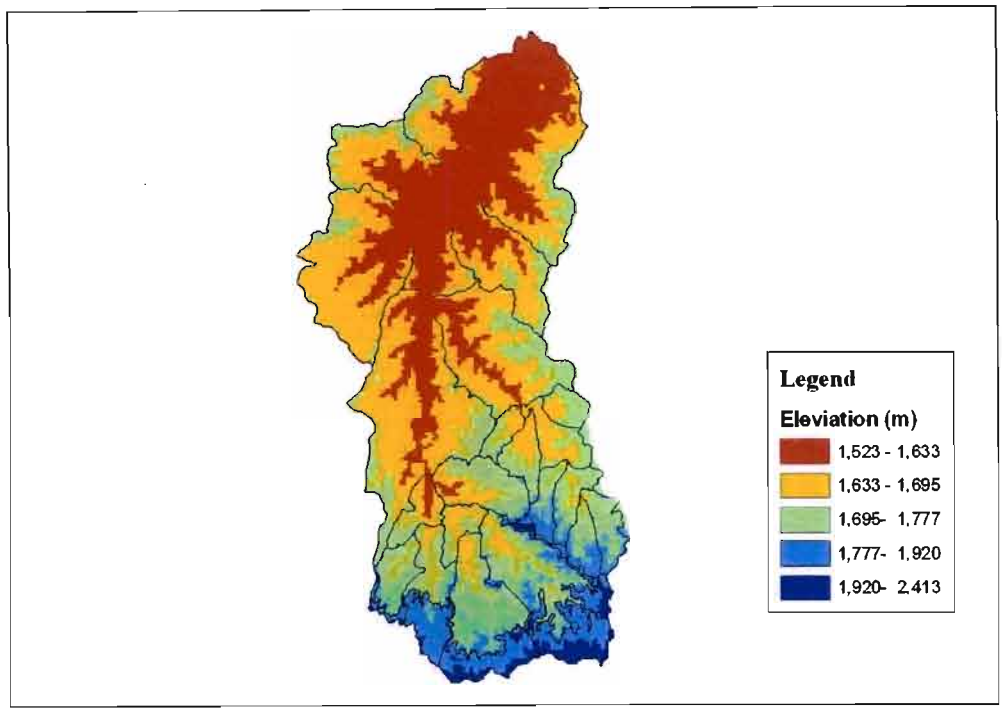

Figure 4.3 Variation in altitude in the Liebenbergsvlei catchment

4.3. Data Representation

Radar rainfall images from 2 November 1998 to 31 March 1999 were used in this study and were provided on compact disk by the SAWS in Meteorological Data Volume (MDV) format. This format is capable of storing multiple levels of multiple fields of data and is designed specifically for meteorological application. On conversion to MDV format, each floating point field is shifted and scaled so that it has a range of 0 to 255 and the scale and shift terms for each field is then converted to character precision and the field is stored row-wise as a one-dimensional array in the MDV file. There is some loss of information in the scaling process of converting to MDV format. The 5 minutes intervals of radar rainfall images were aggregated to daily rainfall images using a computer programme written by Sinclair (2004). The daily rainfall images were accumulated for the period from 8:00 to the next day 8:00 to coincide with the daily raingauges which are recorded between these times. The procedures used to accumulate the tipping bucket raingauge rainfall data into daily rainfall data are showing in Appendix A.

The observed tipping bucket raingauge data were obtained from Meteorological Systems and Technology (METSYS) and consisted of recorded rainfall at 5 minute intervals. A computer programme was written to aggregate the 5 minutes tipping bucket rainfall data into a daily rainfall depth; for the period from 8 a.m. to 8 a.m.

4.3.1. Radar and Raingauge Merging

A computer programme was written by Sinclair (2004) on the basis of the conditional merging technique developed by Ehret (2002), to merge the daily aggregated radar rainfall values and accumulated tipping bucket raingauge rainfall data. Conditional merging makes use of kriging to extract the optimal information content from the observed data. A mean field based on the kriged raingauge data is adopted, while the spatial detail from the radar reduces the bias but retains the spatial variability observed by the radar. The variance of the estimate is reduced in the vicinity of the gauges where they are able to provide good information on the true rainfall field. Full details of the merging process are provided in Chapter 5.

The computer programme used to merge the radar rainfall images and the point rainfall data uses the radar images in MDV format and daily point rainfall data stored ASCII files as an input and the output are in MDV and ASCII formats. The MDV or ASCII format merged rainfall images were viewed and processed in the form of bitmap images and grids.

4.3.2. Image Masking

The areal rainfall for each subcatchment is represented by an average rainfall depth over the subcatchment. These values are obtained by converting the merged daily rainfall values into a grid using ArcInfo Commands (ESRI, 2002). Each output in text format were converted to an ASCII file and stored with header information which includes the number of columns, number of rows, a coordinates of the lower corner of the image or grid, a cell size and a value to represent no data.

Table 4.2 Header information used in ASCII files (after Sinclair, 2004)

ncols	400
nrows	400
xllcorner	-479162.00
yllcorner	-3312540.00
cellsize	1000
NODATA_value	-9999

Once the ASCII files were stored with their respective information, a programme written in the ArcInfo environment to convert the ASCII files into a grid using the "ASCIIgrid" command (ESRI, 2002). Each grid was clipped by all subcatchment polygons using the "GridClip" command. The daily mean values extracted from the clipped grids for each subcatchment represent the spatial rainfall distribution each day for each subcatchment (cf. Appendix A). Figure 4.4 illustrates the image masking process graphically.

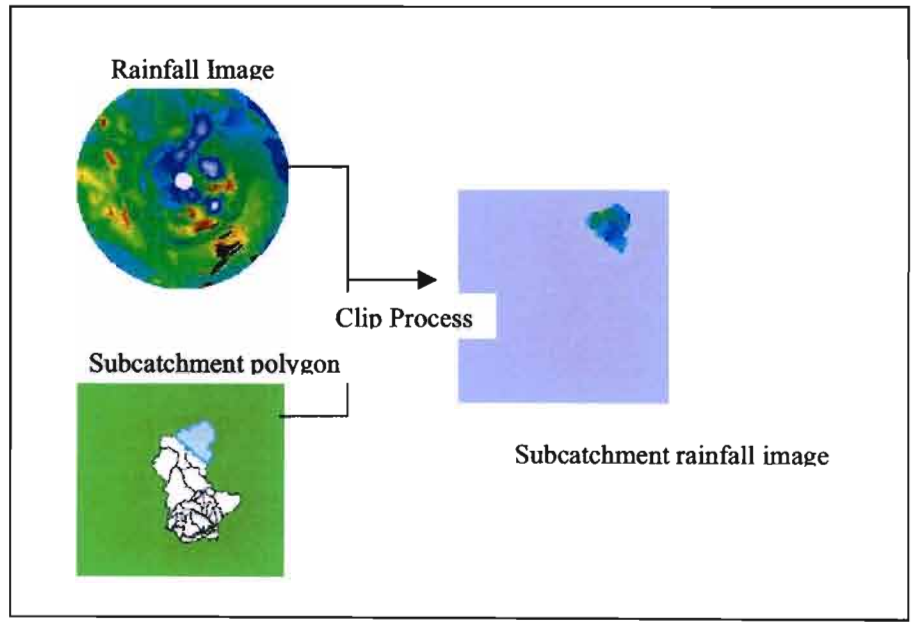

Figure 4.4 Image masking process

* * *

In this chapter, the Liebenbergsvlei catchment, spatial distribution of rainfall distribution in the catchment and data representation and manipulation used for the merging of rainfall values have

been discussed and presented. In the next chapter merged rainfall fields in Liebenbergsvlei catchment are developed and assessed.

5. DEVELOPMENT AND ASSESSMENT OF MERGED RAINFALL FIELDS FOR CONTINUOUS SIMULATION MODELS

Raingauges measure rainfall directly and rainfall depth accumulated over the period of interest is measured with a high degree of accuracy at points where the gauges are located. However, raingauge networks are too sparse to capture the spatial variability of rainfall (Wilson and Brandes, 1979). Radar, on the other hand, measures a volume-averaged returned signal power which is converted to rainfall in a number of steps: first to reflectivity factor (Z), and then to rainfall units (R). Although indirect, radar estimates of rainfall are continuous in space and provide information on the spatial variability of rainfall. However, radar rainfall estimates lack the accuracy of the raingauges provides at a point (Wilson and Brandes, 1979).

Merging of rainfall values from raingauges and radar exploit the complementary characteristics of the techniques. Several methods have been developed for merging raingauge and radar data and merged values have generally produced good results in terms of bias reduction, although little attention has been given to the reduction of variance (Todini, 2002). The different nature of the errors, which implies their independence (Seo and Krajewski, 1990), can be exploited to produce unbiased and more reliable estimates of rainfall. Following this idea, Todini (2001) proposed an original Bayesian combination technique, based on the use of block Kriging and a Kalman filter, which aims at eliminating the bias of meteorological radar estimates of precipitation and at producing minimum variance estimates of precipitation on a pixel of variable size.

Merging of radar and raingauge data using a merging technique enables the best possible estimate of the spatial distribution of rainfall to be made. However, the length of radar records in South Africa is limited and most hydrological models require a long input sequence of rainfall records. Therefore, in this chapter the relationships between average daily rainfall depths for a particular subcatchment, estimated by the merging of radar and raingauge data, and rainfall measured by daily raingauges, which are selected to represent the areal rainfall of the subcatchment, are developed and assessed.

5.1. Conditional Merging

Radar produces an image of the unknown true rainfall field which is subject to several well-known sources of error (e.g, as detailed by Wilson & Brandes, 1979; Habib & Krajewski, 2002), but retains the general covariance structure of the true precipitation field. The information from the radar can be used to condition the spatially limited information obtained by interpolating between raingauges to produce an estimate of the rainfall field that contains the correct spatial structure, while being constrained to raingauge data. This process is illustrated in Figure 5.1. The conditional merging technique of Ehret (2002) makes use of ordinary kriging to extract the information content from the observed gauged rainfall data.

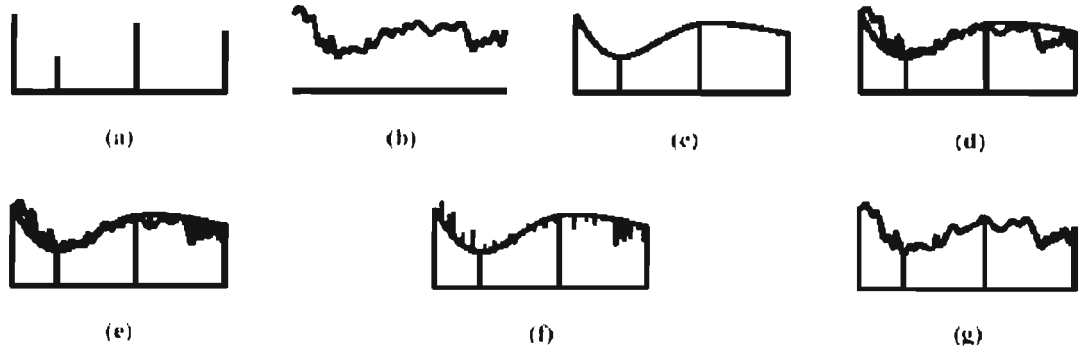

Figure 5.1 Conditional rainfall merging process (Pegram and Sinlcair, 2004)

With reference to Figure 5.1, the conditional merging process is described by Pegram and Sinlcair (2004) as follows:

(a) The rainfall field is observed at discrete points by raingauges.

(b) The rainfall field is also observed by radar on a regular, volume-integrated grid.

(c) Kriging of the raingauge observations is used to obtain the best linear unbiased estimate of rainfall on the radar grid.

(d) The radar pixel values at the raingauge locations are interpolated onto the radar grid using Kriging.

(e) At each grid point, the deviation between the observed and interpolated radar value is computed.

(f) The field of deviations obtained from (e) is applied to the interpolated rainfall field obtained from Kriging the raingauge observations.

(g) A rainfall field that follows the mean field of the raingauge interpolation, while preserving the mean field deviations and the spatial structure of the radar field is thus obtained.

5.2. Spatial distribution of rainfall

Topography plays a major role in the local climate and specifically in the spatial distribution of rainfall. There is a strong relationship between altitude variation and spatial distribution of rainfall of any area (Sotillo *et al.*, 2003). However, the development of this relationship requires downscaling of climate scenarios from meteorological models, as their relationship is complex by nature. The variation in altitude within the subcatchments of the Liebenbergsvlei catchment is shown in Figure 5.2. Subcatchments 11 and 13 have the highest standard deviation of altitude. The effect of variation in altitude in Subcatchment 13 (cf. Appendix B) is clearly evident on the spatial distribution of the rainfall of this subcatchment, but the effect of altitude in the spatial distribution of rainfall of Subcatchment 11 is not as evident. Therefore, this indicates that the orographic effect on the spatial distribution of rainfall is not consistent throughout the 26 subcatchments.

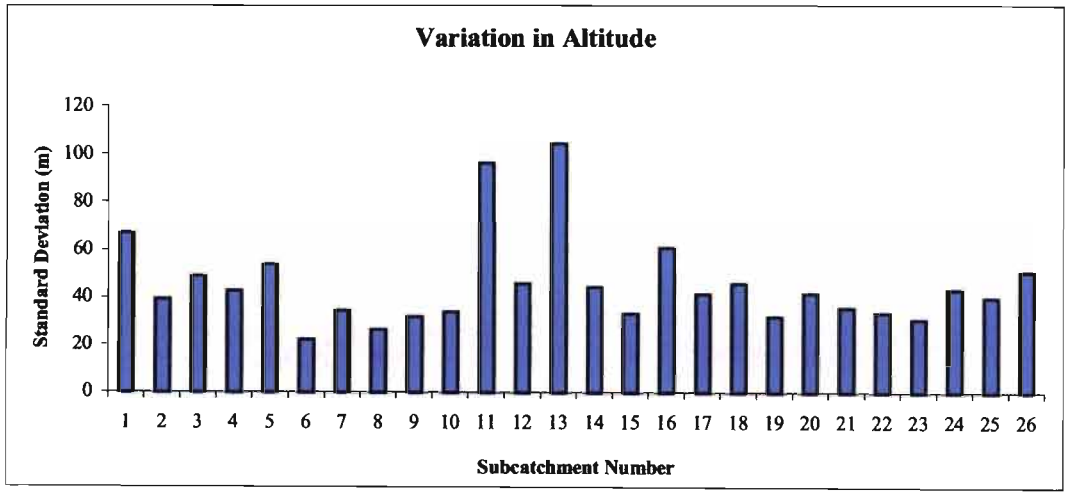

Figure 5.2 Standard deviation of altitude within the 26 subcatchments of Liebenbergsvlei catchment

5.3. Development of Relationships between Daily Rainfall and Merged Rainfall Data

Many hydrological studies require a long temporal sequence and spatially detailed accurate rainfall data. However, the available rainfall data in South Africa are either long series of point rainfall, with no spatial information (raingauge rainfall data), or detailed spatial and temporal rainfall information but with a limited period of record (radar and satellite rainfall values). Therefore, a relationship between the average rainfall depth of a subcatchment, obtained from merging the raingauge data and radar rainfall values, and the long sequence of daily rainfall data from raingauges, is developed in this section.

There are 45 tipping bucket raingauges and 34 daily raingauges in and around the Liebenbergsvlei catchment as shown in Figure 4.2. First, the merging process developed by Sinclair (2004) is verified using rainfall data from the tipping bucket raingauges used in the conditioning of the radar rainfall values. Second, merging process is validated using daily rainfall data measured by daily raingauges which were not used in the calibration of the merging process. Thereafter the reliability of the relationships between the averaged merged rainfall values for the subcatchments, obtained by combining the radar and raingauge data, and the raingauge data selected to represent the areal rainfall of the subcatchment, is investigated.

5.3.1. Verification of the Merging Process

In the merging process, Kriging of the tipping bucket raingauge observations is used to obtain the best linear unbiased estimate of rainfall on the radar pixels and the observed rainfall values at these raingauge pixel locations are fixed in the merged rainfall images without adjustment. Therefore, the average merged rainfall values at the same location as conditioning raingauges, in this case the tipping bucket raingauges, are equal to the measured rainfall at the conditioning gauge. At conditioning raingauge locations where the merging algorithm has "exact" knowledge about the measured rainfall, a 1:1 linear relationship (best fit straight line, $Y = x$; $R^2 = 1$) between the average merged pixel values and the conditioning gauges is expected. Anywhere else in the merged field it is expected that there will be some error between the true rainfall field and the merged estimate ($Y = ax + b$; $R^2 < 1$). If a daily raingauge is located at a point not used to

condition the merging process, the merged value will not necessarily equal the rainfall measured by the raingauge. However, the closer the raingauge is to a location which has a raingauge used in the merging procedure, the more accurate the merged value is expected to be.

The relationship between rainfall values at a tipping bucket raingauge, which was used to condition the radar images, and the merged rainfall values at the conditioning gauge, are shown in Figure 5.3 for all tipping bucket raingauges on 10 October of 1998. A linear regression relationship of $y = 0.9557x - 0.0815; r^2 = 0.8157$ was obtained. According to the merging process developed Sinclair (2004), radar pixels with no rain were masked (i.e. excluded) and hence in regions where the radar registered no rain, the merged value has zero rainfall. This is a trade-off between being wrong at the raingauge in a few cases and having rainfall over the entire data domain which means many "False Rainfalls" elsewhere in the region of interest (Sinclair, 2004). Therefore, when the merged pixel values which had no rainfall as a result of the radar not detecting any rainfall were removed from the relationship, resulted in a perfect relationship, $Y = x; r^2 = 1$, as shown in Figure 5.4.

The verification test was performed for all tipping bucket raingauges and for all days where radar images were available (2 October 1998 to 31 March of 1999) as shown in Figure 5.5, where a linear regression of $y = 0.937x - 0.2326 (R^2 = 0.9225)$ was obtained. When the merged values with zero values, resulting from no rain registered in the radar, are removed from the relationship, a regression relationship of $y = 1.001x - 0.036 (R^2 = 0.9996)$ resulted (Figure 5.6). The masked merged values resulting in zero rainfall due to no rain registered in the radar image make up 6.2 % of the six months of data used in this study and most of these pixels have a conditioning raingauge values of between 1 to 10 mm, while masked values above 10mm are only 0.83 % of all the data considered.

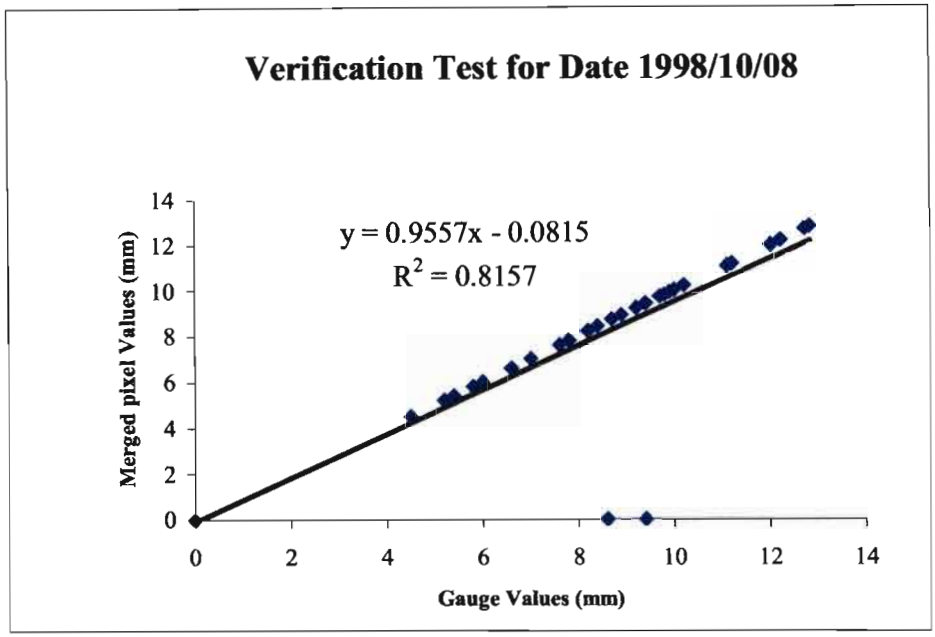

Figure 5.3 Verification of the merging process for 10 October 1998 at all gauges used in the merging process

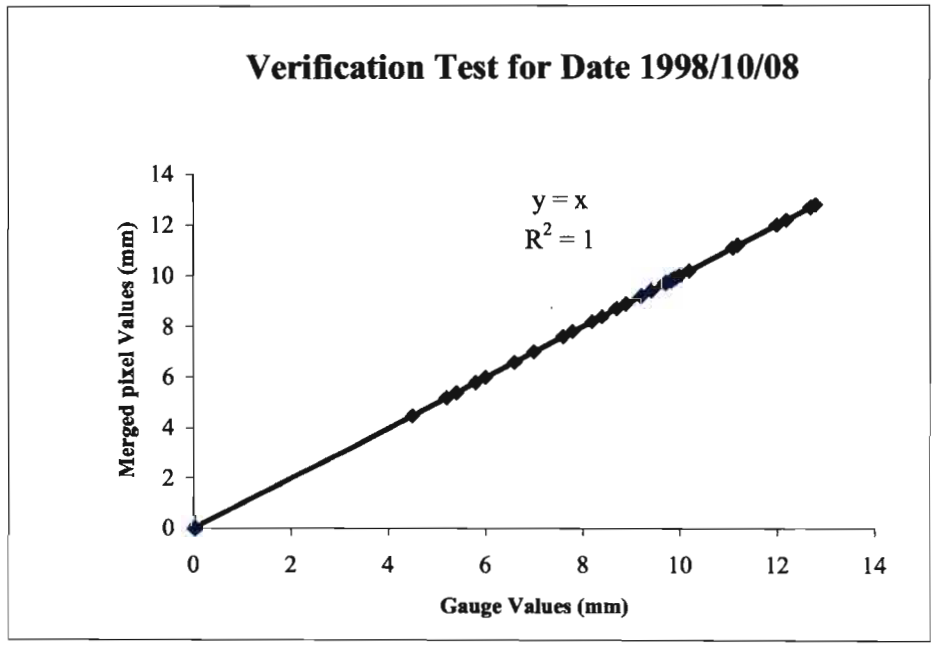

Figure 5.4 Verification of the merging process for 10 October 1998 **at** all gauges used in the merging process after merged zero rainfall values resulting from no rainfall in the radar images were masked

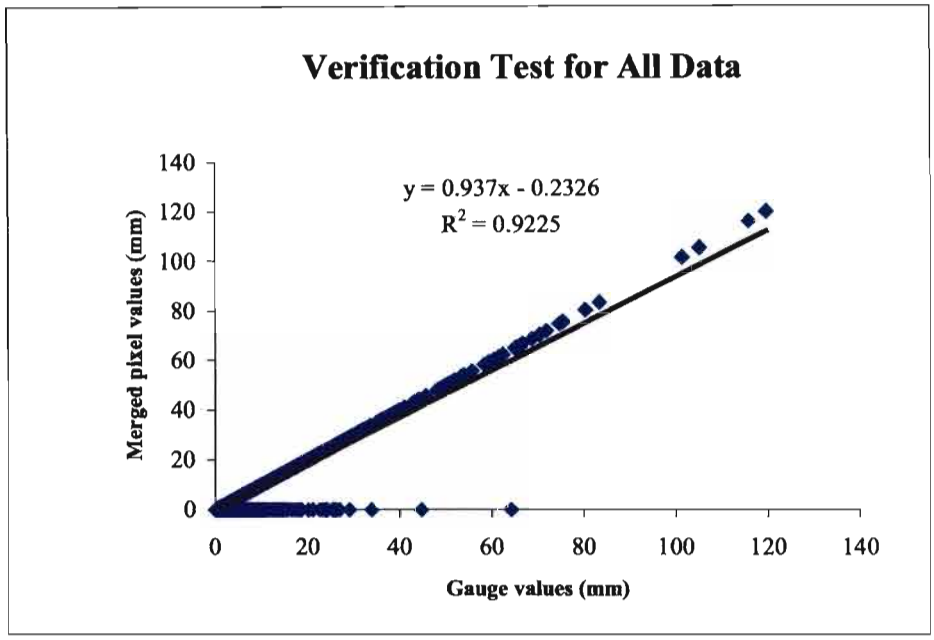

Figure 5.5 Verification of the merging process at all tipping bucket raingauges used in the merging process

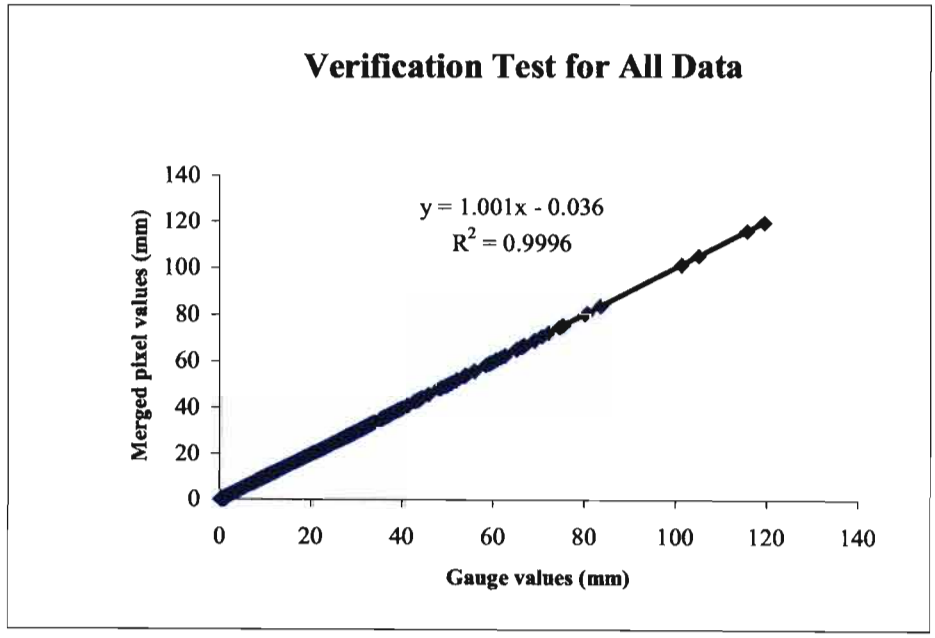

Figure 5.6 Verification of the merging process at all tipping bucket raingauges used in the merging procss after merged zero rainfall values resulting from no rainfall in the radar images were masked

From the verification of the merged rainfall with the tipping bucket raingauges used in the conditioning of the radar images, it is evident that the merging procedure developed by Pegram and Sinclair (2004) successfully assigns rainfall values to the merged pixels from the respective raingauge values used in the conditioning of the radar images.

5.3.2. Verification of Merging Process at Raingauges Not Used in the Conditioning of Radar Images

Average merged pixel values at daily raingauges, which were not used in the conditioning of the radar images, are compared to the daily raingauge values. A linear relationship of $Y = ax + b$ $(R^2 < 1)$ is expected and better relationships are expected where the daily gauge is closer to a tipping bucket raingauge which was used to condition the radar images in the merging process.

Raingauge 0331607W, located in Subcatchment 22 as shown in Figure 5.7, is used as an example of the verifications, where a relationship of $y = 1.0385x - 0.0675$ $(R^2 = 0.7018)$ is obtained from the comparison of rainfall from the daily raingauge and the merged pixel values at the raingauge location (Figure 5.8). However, as explained above, some of the merged pixels were assigned zero values at pixels where the radar registers no rainfall. When these pixel values were removed from the analysis, the relationship improves to $y = 1.1814x + 0.1224$ $(R^2 = 0.8205)$, as shown in Figure 5.9.

Figure 5.10 shows the relationship between tipping bucket Raingauge L015, used in the conditioning of the radar rainfall images, and the average merged pixel rainfall values at the location of the daily Raingauge 0331607W, and shows the rainfall characteristic pattern between the point rainfall from the tipping bucket raingauge and average merged rainfall values and it demonstrates the influence of the tipping bucket Raingauge L015 on the relationship between the point rainfall from daily raigauges and averaged merged rainfall values of pixels at location of the daily raingauges.

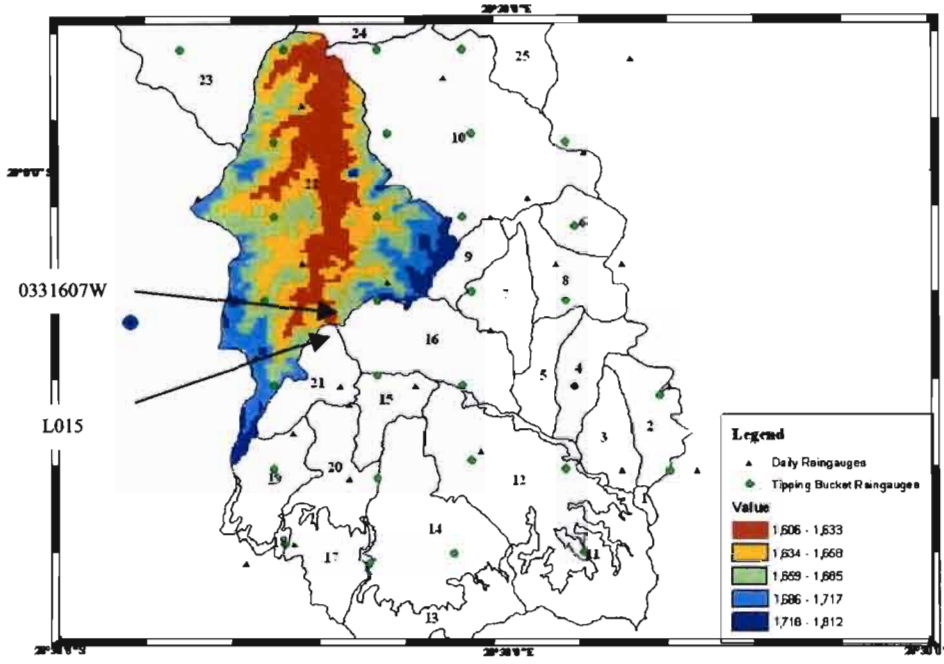

Figure 5.7 Location of Raingauges 0331607W and L015 and altitude distribution in Subcatchment 22

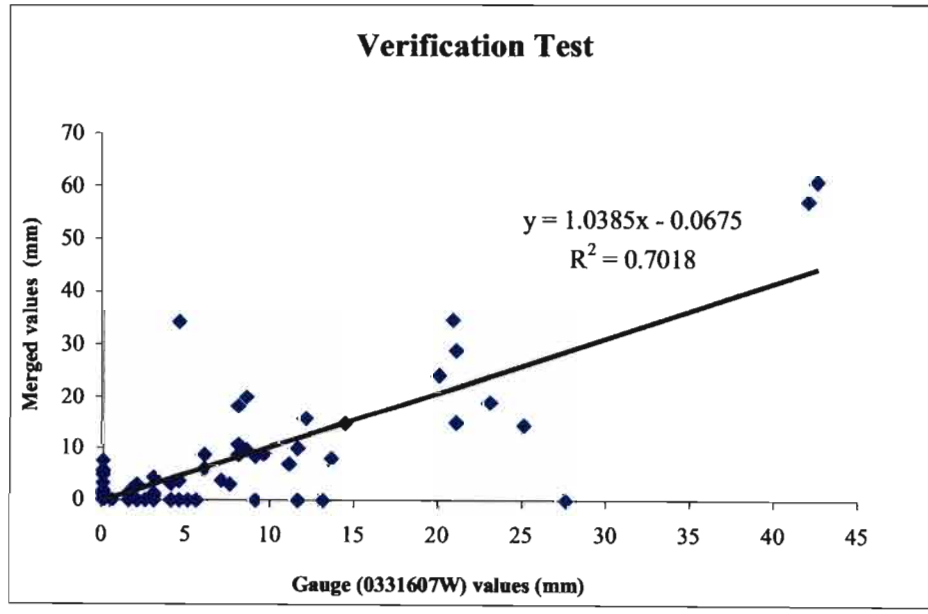

Figure 5.8 Comparison between daily rainfall from Raingauge 03312607W, which was not used in the merging process, and merged daily pixel rainfall values at the raingauge location

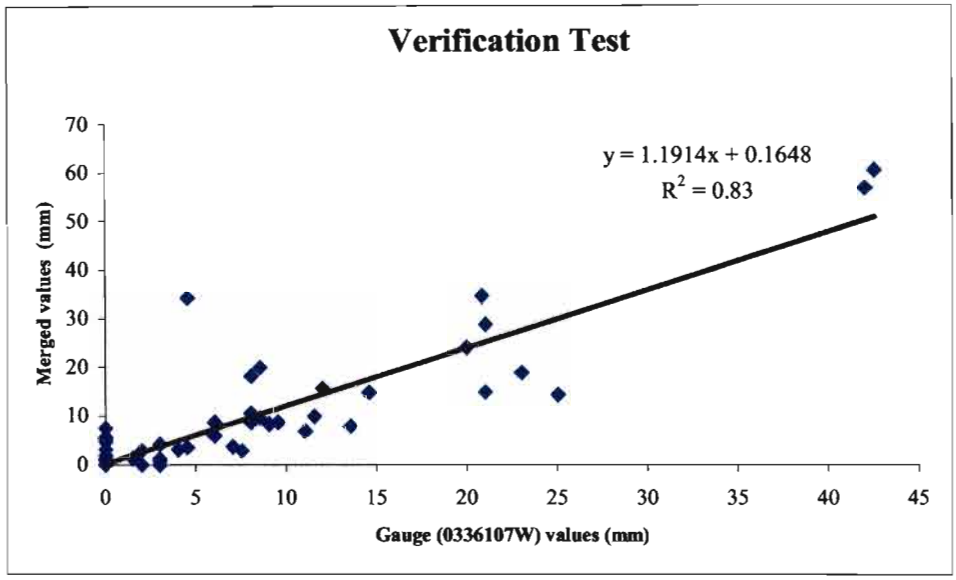

Figure 5.9 Comparison between daily rainfall from Raingauge 03312607W, which was not used in the merging process, and merged daily pixel rainfall values at the raingauge location after merged zero rainfall values resulting from no rainfall in the radar images were removed

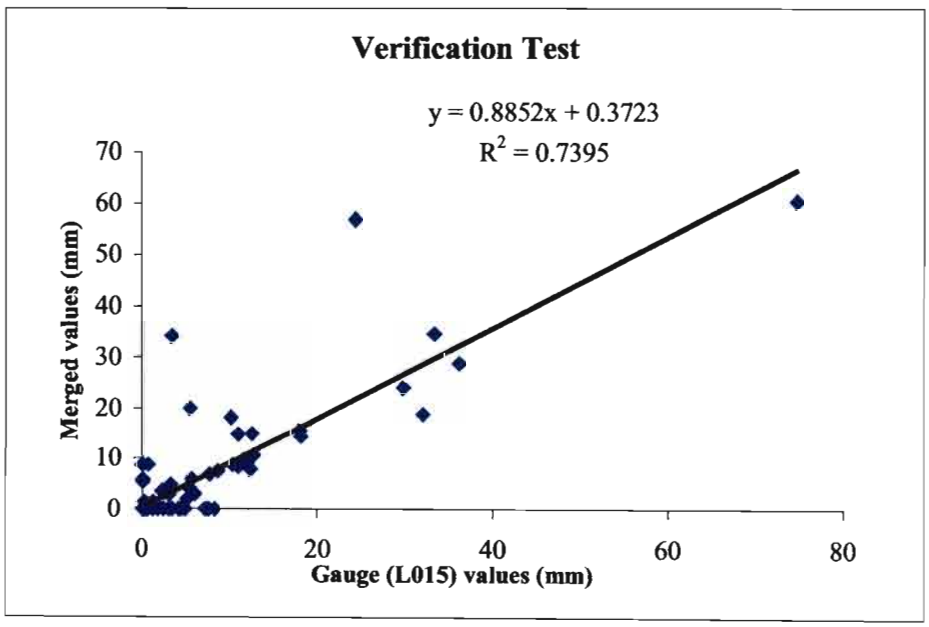

Figure 5.10 Comparison between merged pixel rainfall at location of daily Raingauge 03312607W and a nearby tipping bucket raingauge (L015).

The merged pixel values are a combination of the Kriged interpolated tipping bucket rainfall value at a station and the deviation between the radar rainfall value and the Kriged interpolated rainfall value. Therefore, the relationship between the rainfall values at Raingauge 0336107W and average merged pixel rainfall values are only as good as the merging process and the accuracy of the radar values at the site.

A radar image free of ground clutter, beam attenuation and other errors related with calibration of radar can be referred as a good quality radar image. The relationship between rainfall at Raingauge 0336107W and radar rainfall values at the raingauge site is shown Figure 5.11. On the majority of the days the radar estimates the true rainfall at Raingauge 0336107W reasonably well while on some days the radar estimate of rainfall shows discrepancies from the true value. If the radar estimates of rainfall at the location of the daily raingauges are good, the relationship between the merged pixel rainfall values at location of the daily raingauges and the point rainfall from the daily raingauges can be expected to strong.

A strong relationship, as shown in Figure 5.9, between the merged pixel values and rainfall at Raingauge 0331607W is evident. This relationship is influenced by both the tipping bucket rainfall values and the quality of the radar values at the site. Therefore, consistency between daily raingauge, tipping bucket and radar values is important. The radar does not estimate the true rainfall field as accurately as daily or tipping bucket raingauges. However, the better the estimate of rainfall by the radar, and the small the errors in the tipping bucket and the daily raingauge values, should result in a better relationship between the daily gauges and a merged pixel rainfall value for the same site.

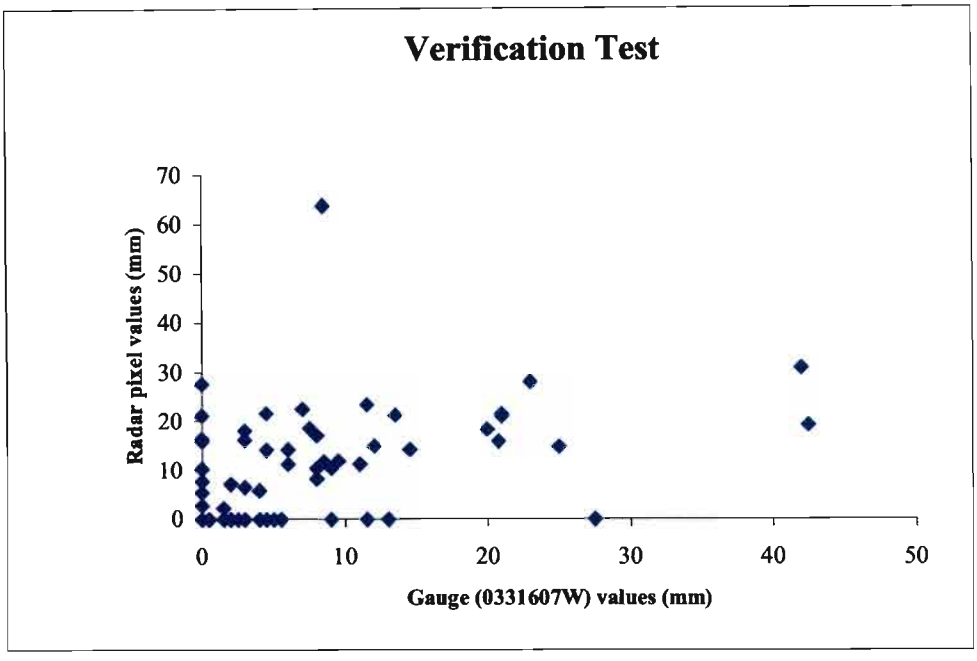

Figure 5.11 Rainfall estimated by radar and measured at Raingauge 0331607W

Table 5.1 contains generally good regressions between the average merged pixel rainfall values at the location of daily raingauges, these daily raingauges are selected randomly and located at different subcatchments inside the Liebenbergsvlei catchment, and gauged daily raingauges at those locations which were not used in conditioning the radar rainfall values. These relationships depends on many factors including the distance between the tipping bucket raingauges used in conditioning of the radar rainfall values and daily raingauges under consideration, the quality of the radar rainfall images, the characteristic rainfall pattern between the tipping bucket raingauges and the daily raingauges which are all manifested in the spatial variability of rainfall.

Table 5.1 Relationship between the mean merged pixel rainfall values at location of daily raingauges and the point rainfall from daily raingauges

Daily Raingauges	X-Coefficient (a)	Correlation (R^2)
0332066W	0.9611	0.6090
0332104W	0.9160	0.9262
0331585W	1.0831	0.8553
0332284W	0.9520	0.5735
0367768W	1.1064	0.5959

5.3.3. Estimation of Subcatchment Rainfall from Daily Merged Rainfall Images

Relationships between the mean areal rainfall of the subcatchments in the Liebenbergsvlei catchment and daily and tipping bucket raingauges were developed to provide the detailed required rainfall inputs to hydrological models.

The downstream part of the Liebenbergsvlei catchment is relatively flat compared to the upstream part of the catchment. As a result the size of the subcatchments delineated by Jewitt *et al.* (1997) are bigger in the downstream portion than in the upstream part. As shown in Figure4.2, Subcatchment 26 is situated in the lower portion of the study area and it is has a standard deviation of altitude 50 m and an area of 827.34 km^2. The location of Station 0367601W is shown in Figure 5.12. Figure 5.13 shows the relationship between the average merged rainfall depth for Subcatchment 26, obtained by averaging all the merged rainfall values at each pixel with the subcatchment, and the daily raingauge (W0367601) values.

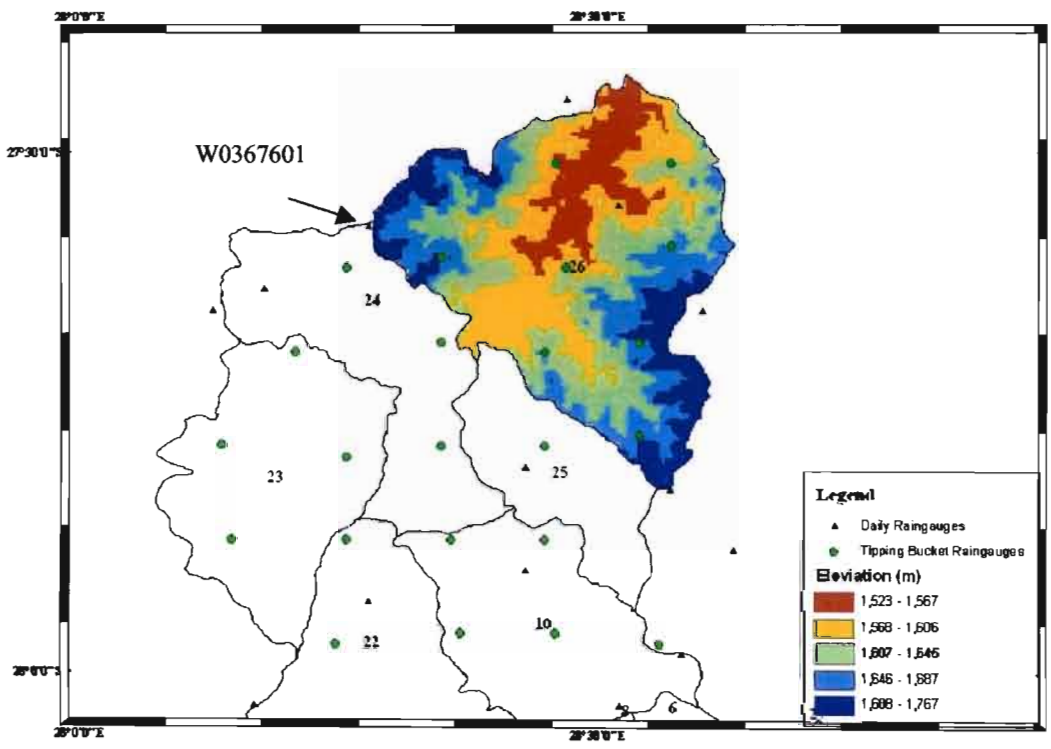

Figure 5.12 Location of Raingauge 0367601W and altitude map of Subcatchment 26

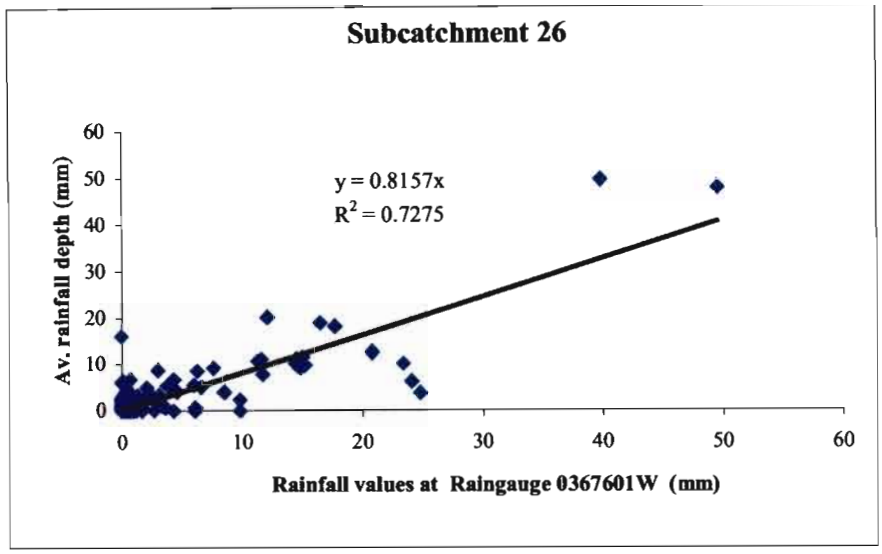

Figure 5.13 Relationship between average subcatchment rainfall depths derived from the merged rainfall and a raingauge (0367601W) selected to represent rainfall in Subcatchmnet 26

The relationship of $y = 0.8157x$ ($R^2 = 0.7227$) between the spatially average merged daily rainfall depth for Subcatchment 26 and rainfall recorded at Raingauge 0367601W indicates that the measured rainfall overestimates the areal rainfall of the subcatchment. The spatial distribution of rainfall within the Subcatchment 26 is relatively uniform as shown in Figure 5.14, where the time series of standard deviation of rainfall on each day over the subcatchment is shown, and where the majority of days have a standard deviation of less than 10 mm. The spatial uniformity of the rainfall over the subcatchment implies that there is little or no orographic effect on the spatial distribution of the rainfall. Although the area of Subcatchment 26 is relatively large as shown in Table 4.1, the spatial rainfall distribution of the subcatchment is relatively uniform as shown in Figure 5.14. Therefore, the reason that rainfall at Raingauge 0367601W overestimates the average merged values for Subcatchment 26, could be due to the fact that raingauge is located at a higher altitude, (1672 m) above sea level, compared to most part of the subcatchment, (1645 m).

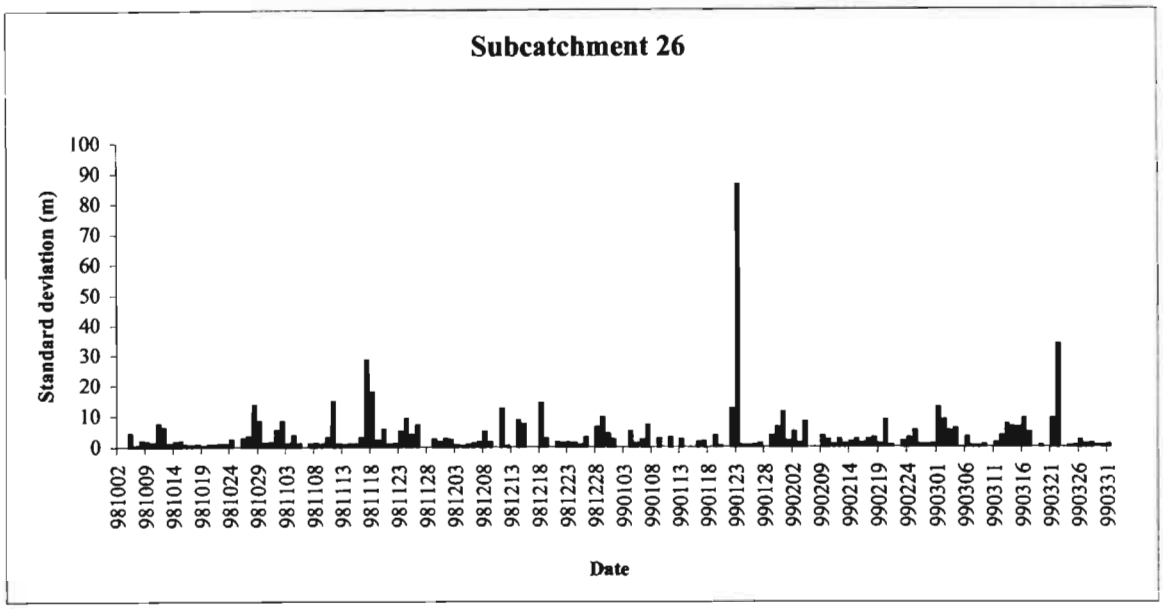

Figure 5.14 Standard deviation of the spatial distribution of daily rainfall within Subcatchment 26

The radar images show that in certain areas there are consistently high or unrealistic values, which could be caused by ground clutter or by other problems related with radar rainfall measurement. Ground clutter is caused by a radar beam, or the side lobes of the radar beam, colliding with the ground at some point and the result is a strong echo which could be interpreted as an intense rainfall cell on Constant Altitude Plan Position Indicators (CAPPI) (Clothier and Pegram, 2002). The radar images consistently show the effect of ground clutter in the Lesotho Mountains, which is outside of the Liebenbergsvlei catchment. Unrealistically high rainfall values lead to a loss of information in the scaling process during conversion of radar images to MDV format.

In the Subcatchment 26, high or unrealistic rainfall values are clearly evident on the image for 23 January 1999 as shown in Figure 5.15 and Figure 5.14. On that day the mean average radar rainfall for the Subcatchment 26 is 16 mm with a maximum pixel rainfall of 712 mm, while the raingauges inside the subcatchment did not record any rainfall. Similarly, on 28 January 1999 and 20 March 1999 no rainfall was registered for the Subcatchment 26 by the radar and hence the merged rainfall pixels inside the subcatchment are automatically set to zero. When the values of

the above days are removed and a graph of mean rainfall of the subcatchment is plotted against the gauged values, the result of the relationship improved to $y = 0.8272x$; $R^2 = 0.7717$, as shown in Figure 5.16.

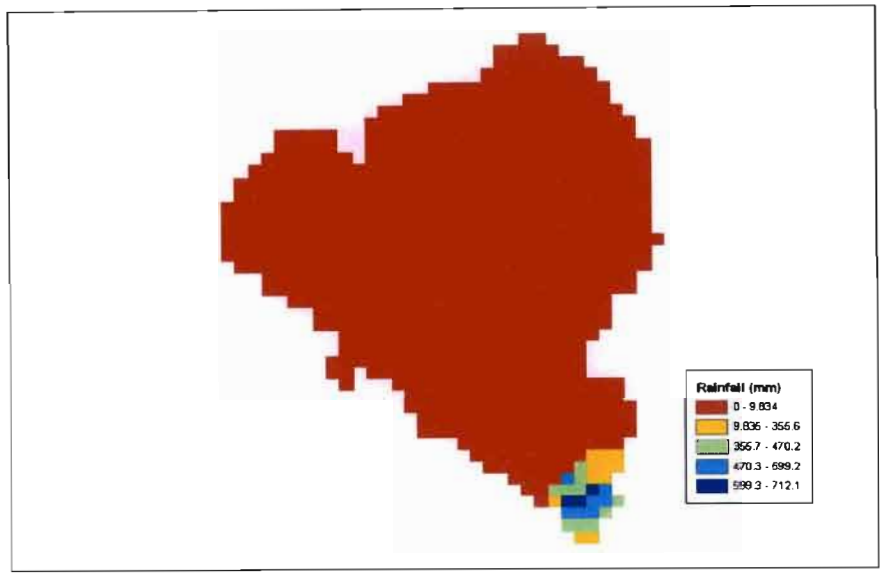

Figure 5.15 Spatial rainfall distribution of rainfall in Subcatchment 26 on 23 January 1999

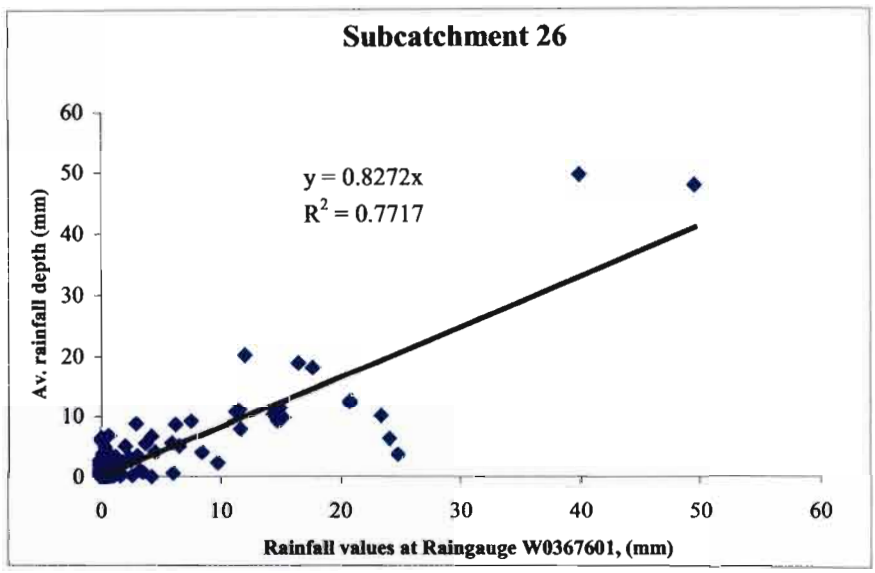

Figure 5.16 Improved relationship between average rainfall depth from merged rainfall field and a representative raingauge rainfall data in Subcathcment 26 after removal of erroneous rainfall caused by ground clutter

Figure 5.17 shows a merged rainfall image for Subcatchment 26 for 7 October 1998, which demonstrates the spatial distribution of rainfall in Subcatchment 26. The image shows that a heavy rainfall storm was restricted to a small area on that day while a relatively uniform and light rainfall fell in the rest of the subcatchment. This illustrates the limitation of using a raingauges, which may be located in an area which generally receives more or less rainfall that the rest of the subcatchment, to represent the areal rainfall of the subcatchment. However, the spatial rainfall distribution also fluctuates with time and the general spatial distribution of rainfall over a subcatchment over a period of time is important when selecting a representative raingauge for the subcatchment.

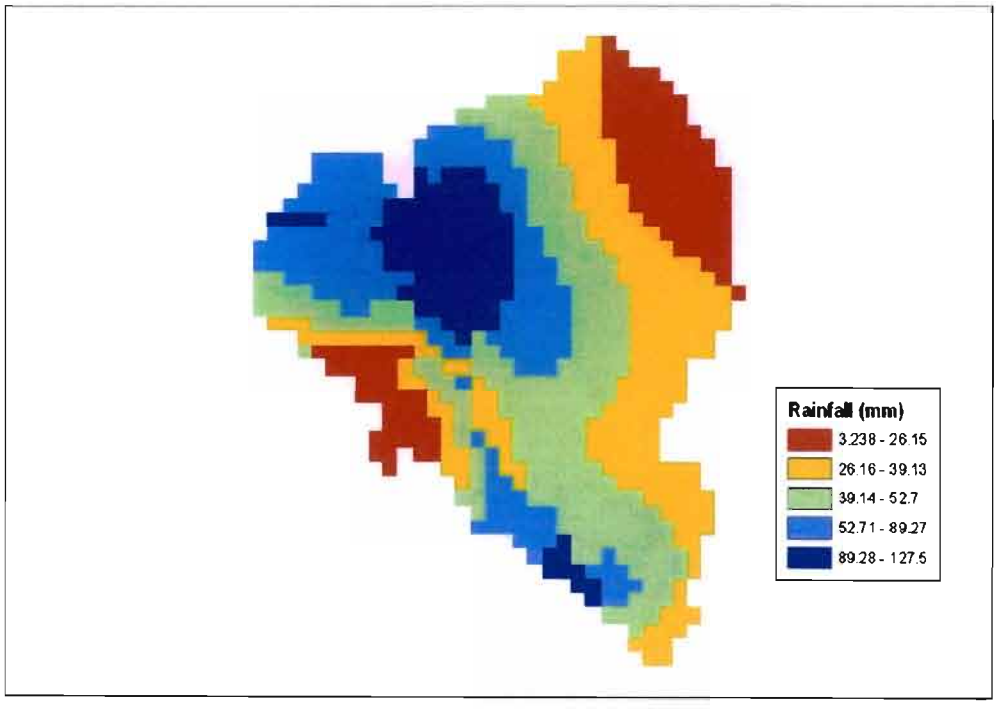

Figure 5.17 Spatial rainfall distribution of rainfall in Subcatchment 26 on 7 November 1998

5.4. Summary of Regressions

In this section the relationship between gauged rainfall at a point and mean areal rainfall of the subcatchment is summarised. Section 5.3.3 contains the relationship between point raingauges located inside Subcatchment 26 and the mean areal rainfall of the subcatchment. The result show

that the raingauges represent the mean areal rainfall satisfactory well, however as it is explained above, Subcatchment 26 is relatively flat compared to other part of the Liebenbergsvlei catchment. Therefore, spatially averaged rainfall values over other subcatchments of Liebenbergsvlei catchment may not be well represented by the point raingauges. Table 5.2 summarises the relationship between both tipping bucket and daily raingauges and the mean areal rainfall over subcatchments.

Table 5.2 Summary of results of relationship between point rainfall data and mean areal rainfall of the subcatchments

Subcachment	Tipping bucket raingauges	Daily Raingauges	X- coefficient (a)	Correlation $-R^2$
1	L008		0.6303	0.3839
2	L008		0.7618	0.5256
	L013		0.7961	0.6984
		0332284W	0.8308	0.5810
3	L013		0.7202	0.5616
4	L012		0.8125	0.8045
		0332104W	0.7438	0.7467
5	L012		0.6996	0.6505
		0332104W	0.6857	0.7061
		0332073W	0.6653	0.6185
6	L021		0.7523	0.7270
		0332066W	0.8803	0.4809
7	L016		0.9388	0.6962
8	L017		1.0558	0.9058
		0332066W	1.2578	0.8219
		0332098W	0.9615	0.7558
9	L016		0.4337	0.8120
		0331845W	0.5124	0.7141
10		0367802W	1.0615	0.7830
11				
12				
13				
14	L001		0.7937	0.7137
15	L010		0.9056	0.7942
16	L015		1.0820	0.7021
17	L045		0.9365	0.8074
18	L045		1.0551	0.7073
19	L004		0.9679	0.8135
20	L005		0.9104	0.7474
		0331590W	0.8578	0.7683
21	L009		1.3507	0.8561
		0331585W	1.0545	0.7723
22	L022		0.6660	0.5685
	L019		0.8677	0.6686
		0331607W	0.9176	0.7217
23				
24	L031		0.6626	0.7865
	L038		0.7781	0.6641
		0367462W	0.7318	0.6247
25	L032		0.7884	0.8740
		0367768W	0.7330	0.6519
26	L036		0.7103	0.8113
	L042		0.8230	0.8996
		0367666W	0.7696	0.7659

As shown in Table 5.2, in most of the cases the point rainfall data represent the areal rainfall of the subcatchments reasonably well and the gauged rainfall generally overestimates the mean areal subcatchment rainfall by between 5% to 50%. Subcatchment 1 has very small area (6.26 km^2) and there is no raingauge data located inside the perimeter of the subcatchment. It has a relatively high variability in the spatial distribution of rainfall as it located in the higher altitude part of Liebenbergsvlei catchment. As consequences none of the raingauges located around of the subcatchment satisfactory represent the mean areal rainfall of the subcatchment. Subcatchments 11, 12 & 13 are located in the very mountainous part of the Liebenbergsvlei catchment and are highly susceptible to ground clutter of the radar image.

In most of the subcatchments, excluding Subcatchments 1, 11, 12 and 13, rainfall measured by raingauges located in and near to the subcatchments generally represents the mean areal subcatchment rainfall reasonably well. However, the representation of the mean areal rainfall of the subcatchment by a raingauge varies between subcatchment. As mentioned in Section 5.3.3, the spatial rainfall distribution of the rainfall in a subcatchment is the main factor which affects the relationship.

Included in Appendix B are the standard deviations of the spatial distribution of rainfall for each subcatchment, averaged on a daily basis, to determine the effect of the spatial distribution of rainfall on the relationship between gauged rainfall data and mean merged areal rainfall of the subcatchment. In all the subcatchments, the standard deviation of spatial rainfall distribution is variable from one day to another. Subcatchment 13 has a high standard deviation of the spatial distribution of rainfall for most of the days considered on this study, while Subcatchments 10, 11 and 12 have relatively higher standard deviations compared to most other subcatchments. Another important factor to the relationship between the point and mean areal rainfall of the subcatchments is the location and altitude of the raingauges.

The spatial and temporal characteristics of the rainfall at the location of the raingauges in reference to the characteristics of averaged areal rainfall of the subcatchment is an important factor to the relationship of the point rainfall and mean areal rainfall. Figure 5.18 shows that there is no clear linear trend between average rainfall variation and subcatchment size or standard

deviation of altitude. The spatially averaged rainfall variation within each subcatchment, and each subcatchment's proportional area of Liebenbergsvlei catchme, are shown in Figure 5.18 for each subcatchments of Liebenbergsvlei catchment. Figure 5.18 also includes standard deviation of subcatchment altitude plotted using the right hand side axis.

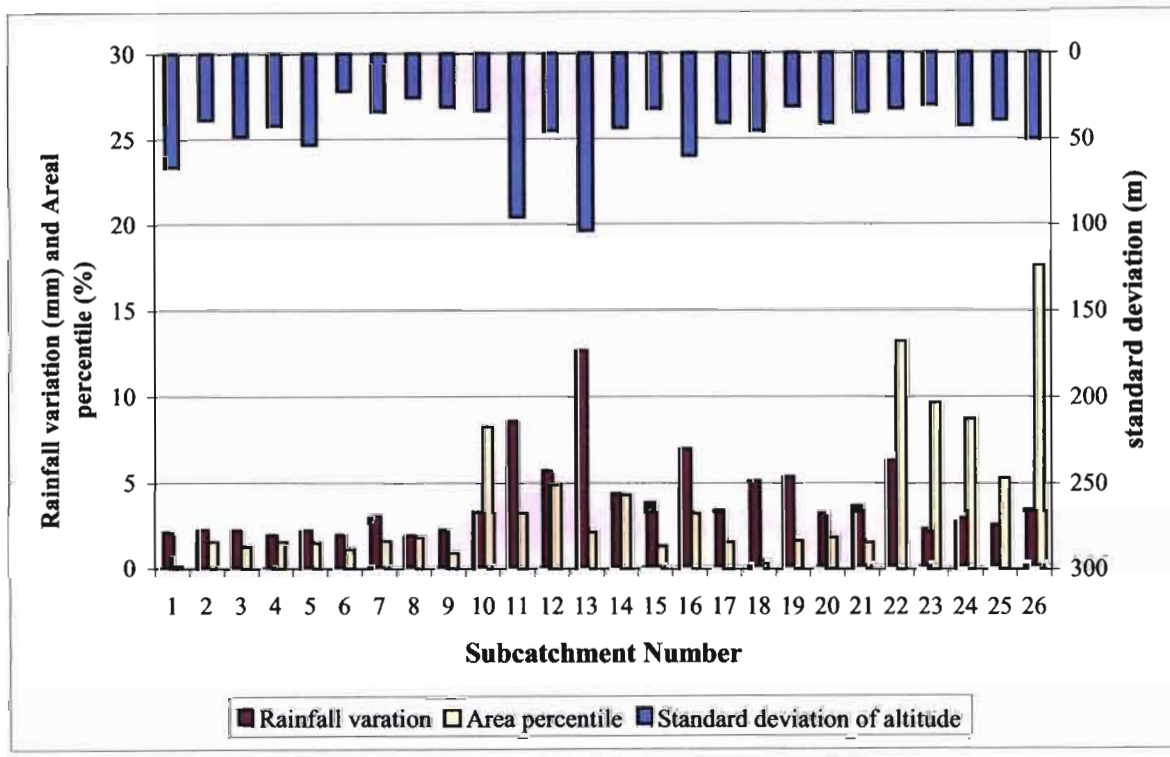

Figure 5.18 Average rainfall variation and average standard deviation of altitude of each subcatchment of Liebenbergsvlei catchment and each subcatchment's proportional area of Liebenbergsvlei catchment

First category is Subcatchments 1 to 9 which have similar average rainfall variation where the subcatchments are located at higher altitude of Liebenbergsvlei catchment and flow into same river route. There is no big difference between their areas except for subcatchment 1. Subcatchment 7 has a higher average rainfall variation, while its standard deviation and area is not higher than the other 8 subcatchments. The second category is Subcatchment 14 to 21 also located at higher altitude part of Liebenbergsvlei catchment. Their size varies while they have similar average standard variation of altitude except for Subcatchment 16 as a consequence have

higher average rainfall variation. The third category is Subcatchment 10, 22, 23, 24, 25 and 26 which are located at the flat part of Liebenbergsvlei catchment and as result they are larger in size. They have similar average standard deviation and similar average rainfall variation except for Subcatchment 22 which could be due to the quality of radar rainfall measurement. It is hard to conclude anything, as there is no trend in the relationship between the standard deviation of altitude, rainfall variation and area of the subcatchment. However it is clear that spatial rainfall distribution is a function of standard deviation of altitude, subcatchment area and altitude.

The relationships between selected daily raingauges and the average merged rainfall depth for the subcatchments in Liebenbergsvlei catchment are generally good as shown in Table 5.2 and Appendix B, with correlation coefficients generally larger than 0.5 for most subcatchments. In most subcachments the use of a daily raingauge to represent the rainfall for a subcatchment overestimates the average areal rainfall depth of the subcatchment. The relationships obtained are largely dependent on the spatial variation of rainfall over the subcatchments and the location and altitude of the daily raingauges. An ideal perfect relationship $(Y = x; r^2 = 1)$ between the daily raingauges and average rainfall depths of the subcatchments can only be obtained under a condition of perfect spatial uniformity of daily rainfall over the subcatchments.

The spatial variation of rainfall over the subcatchments on each day influences the relationship between the daily raingauges and the average rainfall depth over the subcatchments. In areas with uniform rainfall, or with no spatial variability, the relationship between rainfall data from daily gauges and the mean rainfall values of the subcatchment is expected to be good. However, the spatial distribution of rainfall measured within a subcatchment is not uniform and hence the relationship between point rainfall and average catchment rainfall is dependent on the extent of the spatial variability of rainfall. The spatial distribution of rainfall is variable between subcatchments and hence it is not possible to derive a single relationship between gauged rainfall data and subcatchment rainfall which is applicable for all the subcatchments.

* * *

In this chapter the rainfall merging technique developed by Sinclair (2004) and merged rainfall fields are developed for the subcatchments in the Liebenbergsvlei catchment. The merging process is verified against raingauge data used in the merging and is also tested independently against raingauges not used in the merging process.

In the next chapter the String of Beads stochastic rainfall model is used to generate long daily sequence of rainfall values and the characteristics of the synthetic rainfall are compared to the characteristics of the daily rainfall data inside the Liebenbergsvlei catchment.

6. GENERATION OF STOCHASTIC RAINFALL FOR DESIGN FLOOD ESTIMATION USING THE STRING OF BEADS MODEL

Stochastic hydrology is used to generate synthetic streamflow or rainfall sequences that are statistically similar to observed streamflow or rainfall sequences. Statistical similarity implies sequences that have statistics and dependence properties similar to those of the historical record. Therefore, stochastic rainfall generated by rainfall models is designed to mimic the statistics of the observed rainfall data. Stochastic rainfall values should also mimic the observed spatial and temporal variability of rainfall in a catchment and the synthetic rainfall values may be generated at finer spatial and temporal details than the observations (Siriwardena *et al.*, 2002).

Continuous simulation modelling of the hydrologic system requires long-term, high-resolution climate data and, with the continuing advances in stochastic rainfall models, continuous simulation is rapidly becoming a practical tool for hydrological risk assessment and hydraulic engineering designs (Kuczera and Coombes, 2002). In this study, the String of Beads model (Clothier and Pegram, 2002) was selected to generate stochastic rainfall values. The model was selected for evaluation because it was developed locally, and hence was easily availabile, and the ability to produce rainfall values at 1 km x 1 km and 5 minutes spatial and temporal resolutions respectively.

The String of Beads Model (SBM) is a high-resolution space-time model of radar rainfall images. It is a stochastic model that takes advantage of the detailed spatial and temporal information captured by weather radar and combines it with the long term seasonal variation captured by a network of daily raingauges.

Clothier and Pegram (2002) modelled the alternating wet-dry process, or event arrival and duration, as a one-dimensional process, while the detailed wet process is modelled as a three-dimensional (two space and one time) process at 1 km and 5 minute spatial and temporal resolutions respectively, over an area of 16000km^2, which is consistent with the images from the observed radar data. The three-dimensional rainfall events distributed on a one-dimensional time line is analogous to a "String of Beads" (Clothier and Pegram, 2002).

The SBM makes use of a combination of power law numerical filtering techniques and well-known time series models to achieve an efficient algorithm that can be run on a desktop personal computer. Model output is in the form of image files which, when viewed as an animated sequence, are difficult to distinguish from observed radar rainfall images (Clothier and Pegram, 2002). Apart from the realistic appearance of these images, when calibrated to daily raingauge data for a region, analysis of the simulated sequences over periods of up to ten years reveal convincing rainfall statistics for a wide range of spatial and temporal scales. It can be used both as a simulation tool and as a short term forecasting tool (Clothier and Pegram, 2002).

In simulation mode, the SBM can quickly produce long sequences (tens of years) of 128 x 128 km rainfall images at a 5 minute temporal and 1 km spatial resolution. Such simulations can be used as input to distributed and semi-distributed hydrological models to produce "what if" scenarios for applications in water resources management and flood risk assessment, amongst others (Clothier and Pegram, 2002).

According Clothier and Pegram (2002) the SBM has proved effective in producing real time forecasts of up to two hours making it a useful tool for flood warning and management, particularly in steep or urban catchments where fast hydrological responses frequently give rise to flash floods. The SBM can also be used in a combined simulation-forecasting mode to quickly produce many short term "what if" scenarios which can be used to assess the risk of possible storm growth or decay scenarios in real time.

6.1. Structure of the String-of-Beads Model

There are three main stages of rainfall simulation in the SBM and these correspond to the event scale, the image scale and pixel scale statistics. The event, image and pixel scales refer to a rainfall event, radar or equivalent rainfall image and a pixel that stores a rainfall rate for a particular time. The event scale statistics describes the arrival and duration of a rainfall event, as well as the temporal behaviour of the image scale statistics during a rainfall event. The image scale simulation concerns the one dimensional time series of the Wet Area Ratio (WAR_i), Image

size were extracted using ArcGIS software. All the simulated images were converted to grids and all values were extracted using ArcInfo tools (c.f. Chapter 4).

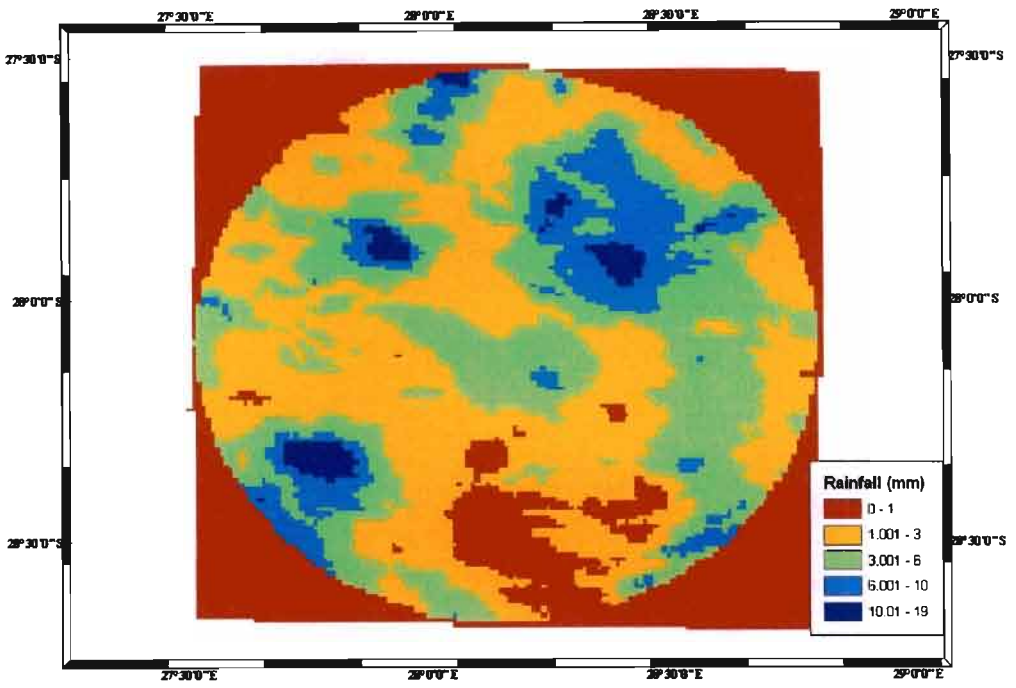

Figure 6.1 Daily rainfall image generated by String of Beads Model

6.3. Statistical Parameters for SBM Evaluation

The String of Beads model is designed to generate rainfall images that simulate the combined statistics of data from the 54 raingauges located inside Bethlehem study area and within the spatial extent of the rainfall images from MRL-5 radar at Bethlehem. As the radar rainfall values for Bethlehem do not extend beyond 1996, Clothier and Pegram (2002) decided to use only the available historical data from raingauges for the temporal structure of the model. Therefore, the temporal structure of the SBM is based on the long record of daily rainfall data and the spatial structure of the model is correlated according to the radar images of the area.

Mean Flux or average rainfall rate (IMF_i) and β_{space} (exponent of a radially averaged, two dimensional power spectrum in space) image scale statistics. The pixel scale simulation concerns the spatial distribution of rainfall on the simulated images.

SBM first stage- Event scale simulation

Two independent sets of event scale statistics are pseudo-randomly generated in this first stage of the simulation, i.e. the event cumulative advection vector and the event arrival, duration and intensity statistics.

Event arrival, duration and intensity

According to Clothier and Pegram (2002), in the SBM the wet and dry spells are alternately sampled from two mutual independent processes, following the ideas of Haberlandt (1998). The principal component in the simulation of the wet spell duration (D_w) and its complementary dry spell duration (D_d) is an alternating renewal process. With only a short record of high temporal resolution data available, the seasonal variation in the wet-dry process is simulated with use of only the long-term dataset available, i.e. the daily raingauge data.

Haberlandt (1998) found that the lognormal distribution and gamma distributions were well suited to describing the distribution of wet spell durations in Germany and Clothier and Pegram (2002) showed that this is also true of the dry spell durations in South Africa and also that there is very little difference between the fitted gamma and lognormal approximations of these distributions. Therefore, they selected a lognormal distribution for SBM, for sake of simplicity.

SBM second stage- image scale simulation

The second stage of simulation uses the event scale parameters, output by the first stage, to generate pseudo-random time series of image scale parameters for each event. Three image scale parameters are required in order to simulate a single image and these are the β_{space}, the WAR_i and the IMF_i. A bivariate autoregressive process is applied to simulate the temporal relationship

between the WAR_i and IMF_i. The String of Beads model output at this stage is a continuous time series of image scale statistics. The WAR_i and IMF_i are assumed to be zero during the dry spells and they start and finish for each wet spell with a WAR of 1%.

SBM third stage – pixel scale simulation

The third and final stage of simulation accepts the event advection and image scale parameters output by the first and second stages and simulates 128 x128 km, two-dimensional images at the pixel scale, consistent with those parameters. The SBM uses a univariate autoregressive and two-dimensional power-law filtering process in this last stage of simulation to combine the three processes, which are the pixel scale temporal process, the field advection process and the pixel scale spatial process. The first is designed to manage the temporal behaviour at the pixel scale between consecutive images. The second is to introduce the advection component of the event. The third is to impose the required spatial structure on individual images.

6.2. Data Representation

Synthetic rainfall values were generated using the SBM, calibrated using the Bethlehem radar and Liebensbergvlei catchment, which made available by Clothier (2004). The model provided generates rainfall images with integer values and generates real (floating point) IMF values at the image. The input required for the String of Beads simulation is the duration of the simulation, the date when simulation starts, the simulation stop date and random seeds. The rainfall image produces by the String of Beads model has a 64 km radius and the model was calibrated by Clothier (2004) the study area near Bethlehem (Figure 6.1). The model can generate rainfall images at an increment of 5 minutes, 1 hour, daily, monthly and yearly. However, in this research only daily, monthly and yearly images were produced.

Daily values were extracted from the generated images at pixel size and image scale to compare the statistics with the available historical raingauge data. IMF or rainfall values at image scale for all time scales (daily, monthly and yearly) are output after the simulation, while values at pixel

In this study and because only a 6 month period of radar images were available, the statistics of the generated images at image and pixel scale were compared to the statistics of the raingauges in the Bethlehem study area. The daily, monthly and annual rainfall totals for the 54-raingauges inside the Bethlehem study area were extracted from Clothier (2004) and these are compared with image scale statistics of the generated images to evaluate the temporal statistics of the images.

According to Siriwardena *et al.* (2002) a key requirement in stochastic data generation is that the synthetic sequence be statistically consistent with the observed characteristics of the historical record. There are different statistical parameters used for evaluation of stochastic rainfall models at different time scale. These include parameters from the following list:

Annual statistics

- Mean annual rainfall
- Standard deviation of annual rainfall
- Coefficient of skewness of Annual rainfall
- Serial correlation (lag-one correlation)
- Maximum annual rainfall (standardised by mean)
- Mean 2-year, 5-year and 10-year low rainfall sums
- Minimum annual number of wet days
- Standard deviation of annual number of wet days

Monthly statistics

- Mean monthly rainfall
- Standard deviation of monthly rainfall
- Coefficient of skewness of monthly rainfall
- Serial correlation of monthly rainfall
- Maximum monthly rainfall (standardised by mean)
- Mean monthly number of wet days

Daily statistics

- Mean daily rainfall (wet days) for each month
- Standard deviation of daily rainfall (wet days) for each month
- Coefficient of Skewness of daily rainfall (wet days) for each month
- Mean daily rainfall for solitary wet days for each month (WET 1)
- Mean daily rainfall for wet days bounded only on one side by a wet day (WET 2)
- Mean daily rainfall for wet days bounded on both sides by wet days (WET 3)

6.4. Evaluation of the SBM

The SBM was evaluated at Bethlehem area, where the model was calibrated by Clothier (2004) and the results are presented in the Sections 6.4.1 to 6.4.3.

6.4.1. Annual Statistics

At the image scale, the statistics of a 50-year period of generated rainfall was compared against statistics computed from the observed rainfall data at 54 raingauges located in the study area. Table 6.1 contains the statistical comparison between the two rainfall series.

Table 6.1 Comparison between SBM generated and observed annual rainfall statistics at the image scale

	Mean (mm)	Standard deviation (mm)	Coefficient of Skewness	Kurtosis	Lag-one auto-correlation	Mean annual number of wet days
Generated	545.2	90.7	-0.034	-0.56	-0.12	198
Observed	654.0	108.0	0.300	-0.03	0.17	313

The generated rainfall images underestimate the mean annual rainfall and standard deviation by 17% and 16% respectively. The differences in the coefficients of skewness, which are a measure of the degree symmetry in the distribution of a variable, implies that the observed rainfall values are skewed above the mean observed rainfall while the generated rainfall values are more symmetric than the observed with rainfall data with only a slightly negative skewed distribution.

Kurtosis is a measure of degree of peakdness or flatness in the variable distribution and both the observed and generated distributions have a flatter distribution than a normal distribution.

Figure 6.2 shows that average annual rainfall total of the 54-rain gauges for a 50 year period of record from 1948 to 1997 and with values ranging from slightly over 900 mm to just below 500 mm.

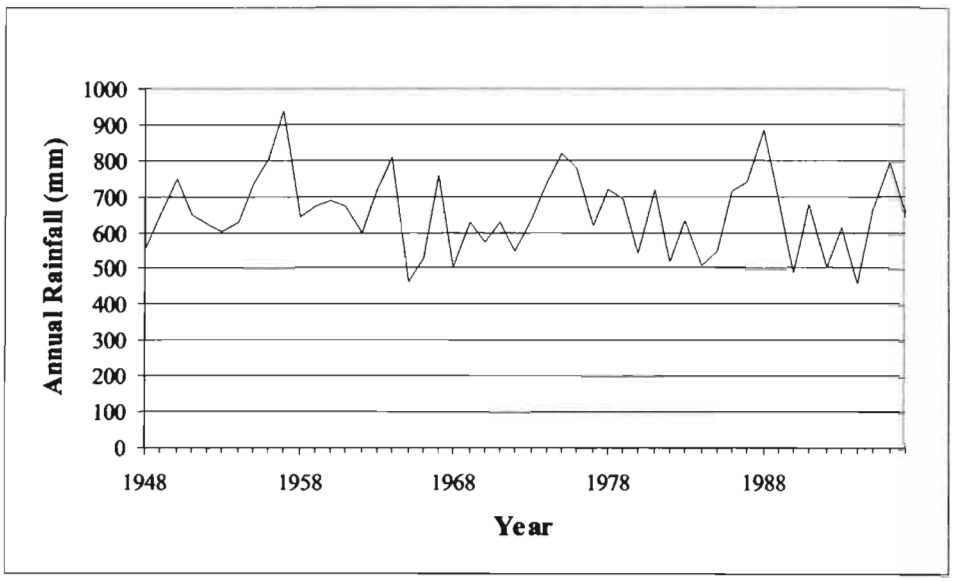

Figure 6.2 Observed average annual total rainfall (Clothier, 2004)

Figure 6.3 shows the average annual rainfall totals of the generated rainfall images for a 50 year period of records. The maximum value is 745 mm and the minimum value is 336 mm. The serial correlations of the generated and observed annual series indicate that the structure of the generated annual series is poor. Other significant difference between the two series of annual rainfall totals is that there are no values exceeding 800 mm in the generated rainfall images and there are values which are less than 400 mm, which do not occur on the observed series.

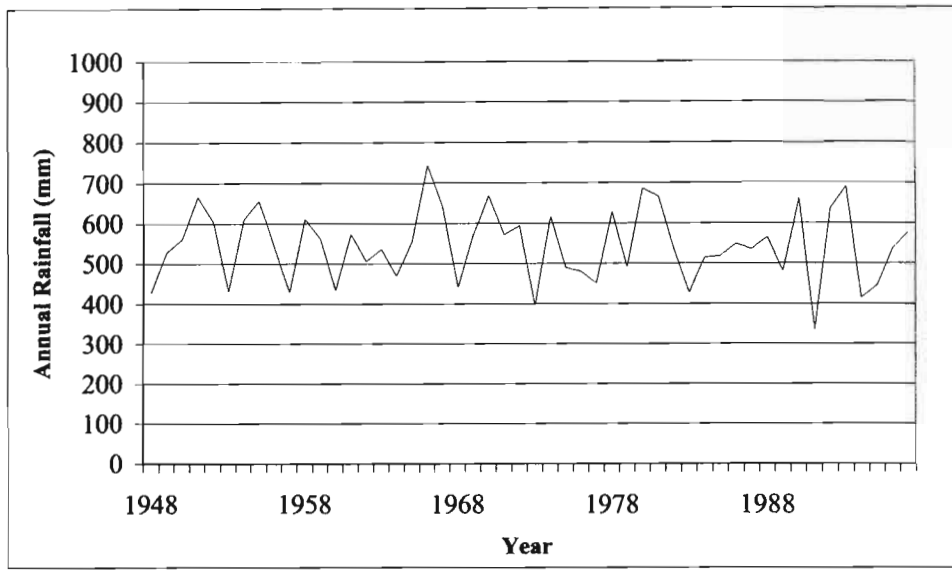

Figure 6.3 Generated average annual total rainfalls

At the pixel scale, raingauges were selected inside the Liebenbergsvlei catchment and compared with a pixel rainfall value from generated rainfall images at the same position as the raingauges. The statistical comparison between the generated and observed rainfall series is summarised in Table 6.2.

Table 6.2 Statistical comparison between SBM generated and observed annual rainfall at pixel scale

Raingauges		Mean (mm)	Standard deviation (mm)	Coefficient of Skewness	Kurtosis	Lag-one auto-correlation	Mean annual number of wet days
0297721W	Generated	506.9	129.8	1.16	1.68	-0.008	79.5
	Observed	720.4	163.7	0.26	-1.11	0.098	102.8
0331271W	Generated	514.7	129.6	0.04	-0.15	-0.174	78.2
	Observed	641.8	152.1	0.53	0.09	-0.011	86.4
0331385W	Generated	506.9	132.6	0.87	0.45	-0.270	80.4
	Observed	673.5	129.1	0.14	-0.84	0.074	129.6
0331402W	Generated	511.4	141.2	0.36	-0.20	-0.238	78.6
	Observed	630.3	112.9	0.21	-0.47	0.164	115.4
0331455W	Generated	542.6	133.8	0.33	-0.15	0.016	78.7
	Observed	720.6	168.0	0.53	-0.24	0.285	107.8
0331467W	Generated	507.9	145.5	0.87	0.31	-0.141	79.9
	Observed	626.7	128.2	0.59	-0.30	0.276	129.4

In all cases the generated mean rainfall at the pixel scale underestimates the observed annual mean raingauge values. The observed rainfall data are more variable than the values generated by the SBM. Although both the selected raingauge data and the generated rainfall series at a pixel have positive coefficients of skewness, the values are not the same. The generated annual rainfall series at the image scale is generally flatter than the observed rainfall data from the 54-raingauges while at a pixel scale the generated rainfall values are more variable in their degree of peakedness. In general, the observed rainfall data in the Liebenbergsvlei catchment are not consistent in terms of their peakedness with some raingauges have sharper peaks than a normal distribution and other flatter peaks. Similarly, the generated rainfall values at the pixel scale are also not consistent in terms peakedness. Moreover, Table 6.2 consistently shows that both series do not have similar serial correlation. As well the mean annual number of wet days is continuously underestimated on the generated series.

6.4.2. Monthly Statistics

Monthly totals are the next temporal scale and a statistical comparison was made between the generated and observed rainfall series. The statistical comparison between the two rainfall series at the image scale is summarised in Table 6.3.

Table 6.3 Statistical comparison between SBM generated monthly rainfall and observed monthly rainfall at image scale

		Jan	Feb	Mar	Apr	May	Jun	Jul	Aug	Sep	Oct	Nov	Dec
Mean Monthly (mm)	Generated	100.60	72.50	69.40	46.00	11.70	2.30	4.00	4.70	20.60	50.90	75.90	89.20
	Observed	105.00	82.00	78.00	50.00	22.00	8.00	8.00	16.00	30.00	70.00	88.00	99.00
Standard dev. (mm)	Generated	46.60	32.3	28.7	20.20	9.80	4.90	6.80	6.60	15.50	27.80	33.40	35.40
	Observed	42.00	39.00	33.00	27.00	22.00	10.00	14.00	21.00	39.00	38.00	37.00	36.00
Coefficient of skewness	Generated	3.20	2.54	2.15	1.49	0.35	0.09	0.12	0.16	0.67	1.69	2.53	2.86
	Observed	1.00	1.00	1.50	0.50	2.00	2.50	1.75	1.60	3.40	1.00	0.50	0.25
Lag-one auto-correlation	Generated	0.67											
	Observed	0.69											

Both the mean monthly and standard deviation of the observed rainfall is reasonably well generated by the SBM, particularly for the wetter months; however, the generated series consistently underestimated the mean monthly observed rainfall data. The smaller differences in the monthly lag-one serial correlations show that the SBM reproduced the monthly rainfall statistics better than the annual statistics. Figure 6.4 shows the monthly rainfall statistics from 54 raingauges over the period of 50 years.

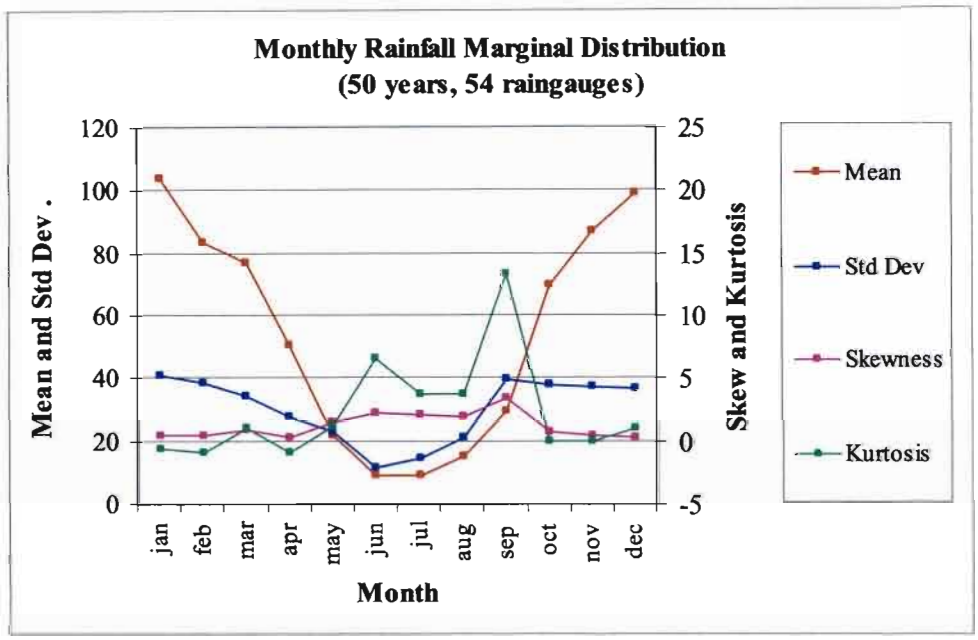

Figure 6.4 Observed monthly rainfall distribution over 50 years period (after Clothier 2004)

There is a significant seasonal variation in the rainfall at Bethlehem. Of the dryer months, it is apparent that September is prone to occasional large monthly totals. The mean of 29.7 mm, standard deviation of 39.5 mm, skewness of 3.4 and kurtosis in excess of 13.3 for September are reduced to 22.6 mm, 18.7 mm, 1.4 and 1.9 respectively if the two extreme events of 1957 and 1987 are excluded (Clothier, 2004). Figure 6.5 shows an equivalent graph to Figure 6.4, which is a SBM generated monthly rainfall distribution for a 50 years period. Figure 6.5 show that the generated mean monthly rainfall values follow the statistical trend of the observed monthly rainfall distribution. However, the other statistics do not follow the statistics of the observed monthly rainfall values as well.

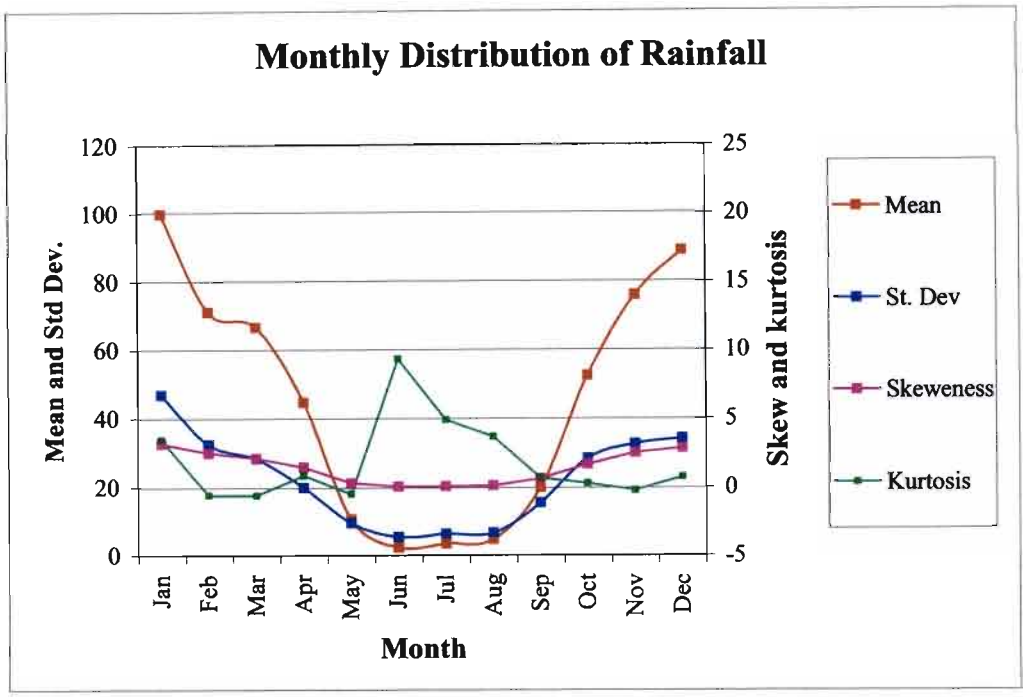

Figure 6.5 SBM generated monthly rainfall distribution over 50 years period (1948-1997)

6.4.3. Daily Statistics

Figure 6.6 contains the frequency distribution for the observed average daily rainfall in the study area. In Figure 6.6, five series are plotted, one for each season and one for the combined analysis considering all of the days, independent of the season. The dry winter season is clearly defined with a probability of observing any rain in the study area of 21%. By contrast, the probability of receiving any rain in the study area on a summer day is 88%. Autumn and spring probabilities are between those of summer and winter, as expected. Spring shows a larger probability of high daily rainfall than autumn over most of the range, but particularly between the 98.0 and 99.5 percentiles (Clothier, 2004). Figure 6.7 shows the frequency distribution of the generated average daily rainfall values in the study area. For the generated series there is a 10% of probability for any rain during the dry winter season. Moreover, the probability of receiving rainfall in the summer season is 75 %, which indicates that the probabilities of generated rainfall occurring for any rainfall amount are less than the probabilities in the observed rainfall series.

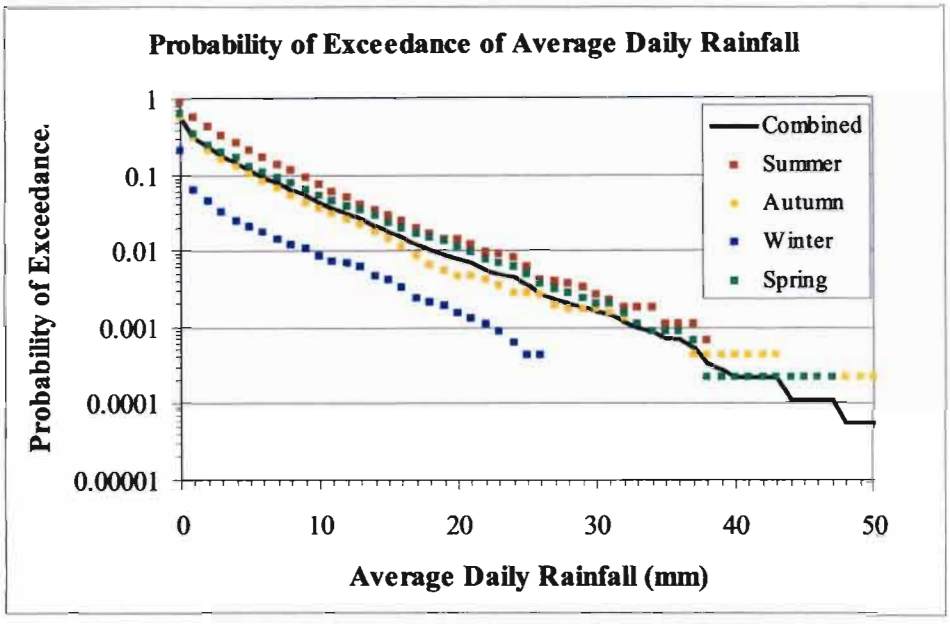

Figure 6.6 Probability of exceedance of observed average daily rainfall over a 50 year period (after Clothier, 2004).

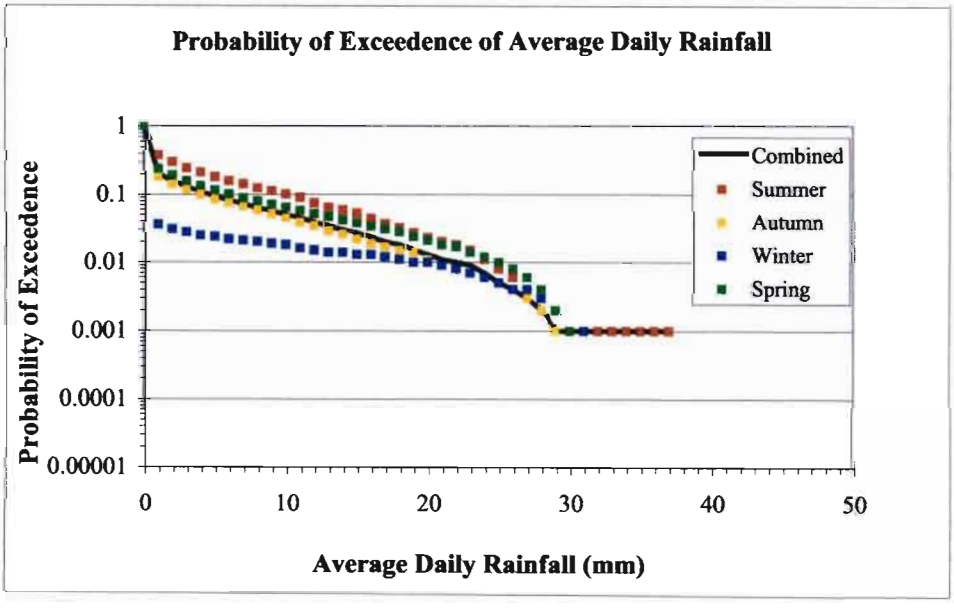

Figure 6.7 Probability of exceedance of generated average daily rainfall over a 50 year period

The statistical comparison between the observed and generated daily rainfall series over a 50 year period at the image scale is summarised in Table 6.4. The SBM is a short duration rainfall model and is expected to give a better result on daily basis than on monthly or annual periods. The generated mean rainfall values reproduce the observed rainfall mean reasonably well. However, as shown in Table 6.4 and Figures 6.8 and 6.9 the SBM generates fewer wet days over the 50 year period than the number wet days in the observed data and assigns more rainfall to the wet days.

Table 6.4 Statistical comparison between SBM generated daily rainfall and observed daily rainfall at image scale

		Jan	Feb	Mar	Apr	May	Jun	Jul	Aug	Sep	Oct	Nov	Dec
Mean Daily rainfall (mm)	Generated	3.24	2.45	2.24	1.53	0.38	0.08	0.13	0.15	0.69	1.64	2.53	2.88
	Observed	3.39	2.90	2.52	1.67	0.71	0.27	0.26	0.52	1.00	2.26	2.93	3.19
Mean daily Rainfall on wet days (mm)	Generated	11.64	11.47	11.76	11.55	10.41	12.91	12.35	9.31	10.64	11.42	11.37	11.53
	Observed	8.85	8.00	8.97	8.33	8.15	9.30	8.00	10.00	10.48	9.59	8.31	8.61
Number of Wet days	Generated	431	302	295	199	56	9	17	25	97	223	334	387
	Observed	593	512	435	300	135	43	50	80	143	365	529	575
Lag-one Autocorrelation	Generated	0.680											
	Observed	0.714											

Unlike the case for annual periods, the lag-one autocorrelations computed from the generated and observed daily series are similar.

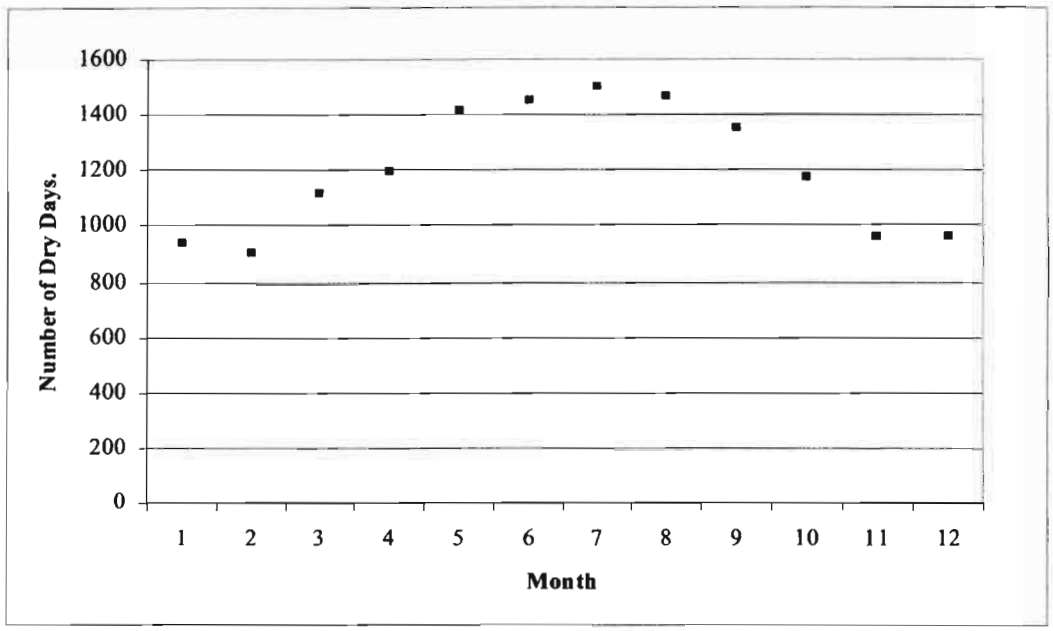

Figure 6.8 Number of observed dry days on each month over the 50 year period (after Clothier, 2004)

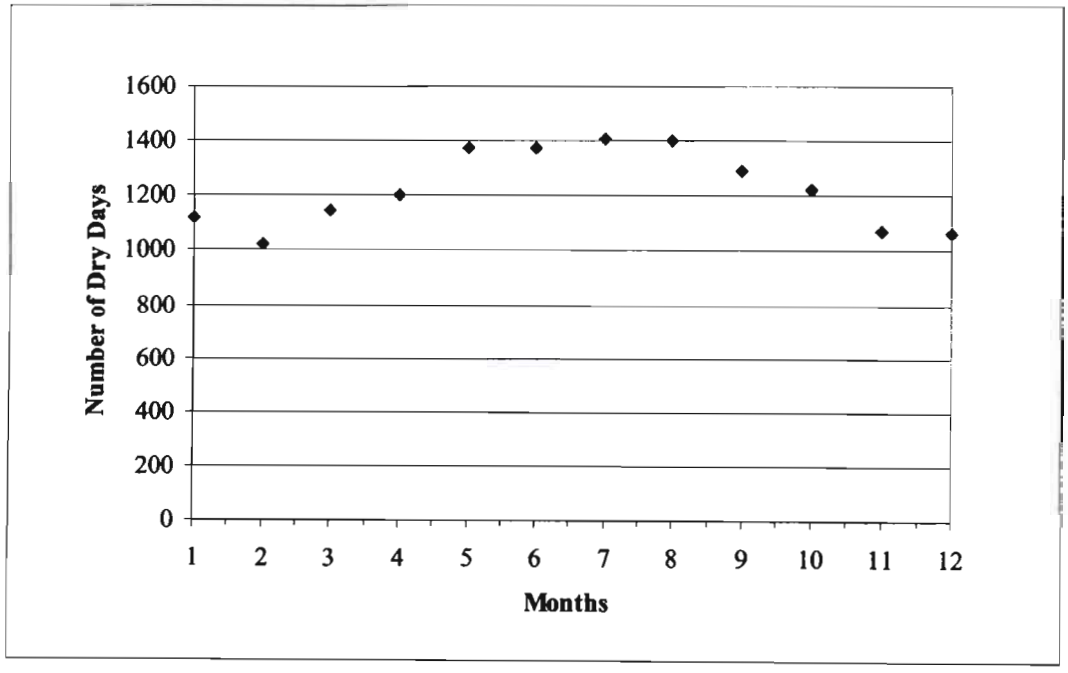

Figure 6.9 Number of generated dry days on each month over 50 year period

The number of dry days in the generated 50 years series follows the trends in the observed data, although the numbers are not exactly the same. The SBM generated almost the same number of dry days in April to June, underestimated the number of dry days during winter (July-September) and overestimated the number of dry days during the summer months (October – March).

The statistics of the generated daily rainfall values were compared with statistics computed from daily raingauges data at both pixel scale and image scale50 year periods. The statistical comparison between the two rainfall series at a pixel scale is summarised in Table 6.5.

Table 6.5 Statistical comparison of SBM generated and observed daily rainfall at a pixel scale

Raingauges		Daily Mean Rainfall (mm)	Number of Wet Days	Daily Mean Rainfall for Wet Days (mm)
0297721W	Generated	1.39	2419	10.48
	Observed	1.97	3130	11.50
0331271W	Generated	1.41	2379	10.80
	Observed	1.76	2629	12.21
0331385W	Generated	1.39	2448	10.35
	Observed	1.84	3945	8.54
0331402W	Generated	1.40	2393	10.67
	Observed	1.73	3514	8.98
0331455W	Generated	1.48	2396	11.27
	Observed	1.97	3281	10.98
0331467W	Generated	1.40	2433	10.5
	Observed	1.71	3939	7.96
0331474W	Generated	1.41	2416	10.69
	Observed	1.78	2674	12.13
0331554W	Generated	1.39	2416	10.49
	Observed	1.73	2867	11.01
0331585W	Generated	1.37	2400	10.50
	Observed	1.67	4347	7.02
0331590W	Generated	1.41	2407	10.71
	Observed	1.69	3797	8.15
0331607W	Generated	1.39	2371	10.71
	Observed	1.87	5181	6.58
0331704W	Generated	1.42	2429	10.69
	Observed	1.69	3713	8.34
0331828W	Generated	1.40	2422	10.59
	Observed	1.88	3442	9.99
0331843W	Generated	1.39	2394	10.60
	Observed	1.61	3356	8.75
0331850W	Generated	1.36	2433	10.17
	Observed	1.56	4325	6.59

Table 6.5 shows that SBM generated rainfall at the pixel scale underestimate the number of wet days over the 50 year period and, at most sites considered, the mean daily rainfall for wet days are bigger in the generated series than in the observed daily rainfall data. The observed mean daily rainfalls are always greater than the generated mean daily rainfall when the all days are considered.

Generally, the SBM reproduced the observed statistics at a daily time scale reasonably well and better than at monthly or annual time scales. The SBM is a short duration rainfall model designed to mimic rainfall values at a detailed temporal and spatial resolution. Hence, small errors at 5 minutes durations accumulate over longer durations to the errors evident at the daily and longer time scales. Spatially, the SBM reproduced the statistics of the selected raingauges considered in this study. The spatial structure of the SBM is designed on the basis of radar images for a 4 year period (1996- 2000) and the observed rainfall from 54 raingauges, while the temporal structure is based solely on the observed rainfall data from the 54 raingauges. Therefore, the quantitative inaccuracy of radar images, compared to the raingauges, may influence the generated rainfall values at pixel size with the raingauge data over the 50 year period.

In this chapter, it was shown that the SBM could reproduce rainfall values better at daily time scales than at monthly or annual periods. Therefore, it is concluded that an appropriately calibrated SBM may be used in rainfall-runoff modelling which requires rainfall at detailed spatial and temporal resolutions. When the rainfall model is required at monthly or yearly time step it is advisable to use model which are designed for monthly and annual time step (e.g. Stochastic Generation of Annual rainfall data by Srikanthan and McMahon. (2001)).

* * *

In this chapter and in Chapter 5, the String of Beads stochastic rainfall model and the merging of information from radar and raingauges are discussed respectively to improve and obtain detailed temporal and spatial rainfall information for long time series. Continuous simulation streamflow models require detailed information of catchment properties and rainfall; and current rainfall measuring instruments either provide rainfall data for long periods of record but with no spatial

detail (raingauges) or good spatial information with less quantitative accuracy and for short periods of record (radar and satellites). The next chapter uses the results acquired in Chapter 5 to simulate streamflow and to compare the results against streamflow simulated using a conventional "driver station" approach. The conventional "driver station" approach is currently used in the ACRU model, where a selected raingauge, with corrections to the data, is used to represent the area rainfall of a subcatchment.

7. STREAMFLOW SIMULATION

"Spatial and temporal variability in meteorology (wind speed, humidity, radiation, and temperature), soils (hydraulic conductivity, porosity, water retention, topography and thermal properties), and vegetation (stomatal resistance, leaf area index, albedo, and root depth) interact in a highly non-linear manner to produce complex heterogeneity in soil moisture, runoff, and evapotranspiration. It is well established that variability in rainfall is among the most important cause of variability in soil moisture and runoff"(Ghan *et al.*, 1997).

The interaction of the distribution of rainfall, both in space and time, and antecedent soil moisture patterns play a major role in the generation of streamflow. Antecedent soil moisture conditions are a consequence of rainfall, evporation and soil characteristics. Therefore, detailed information on the variability of rainfall is important, as it is the major factor in defining streamflow variability. Physically-based hydrological models are used to simplify and simulate the complex relationship between antecedent soil moisture, rainfall and streamflow.

In areas where streamflow is not recorded or the spatial density and period of recorded streamflow are insufficient for the estimation of design floods, design floods are frequently estimated using a rainfall-based approach. In this chapter the physically-based, daily time step *ACRU* agrohydrological simulation model (Schulze *et al.*, 1995) is used to assess the simulation of streamflows in response to spatial rainfall estimated using a conventional "driver-station" approach and an approach which incorporates the merging of the gauged and radar rainfall data.

7.1. Continuous Simulation Model using the ACRU Model

The accuracy of areal rainfall estimated from point measurements depends on the representativeness of the point measurements, the spatial variability of the rainfall (Nicks and Hartman, 1966), the size of the catchment, the duration of rainfall as well as the method used to estimate the areal distribution from the point measurements. Among these techniques, two approaches are recommended by Schulze *et al.* (1995) for estimating daily subcatchment rainfall

and these are the driver station approach and trend surface approach, also termed the ACRU-300 approach. Currently, the driver station approach is the recommended method for use with the ACRU model.

The driver station approach is a technique, which uses a "driver" station to represent a rainfall over a catchment or subcatchment. The "driver" station should be selected to ensure that the selected station is (Schulze *et al.,* 1995):

- as close as possible to, or within, the subcatchment,
- at an altitude similar to the subcatchment's mean altitude, and
- has a long continuous rainfall record with a minimum of missing or suspect data.

The merged rainfall data contain detailed information on the spatial distribution of rainfall for a short period of record while the gauged daily rainfall data contain long periods of record at a particular location. Hence combining these sources of rainfall information has the potential to improve the estimation of subcatchment rainfall for long periods of record.

7.2. Spatial Rainfall Representation

Rainfall for each subcatchment was estimated using two approaches. In the first approach, termed the "Conventional Driver Station" (CDS) approach, areal rainfall for each subcatchment is represented in the *ACRU* model by adjusting data from a selected point rainfall station. The adjustment coefficients, which are input for each month, are derived by dividing the mean monthly rainfall of the gauged rainfall data by the mean monthly rainfall of the centroid of the subcatchment. The rainfall data for the centroid are calculated from the raingauges around the centroid. The raingauge selected to represent the areal rainfall of the subcatchment is selected on the basis of distance from the centroid of the subcatchment under consideration, the length of the reliable data, and the differences in altitude and mean annual precipitation between the raingauge and the centroid of the subcatchment.

In the second approach to estimate subcatchment rainfall, the raingauge values were adjusted using the correction factors for each month derived from the relationship between the 6-months of daily merged rainfall values (October 1998 to March 1999) for the subcatchment and the selected raingauge, as described in Chapter 5. This approach is referred to as the "Modified Driver Station" (MDS) method.

ACRU is a physically-based, daily time step agrohydrological simulation model which was selected for use in this study because it was developed for South Africa and is also relatively widely use in South Africa. Detailed soil, land cover and monthly temperature information were extracted for each subcatchment of Liebenbergsvlei catchment from the South African Atlas of Agrohydrology and Climatalogy (Schulze *et al.*, 1996). Daily maximum and minimum temperatures for the centroid of each subcatchment were used to represent the maximum and minimum temperature for the subcatchments. The same soil, land cover and evaporation information was used in streamflow simulations using both the CDS and MDS rainfall as input.

ACRU is not a parameter fitting or optimising model, which needs to be calibrated to observed flow. Generally variables are estimatedfrom physical properties (Schulze *et al.*, 1996).

Table 7.1 contains the selected driver rainfall stations, tipping bucket raingauges and daily raingauges used in each subcatchment for simulation of streamflow and the correction factors for both the CDS and MDS methods. Although both the conventional and modified driver raingauge approaches use monthly adjustment factors, annual correction factors were used in this study to modify the driver raingauge data as the 6 months of available merged rainfall data did not allow the calculation of monthly factors and, for comparison, annual factors are shown for the CDS approach. The annual correction factor for driver rainfall stations were derived using mean annual rainfall, while the correction factor for the raingauges used in the modified method were derived from the 6 months of merged rainfall values, as described in Chapter 5.

Table 7.1 Selected driver rainfall stations with their correction factors for the Conventional and Modified Driver Station approaches for each subcatchment in the Liebenbergsvlei catchment

Subcatchment	Conventional Driver rainfall Station Approach		Modified Driver Rainfall Station Approach		
	Station	Annual Correction factor	Tipping Bucket Raingauge	Daily Raingauge	Correction Factor used
1	0332349W	1.03	Same as conventional*		
2	0332349W	1.03	L008		0.76
3	0332104W	1.02	L013		0.72
4	0332073W	1.02	L012		0.81
5	0332073W	1.03	L012		0.69
6	0332066W	1.14	L021		0.75
7	0332073W	0.85	Same as conventional*		
8	0332066W	1.00		0332066W	1.25
9	0367768W	1.02	Same as conventional*		
10	0367802W	0.98		0367802W	1.06
11	0332349W	1.04	Same as conventional*		
12	0331828W	1.01	Same as conventional*		
13	0297721W	1.01	Same as conventional*		
14	0331828W	0.98	L001		0.79
15	0331560W	0.78	L010		0.91
16	0331607W	0.89	L010		0.95
17	0331474W	0.98	L045		0.94
18	0331474W	1.01	L045		1.06
19	0331560W	1.00	L004		0.96
20	0331560W	0.98	L005		0.91
21	0331554W	0.97	L009		1.35
22	0331455W	0.95		0331607W	0.91
23	0367256W	1.08	Same as conventional*		
24	0367432W	0.91		0367432W	0.73
25	0367768W	0.98		0367768W	0.73
26	0367666W	0.94		0367666W	0.76

* In Subcatchments 1, 7, 9, 11, 12, 13 and 23 no definite relationship between the mean merged areal rainfall and point rainfall either from tipping bucket raingauges or daily raingauges was obtained and hence the adjustment factor for the modified approach is the same as that used for the conventional approach

The CDSs are selected based on their availability of data fro the required period, their closeness to the subcatchment under consideration, consistency of their MAP and altitude with the subcatchment MAP and mean altitude. While the tipping buckets and daily raingauges selected for the modified approach were selected on the availability of data for the period from 1995 to 1999 and on the strength of the relationship between raingauge values and the merged areal rainfall for the subcatchment.

7.3. Verification of Simulated Streamflow

There are three flow gauging weirs in the Liebenbergsvlei Catchment, as shown in Figure 4.1. According to Midgley *et al.* (1994), data from gauge C8H009 are not reliable, while data from Gauge C8H026 are not available for the required period. Gauge C8H020 does have continuous streamflow data for the required period. However, from the data for the period of 1998 to 1999, it is evident that there is water pumped into the catchment from upstream of the Liebenbergsvlei catchment as part of an inter-catchment transfer from the Lesotho Highlands Water Scheme. As a consequence, the verification of the simulation streamflow was performed using only observed streamflow data from Gauge C8H020 for the period from January 1995 to December 1996.The observed streamflow for this period are reliable and realistic. Simulated and observed runoffs for this period are shown in Figures 7.1 and 7.2 and the associated summary statistics are contained in Table 7.2.

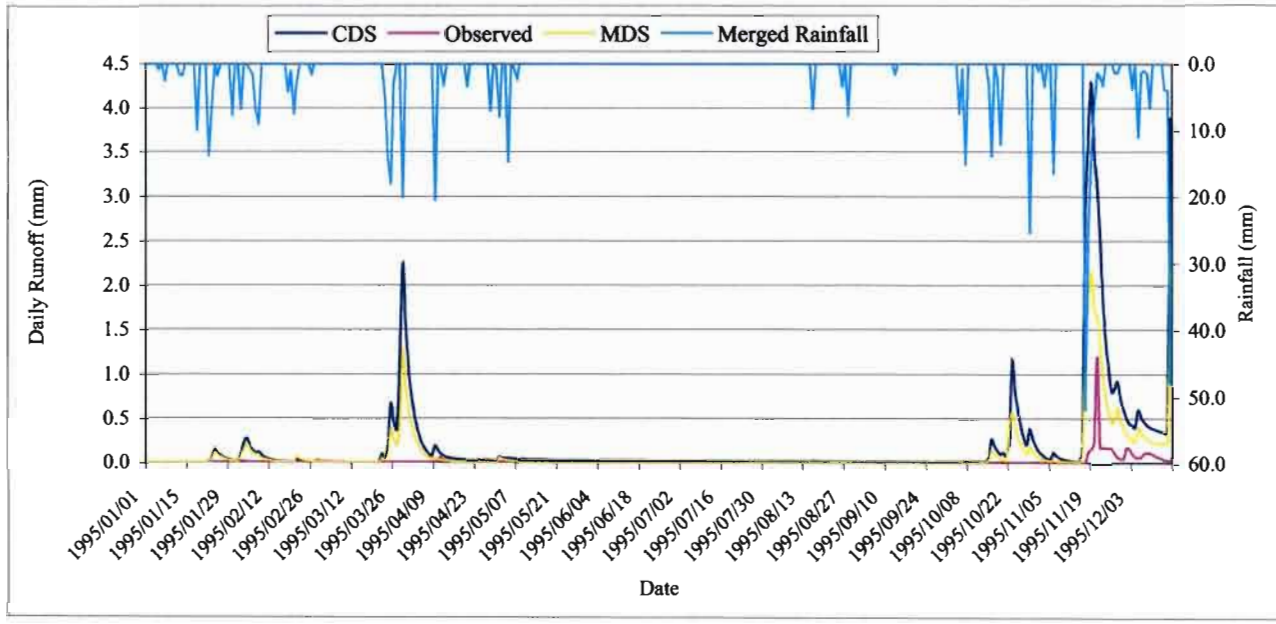

Figure 7.1 Simulated and observed daily streamflow at Gauge C8H020 for 1995

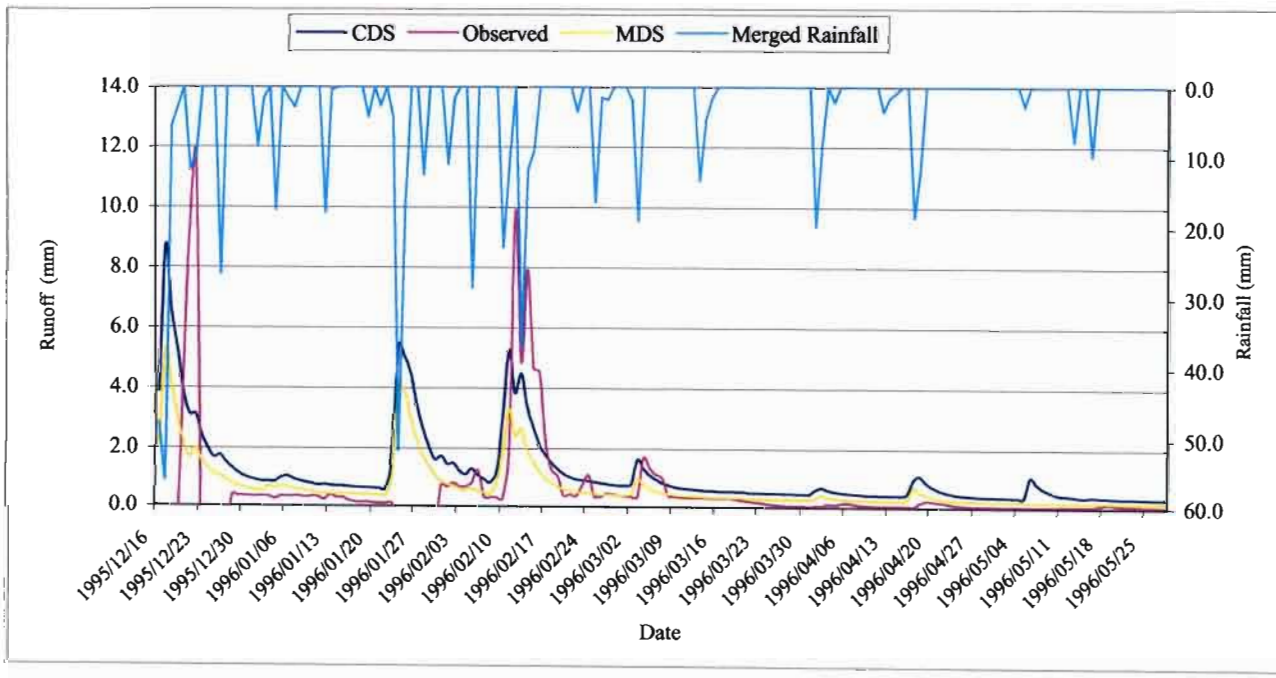

Figure 7.2 Simulated and observed daily streamflow at Gauge C8H020 for 1996

Table 7.2 Daily simulated and observed streamflow statistics at Gauge C8H020 for 1995 and 1996

	Merged Annual Rainfall at Subcatchment 24		Observed Runoff		Simulated runoff using Conventional Driver Stations (CDS)		Simulated runoff using Modified Driver Stations (MDS)	
Year	1995	1996	1995	1996	1995	1996	1995	1996
Total (mm)	631.03	764.33	30.97	84.35	102.18	155.64	63.80	109.26
Mean (mm)	1.73	2.08	0.08	0.23	0.28	0.43	0.17	0.30
Median (mm)	0.00	0.00	0.12	0.05	0.93	0.27	0.66	0.19
Standard Deviation (mm)	6.04	6.12	20	37	61	25	26	15
Coefficient of Skeweness	5.84	4.06	7.41	5.43	4.73	4.44	5.08	5.24
Kurtosis	41.60	19.87	60.50	34.98	27.40	28.81	32.90	40.75
Maximum (mm)	56.24	51.68	4.73	5.43	7.09	4.78	4.88	4.33
Minimum (mm)	0.00	0.00	0.00	0.00	0.00	0.00	0.00	0.00

From Table 7.2 it is evident that the simulated streamflow exceeds the observed streamflow and that more streamflow is simulated by the conventional driver station approach compared to the modified driver station approach. With respect to the shape of the streamflow distribution for 1995, the observed variance, coefficient of skewness, kurtosis and maximum values are a lot closer to the respective values simulated using the MDS approach than when subcatchment rainfall was estimated using the CDS approach, the CDS uses the annual correction factor to adjust the driver raingauge data to the centroid rainfall data. However, for 1996 where the observed streamflow has some missing data, the variance, kurtosis and maximum of the CDS method simulated streamflow closer to the observed than the MDS method. The coefficient of skewness is better simulated in MDS than the CDS simulated streamflow. The streamflow simulated using both the methods significantly overestimated the observed streamflow. The poor simulation of the streamflow could be due to error in recording of observed streamflows or inappropriate configuration and/or parameterisation of the *ACRU* model. For example, in the configuration used, the wetland routines were not invoked to simulate the wetland in the catchment.

A comparison between the simulated streamflow, estimated using the CDS and MDS approaches is shown in Figure 7.3 for the period from January 1995 to December 1999 at the location of Gauge C8H020. From the relationship obtained, it is evident that the streamflow generated using the MDS method is only 71 % of the streamflow generated the CDS method. The rainfall

correction factors used in *ACRU* to correct the driver station in order to more adequately represent the subcatchment areal rainfall are derived from the ratio of mean monthly rainfall at the centriod of the subcatchment and the value at the driver rainfall station. The centriod of the subcatchment rainfall may not always be representative the subcatchment areal rainfall and it can only have a 1:1 relationship with the areal rainfall of the subcatchment when the spatial rainfall distribution over the subcatchment is perfectly uniform on all the days under consideration. While the probability of the centroid subcatchment rainfall to be representative the subcatchment areal rainfall is strong, the same probability exists for any other location in the subcatchment. Therefore, the monthly corrections applied to conventional driver station rainfall values may not always result in an improved relationship between the conventional driver station rainfall and subcatchment areal rainfall. Any corrections factor applied to a point rainfall should be derived from the relationship of the point mean monthly rainfall and the best estimate mean monthly areal rainfall of the subcatchment.

The correction factors applied to the gauged rainfall in the MDS method were derived from only 6 months of merged rainfall values, as explained in Chapters 4 and 5. More reliable factors would be derived if longer periods of radar and tipping bucket rainfall data were available.

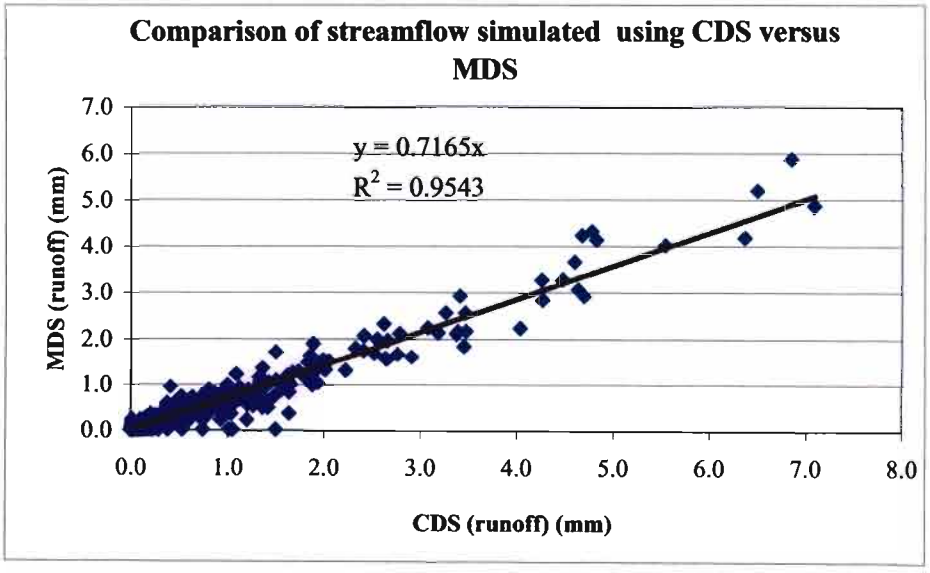

Figure 7.3 Comparisons between streamflow simulated at Gauge C8H020 using the CDS and MDS rainfall estimation methods

The ideal situation would be to have detailed merged areal rainfall for the subcatchment for the required period of record. However, as explained in the previous section there are only limited historical rainfall records with detailed spatial and temporal information. Raingauges provide long sequences of rainfall data for a point while radar and satellites can provide more spatial information of rainfall, but with less accuracy and, currently, only for a limited period of time. If longer lengths of the merged rainfall values were available to relate the merged rainfall values with the point rainfall values on monthly or seasonal bases, than more confidence in the results could be attained.

Despite the limited length of the merged rainfall values used in this study, the results show that there is a significant difference between streamflow simulated using the CDS and MDS approaches. Ideally streamflow should be simulated using spatially detailed mean areal rainfall information of the subcatchment if there are no recorded streamflow data. However, this is not always available for all areas and for all the required periods. As discussed in Chapter 5, the mean areal rainfall of the subcatchment is best estimated by merging rainfall information from the raingauge, radar and satellite data. Hence the raingauge data selected to represent a subcatchment should be compared with the best estimate areal rainfall values of the subcatchment, to check if there is a good correlation between the areal rainfall and point rainfall. In CDS method which is frequently used with the ACRU model, the point rainfall is selected by comparing with the raingauge data to the mean rainfall at the centriod of the catchment and which may not be representative of the general rainfall in the catchment.

7.4. Driver Stations Vs Merged Rainfall Values

The driver rainfall stations corrected by monthly correction factors (i.e. CDS method) were compared against the merged areal rainfall values for each subcatchment for the 6-months period when the merged rainfall values are available. Figure 7.4 (a) and (b) show the comparison of uncorrected and corrected (CDS) rainfall values of the Raingauge 0367432W against the merged areal rainfall values for the Subcatchment 24. In this case, the adjustment of the gauged rainfall depths results in a better estimate of the "true" spatial rainfall field, depicted by the merged rainfall values. However, this is not always true as shown in Figure 7.5 (a) and (b), where the

unadjusted rainfall values of the driver rainfall station have a better relationship with the merged areal rainfall in Subcatchment 16.This could explain that centroid rainfall data do not always represent better the subcatchment mean rainfall than the raingauges in and around the subcatchment.

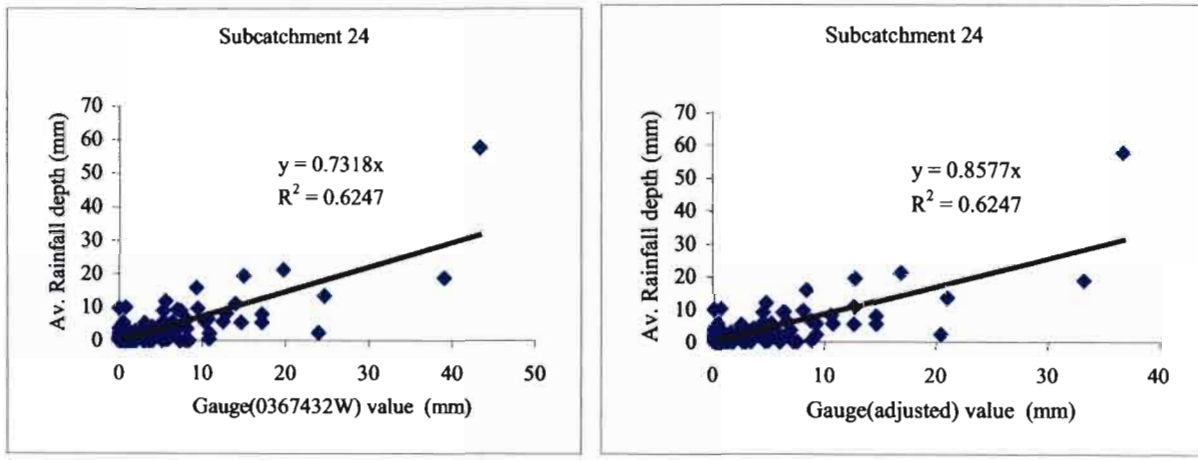

(a) (b)

Figure 7.4 Comparison of merged areal rainfall values against (a) measured rainfall at Station 0367432Wand (b) adjusted (CDS) rainfall in Subcatchment 24

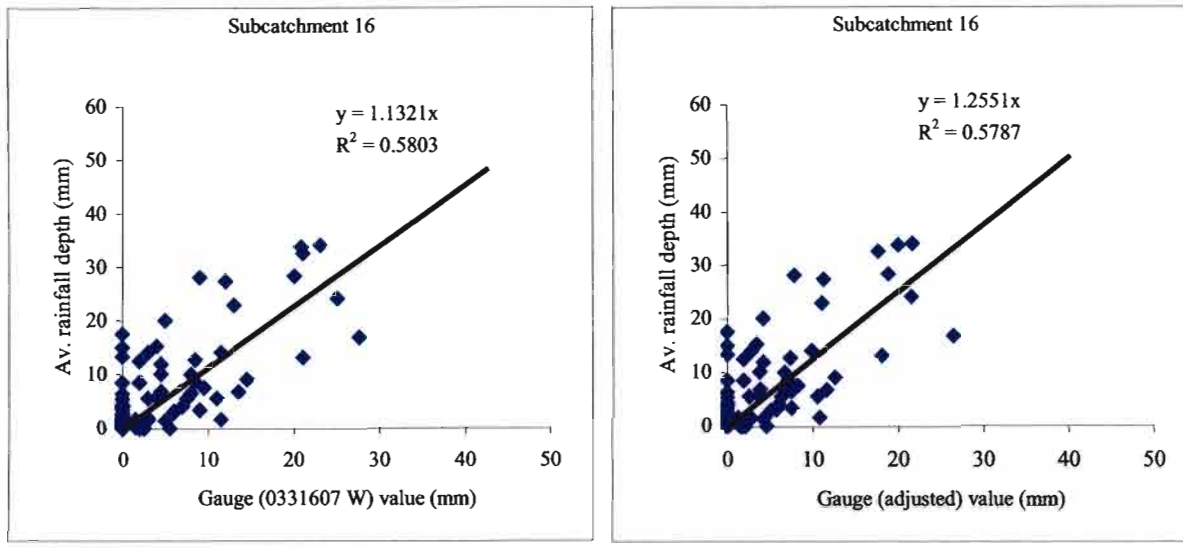

(a) (b)

Figure 7.5 Comparison of merged areal rainfall values against (a) measured rainfall at Station 0367432Wand (b) adjusted rainfall in Subcatchment 16

Table 7.3 compares the measured and adjusted point rainfalls of the daily raingauges selected to represent the mean areal rainfall, using CDS, of the respective subcatchment against the mean merged areal rainfall of the subcatchment for 6 months period developed in Chapter 5.

Table 7.3 Regression coefficients and correlation between both measured and adjusted daily gauge data and merged rainfall values

Subcatchment	Area (km^2)	Station	Measured Rainfall		Adjusted Rainfall (CDS method)	
			X-coefficient	Correlation- R^2	X-coefficient	Correlation- R^2
1	6.26	0332349W	0.3717	0.0463	0.3673	0.052
2	71.65	0332349W	0.4786	0.3166	0.4670	0.320
3	60.31	0332104W	0.5252	0.4579	0.5136	0.458
4	70.65	0332073W	0.6343	0.6415	0.6139	0.638
5	70.11	0332073W	0.6653	0.6185	0.6463	0.629
6	52.65	0332066W	0.8803	0.4809	0.8153	0.441
7	71.52	0332073W	0.4863	0.3029	0.5760	0.268
8	84.86	0332066W	1.2578	0.8219	0.8868	0.570
9	42.04	0367768W	0.4744	0.0585	0.4328	0.063
10	387.14	0367802W	1.0615	0.7830	1.1205	0.780
11	153.36	0332349W	0.4700	-0.1582	0.6271	-0.071
12	230.75	0331828W	0.2120	-0.1306	0.2120	-0.130
13	100.41	0297721W	1.0070	-0.1200	0.9936	-0.120
14	203.31	0331828W	0.1845	-0.1388	0.1912	-0.139
15	55.86	0331560W	0.7023	0.4980	0.9442	0.467
16	151.84	0331607W	1.1321	0.5803	1.2551	0.578
17	73.41	0331474W	0.3418	-0.0530	0.3494	-0.033
18	14.91	0331474W	0.4038	-0.0619	0.4016	-0.075
19	77.84	0331560W	0.7716	0.4896	0.7887	0.467
20	86.38	0331560W	0.7286	0.5992	0.7556	0.581
21	68.42	0331554W	0.8170	0.4483	0.8404	0.460
22	621.46	0331455W	0.7108	0.4914	0.7394	0.495
23	453.08	0367256W	0.3514	0.5886	0.3776	0.577
24	409.63	0367432W	0.7318	0.6247	0.8557	0.624
25	249.10	0367768W	0.7330	0.6519	0.7431	0.631
26	827.34	0367666W	0.7696	0.7659	0.5778	0.590

Not all selected driver stations have a strong relationship with the mean merged areal rainfall of their respective subcatchments as it is showing in Table 7.3. From the results presented in Table 7.3 it is clear that rainfalls measured at a point often do not represent the areal catchment rainfall for the catchment sizes used in this study.

7.5. Summary of Chapter

Streamflow should be simulated from detailed rainfall information, where both the spatial and temporal distribution of rainfall is available for the area under consideration. Radar rainfall information contains the spatial and temporal detail required, but their accuracy is poor compared to rainfall measured at a point by raingauges. Therefore, it is important to merge the rainfall information from these two instruments to provide the best estimate of the "true" rainfall field for the area under consideration, where radar, and raingauge rainfall information are available. Radar and satellites have only recently been used to estimate rainfall in South Africa, and hence are only available for short periods of record. In such cases the merged rainfall information can be related to point rainfall from raingauges to adjust the point rainfall data to better represent the true area rainfall.

Streamflow is a product of an interaction between the antecedent of soil moisture and and the major hydrological driving force of rainfall If the areal rainfall of a catchment under consideration is overestimated in a streamflow simulation, the streamflow will be overestimated. To estimate streamflow accurately for design flood and other hydrological studies, the areal rainfall of the catchment under consideration should be estimated as accurately as possible. In Section7.3, the streamflow simulated using CDS was expected to overestimate the actual streamflow of the catchment, as the measured and adjusted point rainfalls used overestimate the mean merged areal rainfall of the respective subcatchments (cf. Section7.4), which is the best estimate of the "true" areal rainfall of the subcatchments.

In continuous simulation models like ACRU, the mean areal rainfall of a subcatchment under consideration should be estimated as accurately as possible from detailed spatial and temporal rainfall information. Areal rainfall estimated from point raingauges using different interpolation techniques do not provide the best estimate of the mean areal rainfall of the subcatchment and hence, where available, rainfall information from radar and satellite should be used to complement the raingauge rainfall information.

8. DISCUSSION, CONCLUSIONS AND RECOMMENDATIONS

Accurate estimates of design floods are critical to the design of hydraulic structures, risk assessment or water management from dams or reservoirs. As explained in the introduction to this document, rainfall is the main input for design flood estimation at ungauged stream sites. Therefore, accurate measurement of rainfall is important for the estimation of accurate design floods. Traditionally, rainfall has been measured using raingauges, and this is currently the only direct means of rainfall measurement. However, recently radar and satellites have been used as indirect sources for rainfall measurement and they are successful in addressing some shortcomings of raingauges, the most important of which are that the raingauge only measures rainfall at a point and does not adequately represent the spatial distribution of rainfall.

Accurate estimation of design floods from rainfall using continuous simulation modelling (CSM) requires detailed information of the rainfall distribution in space and time for a long period record. Rainfall is highly variable in space and time. Traditional mathematical interpolation techniques have been used to determine the spatial distribution of rainfall over an area from raingauge networks. However, the rainfall fields from these techniques fall short of describing the "true" rainfall fields. Since the introduction of weather radar as a rainfall measuring technique, researchers have been working to develop a meaningful link between the radar estimated and raingauge measured rainfall data. As a result, statistical models have been developed which combine the rainfall fields from the radar and raingauge networks and these rainfall fields represent the highly variable rainfall fields reasonably well. However, the length of record and the spatial coverage are the main limitation of the merged rainfall fields, as the overlapping period of record for the radar and raingauge measured rainfall data is limited and the spatial coverage of the radar information also limited to some regions, especially in a country such as South Africa. Therefore, rainfall models are required which mimic the statistics of the historical rainfall data and transfer the statistics to areas where there is a missing data or no spatial data at all.

Rainfall distribution across a catchment is variable and it is very complex to describe the distribution in one or two statistical functions. With present technology, there is no instrument

which can measure rain that falls over an area unit with 100 % accuracy. This means that the true rainfall field is unknown. However, developments accomplished up to now show positive progress on estimating a "best" rainfall field which represents the true rainfall field reasonably well.

As explained in the above sections hydrological modelling and particularly for the estimation of design floods from rainfall using CSM, requires long series of rainfall record rainfall at fine resolution both in space and time. The rainfall measuring instruments discussed in Chapter 2 do not currently individually provide the required input. Therefore, in order to estimate rainfall at a finer spatial resolution than observed by raingauges, numerous interpolation techniques are discussed in Chapter 3 which provides smooth curves with fine spatial resolution of rainfall. However, smooth interpolation of gauged rainfall generally does not represent the true rainfall realistically over a catchment. Both single-site and multi-site stochastic rainfall models may also be used to generate realistic rainfall series. While single-site models only mimic rainfall values at gauged sites, the multi-site models forge a spatial correlation between sites and allow them to simulate rainfall values at both gauged and ungauged sites. The simulated rainfall fields generated by multi-site models do not necessarily represent the "true rainfall field". Stochastic downscaling and intermediate stochastic models are also are among the numerous techniques discussed in Chapter 3. Stochastic downscaling modelling appears to be the most promising approach to simulate rainfall values both at gauged and ungauged sites using information gathered by raingauges and radar.

Three appropriate options to provide rainfall input to detailed hydrological models can be deduced from the review in Chapter 3.. The first option is to find a meaningful link between the merged fields of radar values and observed raingauge data, and the long series of historical rainfall data. The second option is to simulate a long series of rainfall at gridded sites using the stochastic String of Beads model of Clothier and Pegram (2002) calibrated for the area of interest. The third option is the multi-site rainfall model developed by Wilks (1998) and which can generate rainfall values at gauged and ungauged sites.

The first two options were selected as methodologies assess during this research with the Liebenbergsvlei catchment selected as a study area. The rainfall in the Liebenbergsvlei catchment has been an intensively monitored with 45 tipping bucket raingauges and 34 raingauges located in and around the catchment and it also has full coverage of the MRL-5 radar located near Bethlehem. Six months of radar images, tipping bucket raingauges data from 1995 to 1999 and 50 years of historical daily raingauges data were available and used to assess the two selected methodologies.

As presented in Chapter 5, rainfall data from 45 tipping bucket raingauges and radar rainfall images were merged using a programme developed by Sinclair (2004) which is based on the conditional merging techniques developed by Ehret (2002). The merging technique was validated against tipping bucket raingauges used in the conditioning of the radar images and verified against daily raingauges which were not used to condition the radar images. The conditional merging technique should retain the rainfall values at the raingauges used to condition the radar images. Hence, the relationships between the merged pixel rainfall values at the location of the raingauges were expected to correspond exactly to the observed rainfall values. However, some differences in the merged and observed rainfall were noted at the raingauge sites used in the merging process. This was because the merging technique developed masks the area (i.e. assigns values) where the radar did not register any rain, even though raingauges in the area did report rainfall. This approach was adopted by Sinclair (2004) to avoid false rainfall results in other parts of the area. When the merged pixel values with zero rainfall as a result of the masking process are removed, then the remaining merged pixel values corresponded perfectly with the observed raingauge data. From the verification of the merged rainfall with the tipping bucket raingauges used in the conditioning of the radar images, it is evident that the merging procedure developed by Pegram and Sinclair (2004) successfully assigns rainfall values to the merged pixels from the respective raingauge values used in the conditioning of the radar images.

The merging technique was also independently verified against daily raingauges not used in the conditioning of the radar images. Where a daily raingauge is located close to the tipping bucket raingauges used in conditioning of the radar images then a strong linear regression between the merged pixel rainfall and daily rainfall was expected. Generally reasonably good linear

regressional relationships, where X-coefficient are between 0.8 and 1.2 and R^2 is greater than0.5, were achieved between the independent daily raingauges and merged pixel values at the same location as the daily raingauges. Therefore, the merging technique reasonably reproduce the daily raingauges not used in the conditioning of radar but this could be improve with the improvement of the quality of radar rainfall measurement and denser network of raingauges used in merging process.

Linear regression relationships were developed between the daily raingauges and the mean merged rainfall values of each of the 26 subcatchments in the Liebenbergsvlei catchment. In most of the subcatchments, reasonably strong regressions ($R^2 > 0.5$) were achieved between the daily raingauges and the mean merged rainfall of the subcatchments. However, the raingauges selected to represent the areal rainfall of the subcatchments generally overestimated the mean areal merged rainfall values of the subcatchments by between 5% and 50%. It was noted that in catchments where a relatively uniform spatial rainfall distribution was observed for the 6 month period considered, the relationship between the point rainfalls and mean merged rainfall of the subcatchments was better, thus indicating that the spatial rainfall distribution in a catchment is a major factor determining how well a raingauge can be used to estimate the rainfall in a catchment. In general, rainfall variability across a subcatchment is a function of subcatchment size, standard deviation of altitude and altitude of the subcatchment.

The stochastic String-of-Beads rainfall model developed by Clothier and Pegram (2002) was the model assessed in Chapter 6. The model was calibrated for Bethlehem by Clothier (2004) and a daily rainfall values were generated for a 50 year period. The statistics of daily, monthly and annual periods of the generated rainfall values were compared to the corresponding statistics computed from the historical daily rainfall data from daily raingauges located in and around of the Liebenbergsvlei catchment. At both the image and pixel scale, the model reproduces the daily statistics better than the monthly statistics and, similarly, the monthly statistics were reproduced better than the annual statistics. The String-of-Beads model was designed to generate rainfall values at short durations (5 minutes) and with a fine spatial resolution (1 km). Hence, it might be expected to reproduce the short time scale statistics better than the ststistics for longer periods. From this study is concluded that the String-of Beads model can be useful for generating long

time series of daily or shorter time scale rainfall, which can be used in hydrological modelling and other studies. It is recommended that for monthly and annual stochastic rainfall generation a long duration stochastic rainfall model should be used. It is further recommended that the String-of Beads model should be further developed to improve the statistics of values for time periods longer than a day and to include both intra-annual and inter-annual variability.

As reported in Chapter 7, streamflow was simulated using both conventional driver station (CDS) and modified driver station (MDS) approaches. The CDS was used as the standard procedure in the *ACRU* model to estimate catchment rainfall. The streamflow generated appeared to be relatively poorly simulated compared to the observed streamflow. This may be attributed to error in recording of observed streamflows or inappropriate configuration and/or parameterisation of the ACRU model. For example, in the configuration used, the wetland routines were not invoked to simulate the wetland in the catchment.

The comparison between the streamflow simulated using the CDS and MDS rainfall gave a good indication of the effect of using an improved estimate of catchment rainfall on streamflow simulation. In most of the cases, the driver rainfall data selected to represent the areal rainfall of the subcatchment overestimated the mean areal rainfall of the subcatchment. As a consequence more streamflow (40%) was simulated using CDS compared to the MDS rainfall, and both simulations generated more streamflow than observed. Therefore, the estimate of the subcatchment rainfall should utilise available data and the best existing techniques and instruments to achieve a best possible estimate of the mean areal rainfall of the subcatchments. MDS is a way forward, however the same driver station may be need to be used to see clearly the difference between the CDS and MDS. In general, MDS approach is should be used in generating streamflow with recommendation mentioned above.

In, general, catchment rainfall is a major factor in estimating runoff for design flood estimation, risk associated with water management activities and other hydrology and engineering projects. Accurate design flood estimation using a continuous simulation modelling approach requires a long series of detailed spatial and temporal rainfall information which the existing three rainfall measuring instruments do not provide individually. Merging rainfall information from the three

instruments is the best estimate of the "true" rainfall. However the length of the radar and satellite records are currently limited. Therefore, extending merged rainfall information to the historical gauged point rainfall or developing a stochastic rainfall model which generates long series of realistic rainfall fields at the required detailed spatial and temporal resolution enable design floods to be estimated more confidently using a continuous modelling approach. The results of this study indicate that currently techniques used to estimate mean areal catchment rainfall in South Africa needs to move towards adopting the radar and raingauge merging approach used in this study. Moreover, the application of stochastic rainfall models which provide long time series of sysnthetic rainfall at a detailed spatial and temporal resolution can be used for hydrological risk assessment in South Africa. Based on the results obtained from this research, the following paragraphs outline some recommendations for future work.

- Merging the rainfall information from the three rainfall measuring instruments is the best estimates of the "true" rainfall. Therefore, rainfall information in South Africa need to merged from the three instruments where the data are available, as already being under study by Pegram and Sinclair (2004). Moreover, the merged rainfall information should be used to extend and improve the estimation of catchment rainfall from daily raingauges using the MDS approach developed in this study. This will result in the mean areal rainfall for catchments in South Africa to be estimated using the best available techniques and data, which will benefit hydrological studies which require the estimation of catchment rainfall.

- In the merging process of rainfall information from radar and raingauges in Liebenbergsvlei catchment, areas of no rainfall recorded by the radar were masked and the issue of ground clutter of the radar signal remains a problem for rainfall estimation. Therefore, the merging process needs to address these two problems to improve the reliability of the merged rainfall values

- The stochastic SBM rainfall model was used to generate rainfall values for Liebenbergsvlei catchment, using parameters calibrated for the model by Clothier (2004). It is recommended that a user-friendly version of the model, with easy-to-use calibration

routines be developed for the SBM. This will enable the model to be calibrated for all the existing radars in South Africa and thus long periods of realistic rainfall fields could be generated for hydrological studies and risk assessment in South Africa.

- The SBM is a short duration time step rainfall model, and should be used in a daily or shorter duration rainfall-runoff models. A suitable stochastic rainfall model should be developed or adopted for monthly and yearly durations, if accurate results are required from a monthly or yearly time step rainfall-runoff models.

9. REFERENCES

Adamowsky, K. and Smith, A.F., 1972. Stochastic generation of rainfall. *Journal of Hydraulic Engineering,* 98: 1935-1945.

Balascio, C.C., 2001. Multiquadric equations and optimal areal estimation. *Journal of Hydrologic Engineering*, 6: 498-505.

Bardossy, A. and Plate, E.J., 1991. Modelling daily rainfall using a semi-Markov representation of circulation pattern occurrence. *Journal of Hydrology*, 122: 33-47.

Bardossy, A. and Plate, E.J., 1992. Space time model for daily rainfall using atmospheric circulation pattern. *Water Resources Research,* 28: 1247-1259.

Borga, M. and Vizzaccaro, A., 1997. On the interpolation of hydrologic variables: Formal equivalence of multiquadric surface fitting and kriging. *Journal of Hydrology*, 195: 160-171.

Boughton, W. C., 1999. A daily rainfall generating model for water yield and flood studies. Report 99/9, *CRC for Catchment Hydrology*, Monash University, Melbourne, AU, 21 pp.

Buishand, T.A., 1977. Stochastic modelling of daily rainfall sequences. Dissertation. Communication Agriculture University. Wageningen. NZ.

Burrough, P.A., 1986. Methods of spatial interpolation. In: *Principles of Geographical Information Systems for Land Resource Assessment,* ed. P.H.T. Beckett. Oxford University Press, New York, USA, 147-165.

Cameron, D.S., Beven, K.J., Tawn, J., Blazkova, S. and Naden, P., 1999. Flood frequency estimation by continuous simulation for a gauged upland catchment (with uncertainity). *Journal of Hydrology,* 219: 169-187.

Chandler, R.E. and Wheater, H.S., 2002. Analysis of rainfall variability using generalised linear models: A case study from the West of Ireland. *Water Resources Research*, 38: 1-11.

Chandler, R.E., Wheater, H.S., Isham, V.S., Onof, C., Bate, S., Northrop, P.J., Cox, D.R. and Koutsoyiannis, D., 2000. Generation of spatially consistent rainfall data. BHS Occasional Paper, 13: 59-65, London, UK.

Chapman, T., 1994. Stochastic modelling of daily rainfall. In: *15th Hydrology and Water Resource Symposium.* The Institution of Engineers. Melbourne, AU, 7-12.

Charles, S.P., Bates, B.C and Hughes, J.P., 1999. A spatiotemporal model for downscaling precipitation occurrence and amounts. *Journal of Geophysical Research*, 104: 31657-31669.

Chin, E.H. and Miller, J.F., 1980. On the conditional distribution of precipitation amounts. *Monthly Weather Review*, 108: 1462-1464.

Clothier, A., 2004. High resolution space-time modelling of rainfall: The String of Beads Model. PhD Thesis. University of Natal, Durban. South Africa.

Clothier, A.N. and Pegram, G.G.S., 2002. *Space-time modelling of rainfall using the string of beads model: integration of radar and raingauge data.* WRC Report No. 1010/1/02. Water Research Commission, Durban, RSA.

Cole, J.A. and Sherriff, J.D.F., 1972. Some single and multisite models of rainfall with discrete time increments. *Journal of Hydrology,* 17: 97-113.

Cox, D.R. and Isham, V., 1994. Stochastic models of precipitation. In: *Statistics for the Environment 2. Water Issues*. Barnett, V. and Turkman, K.F. (eds). Wiley, New York, USA, 3-18.

Cox, D.R. and Isham, V.S., 1988. A simple spatial-temporal model of rainfall. In: *Proclamation of Royal Society of London,* UK, A415: 317-328.

Dawdy, D.R. and Bergman, J.M., 1969. Effects of rainfall variability on streamflow simulation. *Water Resources Research,* 5: 958-969.

Deyzel, I.T.H., Pegram, G.G.S., Visser, P.J.M., and Dicks, D., 2004. *Spatial interpolation and mapping of rainfallb (Simar).* WRC Report No 1152/01/04. Water Research Commission, Pretoria, RSA.

Ehret, U., 2002. Rainfall and flood nowcasting in small catchments using weather radar. PhD Thesis. University of Stuttgart, Germany.

Foufoula-Georgiou, E. and Lettenmeier, D., 1987. Markov renewal model for rainfall occurrence. *Water Resources Research*, 23: 875-884.

Foufoula-Georgiou, E. and Vuruputur, V., 2000. In: *Spatial patterns in catchment Hydrology-observations and modelling. Patterns and organisation in precipitation.* Grayson, R. and Blöschl, G. (eds). Cambridge university press, Cambridge, UK.

Gandin, L.S., 1970. The planning of meteorological station networks. *Technical Note No.111.* WMO Report No.265, Geneva, Switzerland.

Ghan, S.J., Liljegren, J.C., Shaw, W.J., Hubbe, J.H. and Doran, J.C., 1997. Influence of subgrid variability on surface Hydrology. *Journal of Climate,* 10: 3157-66.

Grimes, D., 1999. Satellite and images. [Internet] Department of Meteorology. University of Reading, United Kingdom. Available from: http://www.met.reading.ac.uk/ ~swsgrime/artemis/. [Accessed: 30 Sep 2004]

Gupta, V.K. and Waymire, E.C., 1993. A statistical analysis of mesoscale rainfall as a random cascade. *Journal of Applied Meteorology*, 32: 251-267.

Haberlandt, U., 1998. Stochastic processes using regionalized model parameters. *Journal of Hydrologic Engineering,* 3: 60-168.

Habib, E. and Krajewski, W.F., 2002. Uncertainty Analysis of the TRMM Ground Validation Radar-Rainfall Products: Application to the TEFLUN-B Field Campaign. *Journal of Applied Meteorology*, 41: 558–572.

Hay, L.E., McCabe Jr, G.J., Wolock, D.M. and Ayers, M.A., 1991. Simulation of precipitation by weather type analysis. *Water Resource Research,* 27: 493-501.

Hutchinson, P., 1974. Progress in the use of the method of optimum interpolation for the redesign of the Zambian rain gauge network. *Geoforum,* 20: 49-62.

Hutchinson, P., 1995. Stochastic space time weather models from ground based data. *Agriculture and Forest Meteorology,* 73: 237-264.

Jewitt, G.P.W., Terblanche, D., Mittermaier, M. and Görgens, A.H.M., 1997. Radar measured precipitation as input to a distributed hydrological model: An example from the Liebenbergsvlei. In: *Proceedings of the Eighth South African National Hydrological Symposium.* Nov. 17-19, 1997, Water Research Commission, Pretoria, RSA.

Jimon, O.D. and Webster, P., 1999. Stochastic modelling daily rainfall in Nigeria, intra-annual variation of model parameters. *Journal of Hydrology*, 222: 1-17.

Jothityangkoon, C., Sivapalan, M. and Viney, N.R., 2000. Tests of a space-time model of daily rainfall in Southern Western Australia based on non-homogeneous random cascades. *Water Resource Research,* 36: 267-284.

Kuczera, G., and Coombes, P.J. (2002). Towards continuous simulation: a comparative assessment of the performance of volume-sensitive systems. Storm water Industry Association Regional Conference. Orange, NSW.

Lall, U., and Sharma, A., U., 1996. A nearest neighbour conditional bootstrap for resampling of hydrological time series. *Water Resource Research,* 32: 679-693.

Lall, U., Rajagopalan, B. and Tarboton, D.G., 1996. A non-parametric wet/dry spell model for resampling daily precipitation. *Water Resources Research,* 32: 2803-2823.

Lanza, L.G., Ramírez, J.A. and Todini, E., 2001. Stochastic rainfall interpolation and downscaling. *Hydrology and Earth System Sciences*, 5: 139-143.

Livezzani, V., Amorati, R. and Meneguzzo, F., 2000. A review of satellite-based rainfall estimation methods. [Internet] Multi-sensor Precipitation Measurements, Integration and Calibration, Italy: Available from: http://www.geomin.unibo.it/orgv/hydro/music/reports/D6.1_SatPrecEst.pdf. [Accessed: 30 September 2004]

Lynch, S.D., 2003. *Development of a raster database of annual, monthly and daily rainfall for southern Africa.* WRC Report No. 1156/1/03, Water Research Commission, Pretoria, RSA.

Menabde, M., Seed, A.W., Harris, D. and Austin, G., 1999. Multi-affine random field model of rainfall. *Water Resources Research*, 35: 509-514.

Michaud, J.D. and Sorooshian, S., 1994. Effect of rainfall sampling errors on simulation of desert flash floods. *Water Resources Research*, 30: 593-605.

Midgley, D.C., Pitman, W.V. and Middleton, B.J., 1994. *Surface water resources of South Africa 1990.* Water Research Commission. WRC Report No. 298/2.1/94. Pretoria. South Africa.

Mittermaier, M.P. and Terblanche, D.E., 1997. Converting weather radar data into cartesian space: A new approach using DISPLACE averaging. *Water SA*, 23: 46-50.

Nicks, A.D. and Hartman, M.A., 1996. Variation of rainfall over large gauged area. *Transactions of the American Society of Civil Engineers*, 9:437-439.

Northrop, P.J., 1998. A clustered spatial-temporal model of rainfall. In: *Proclamation of Royal Society of London,* UK, A454: 1875-1888.

Over, T.M. and Gupta, V.K., 1994. Statistical analysis of mesoscale rainfall: Dependences of a random cascade generator on large scale forcing. *Journal Applied Meteorology*, 101: 319 –326, 331.

Pegram, G.G.S. and Clothier, A.N., 2001. Downscaling rainfields in space and time, using the string of beads models in causal mode. *Hydrology and Earth System Science,* 5: 175-186.

Pegram, G.G.S. and Seed, A.W., 1998. *The feasibility of stochastically modelling the spatial and temporal distribution of rainfields*. WRC Report No. 550/1/98. Water Research Commission, Pretoria, RSA.

Pegram, G.G.S. and Sinclair, D.S., 2004. A flood nowcasting system for the eThekwini metro: Umgeni nowcasting using radar - an integrated pilot study. WRC Report No. 1217/2/04. Water Research Commission, Durban, RSA.

Rajagopalan, B. and Lall, U., 1999. A k-nearest-neighbour simulator for daily precipitation and other weather variables. *Water Resource Research,* 35: 3089-3101.

Rajagopalan, B., Lall, U. and Tarboton, D.G., 1996. A nonhomogeneous markov model for daily precipitation simulation. *Journal of Hydrologic Engineering*, 1: 33-40.

Rodriquez-Itrube, I., Cox, D.R. and Isham, V., 1987. Some models for rainfall based on stochastic point process. In: *Proc. Royal Society of London,* UK, A410: 269-288.

Schäfer, N.W. 1991. Modelling the areal distribution of daily rainfall. MSc.Eng. Thesis. Department of Agricultural Engineering. University of Natal, Pietermaritzburg, RSA.

Schulze, R.E., 1976. On the application of trend surfaces of precipitation to mountains areas. *Water SA,* 2: 110-118.

Schulze, R.E., Dent, M.C., Lynch, S.D., Kienze, S.W. and Seed, A.W., 1995. Rainfall. In *Hydrology and Agrohydrology. A Text to Accompany the ACRU 3.00 Agro hydrological Modelling System.* Schulze, R.E. (ed.). ACRU Report No.8. Department of Agricultural Engineering, University of Natal, Pietermaritzburg, RSA.

Schulze, R.E., Schäfer, N.W. and Lynch, S.D., 1989. An assessment of regional runoff production in Qwa Qwa: A GIS application of the ACRU modeling system. *South African Journal of Photogrammetry, Remote Sensing and Cartography*, 15: 141-148.

Seed, A.W., 1992. Generation of a spatially distributed daily rainfall datatbase for various weather modification scenarios. WRC Report No 373/1/92. Water Research commission, Pretoria, RSA.

Seed, A.W., Draper, C., Srikanthan, R. and Menabde, M., 2000. A multiplicative broken-line model for time series of mean areal rainfall. *Water Resources Research,* **36:** 2395

Seo, Dong-Jun. and Krajewski, F.K., 1990. Stochastic interpolation of rainfall data from raingauges & radar using cokriging. *Water Resources Research,* 26: 915-924.

Simanton, J.R., and Osborn, H.B., 1980. Reciprocal-distance estimate of point rainfall. *Journal of Hydrologic Engineering Division,* ASCE, 106(7): 1242-1246.

Sinclair, D.S., 2004. Personal communication. Department of Civil Engineering, University of Kwazulu-Natal,Durban,RSA.

Singh, V.P., 1976. A rapid method of estimating mean areal rainfall. *Water Resource Bulletin*, 12: 307-315.

Siriwardena, L., Srikanthan, R. and McMahon, T., 2002. Evaluation of two daily rainfall data generation models. Report 02/14, *CRC for Catchment Hydrology*. Melbourne, AU.

Sokol, Z., 2003. Utilization of regression models for rainfall estimates using radar-derived rainfall data and aringauge data. *Journal of Hydrology,* 278: 144-152.

Sotillo, M.G., Ramis, C., Romero, R. and Alonso, S., 2003. The Role of the orography on the spatial distribution of precipitation over the Spanish Mediterranean zone. *Climate Research*. 23: 247- 261

Srikanthan, R. and McMahon T.A., 1985. *Stochastic generation of rainfall and evaporation.*. AWRC Technical Paper No. 84, 301 pp. Australian Water Resource Council, Sydney, AU.

Srikanthan, R. and McMahon, T.A., 2001. Stochastic generation of annual, monthly and daily climate data: A review. *Hydrology and Earth System Sciences*, 5(4): 653 –670.

Tabios, G.Q, and Salas, T.D., 1985. A comparative analysis of techniques for spatial interpolation of precipitation. *Water Research Bulletin*, 21(3): 365-380.

Todini, E., 2001. Bayesian conditioning of RADAR to rain gauges. *Hydrology and Earth System Science,* 5: 225-232.

Wang, Q.J. and Nathan, R.J., 2002. A daily and monthly mixed algorithm for stochastic generation of rainfall time series. In: *Pro. The 27th Hydrology and Water Resources Symposium*, Melbourne, Australia.

Weather, H., Isham, V., Cox, D.R., Chandler, R., Kakou A., Northrop, P.J., Oh, L., Onof, C. and Rodriquez-Itrube, I., 2000. Spatial-temporal rainfall fields: modelling and statistical aspects. *Hydrological and Earth Systems Science.* 4: 581-601.

Wilks, D.S., 1989. Conditioning stochastic daily precipitation models on total monthly precipitation. *Water Resource Research*, 23: 1429-1439.

Wilks, D.S., 1998. Multisite generation of a daily stochastic precipitation generation model. *Journal of Hydrology*, 210: 178-191.

Wilson, J. W., and E. A. Brandes, 1979: Radar measurement of rainfall: A summary. *Bulletin of American Meteorology Society*. 60 (9), 1048-1058.

Wilson, L.L., Lettenmaier, D.P. and Skyllingstad, E., 1992. A hierarchical stochastic model of large-scale atmosphere circulation patterns and multiple stations daily precipitation. *Journal of Geophysical Research,* 97: 2791-2809.

Woolhiser, D.A., Keefer, T.O. and Redmond, K.T., 1993. Southern oscillation effects on daily precipitation in the southwestern United States. *Water Resource Research*, 18: 1461-1468.

Zhou, S.L., Srikanthan, R. and McMahon T.A., 2002. Stochastic modelling of daily rainfall. Report 02/5, *CRC for Catchment Hydrology*, Melbourne, AU.

Zucchini, W. and Adamson, P.T., 1984. The occurrence and severity of drought in South Africa. WRC Report 91/1/54. Water Research Commission, Pretoria, RSA.

Zucchini, W. and Guttorp, P., 1991. A hidden markov model for space-time precipitation. *Water Resource Research,* 27: 1917-1923.

APPENDIX A

DATA FORMATS AND MANIPULATION

A.1. Raingauge Accumulation

The tipping bucket raingauge data, provided by METSYS, were in the format illustrated in the Figure A1. The first column of the data contains the gauge name. The next six columns of two digit integer numbers represent, the year, month, day, hour, minute and second at which the reading was taken. The next column (accurate to two decimal places) is the rainfall depth represented by each tip; always 0.2mm. Column 9 is the Julian day for the current year. The final column is a tip count.

Stn	yy	mm	dd	hh	mm	ss	trip	yd	count
L001	98	09	30	13	51	03	.20	273	00048
L001	98	09	30	13	51	28	.20	273	00049
L001	98	09	30	13	51	55	.20	273	00050
L001	98	09	30	13	52	21	.20	273	00051
L001	98	09	30	13	52	59	.20	273	00052
L001	98	09	30	13	53	45	.20	273	00053
L001	98	09	30	13	54	40	.20	273	00054
L001	98	09	30	13	56	34	.20	273	00055

Figure A1 Example of tipping bucket gauge data

Each data file stores an entire month's data, with the data for each of the 45 gauges following consecutively. Every gauge makes at least one reading per day to confirm that the gauge was operational on each day of the month. A computer programme was written to aggregate the data into daily rainfall totals which are output in the format required by the raingauge and radar merging programme. The raingauge and radar merging programme developed by Sinclair (2004), merges the radar and gauge values on a daily basis. Therefore, the daily totals for each of the 45 tipping bucket raingaues were stored as shown in Figure A2. The first column of the data contains the location of the tipping buckets and the following column is the daily accumulated rainfall depth.

Geog. Location	R. Depth
(-259700,-3147600)	36.6
(-250900,-3146300)	37.2
(-237175,-3146010)	20.2
(-269757,-3136730)	39.2
(-258938,-3137600)	32.0

Figure A2 Example of daily accumulated tipping bucket of rainfall data.

The daily total from the tipping raingauge rainfall data was stored for each day in a separate file for each tipping bucket raingauge.

The algorithm used to accumulate and format the data is as follows:

- The count values are converted into rainfall data as each count is 0.2mm.
- The algorithm then aggregates the rainfall data into hourly totals.
- The daily rainfall values from day 8:00 a.m. to the following day at 8:00 a.m. are computed and registered for the current day.
- The rainfall data for all the 45 tipping buckets for the same day are stored in a single file. The files have two columns, namely the location of the stations in Gauss coordinates and the value of each tipping bucket for that day.

* * *

A.2. Radar accumulation

The rainfall accumulation from radar rainfall images was performed by simple linear addition of the rainfall rates estimated from each radar scan. The rain rate at a pixel in the first scan (r_0) as well as the rain rate at the same pixel in the second scan (r_1) and the time between scans is known. The total rainfall for the pixel between scans is based on the average of r_0 and r_1, multiplied by the time between scans. The data are stored MDV format which is based on the scaling between maximum and minimum value.

* * *

A.3. Extracting point rainfall values: radar and merged rainfall image sets

Daily rainfall values were extracted from the radar and merged rainfall sets to compare against the gauged rainfall data, either from daily raingauges or tipping bucket raingauges. These values were extracted using ArcGIS tools.

The procedures followed to extract the point rainfall values are as follows:

- A text file was saved with three columns, which contain the names, longitudes and latitudes of the stations. The locations were in the same geographical projection as the rainfall image or grid.
- All the rainfall images were converted from bitmap to grid format.
- The "Sample" ArcInfo command was used to extract the values for each point from the respective rainfall grids.

* * *

APPENDIX B

SPATIAL RAINFALL DISTRIBUTION OF LIEBENBERGSVLEI CATCHMENT

This section contains a summary of results which includes, for each subcatchment, an altitude map, the standard deviation of the distribution spatial rainfall distribution on a daily basis and the relationship between mean areal rainfall and a selected daily raingauge.

B.1. Subcatchment 1

The variation in altitude within Subcatchment 1 (area = 6.26 km^2) is highly variable and has a standard deviation of 66 m, as shown in Figure 5.2. All daily and tipping bucket raingauges are located outside of the subcatchment as shown in Figure B.1a. The L008 tipping bucket raingauge, located at an altitude of 1750 m, was selected to compare the daily areal rainfall of the subcatchment with gauged rainfall data. As shown in Figure B.1b, rainfall recorded at Raingauge L008 does not represent the areal rainfall of the subcatchment well. The daily Raingauge 0332199W (1810 m) does not have a continuous data for the required period. As shown in Figure B.1c, the spatial distribution of the subcatchment daily rainfall consistently shows similar variability on all the days, with the exception for 18 December 1998. On this day the radar image contains daily rainfall values as high as 6800 mm, which is impossible and is caused by the problem of ground cluttering in the radar image.

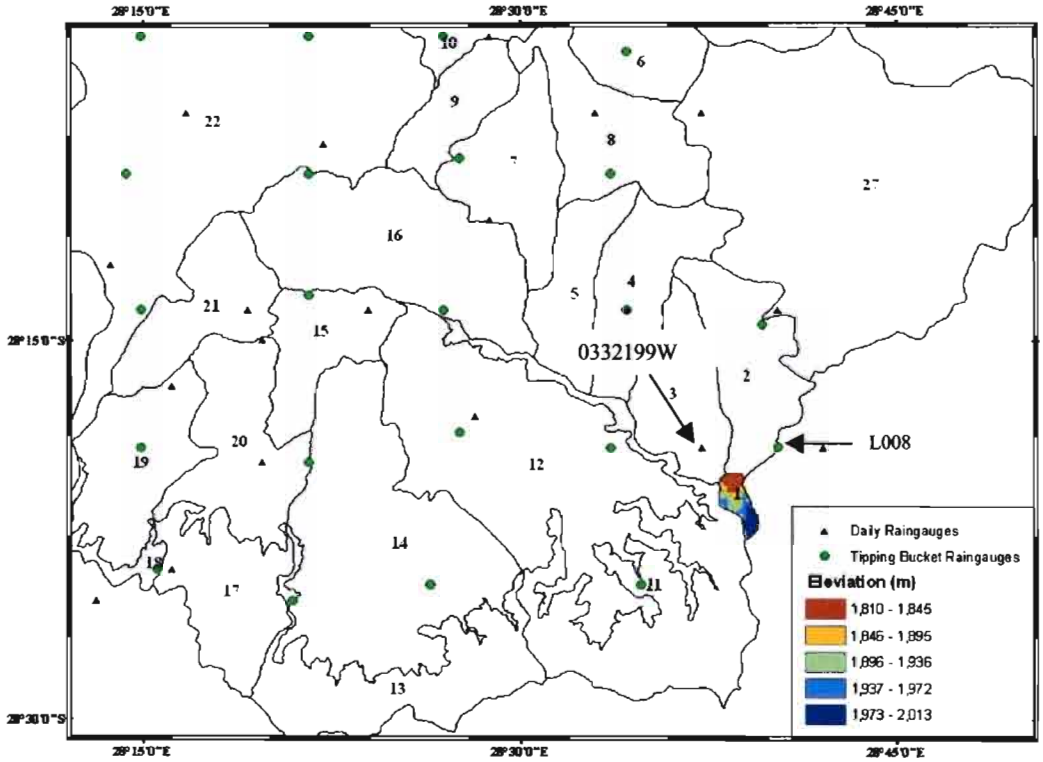

Figure B.1a Altitude map of Subcatchment 1

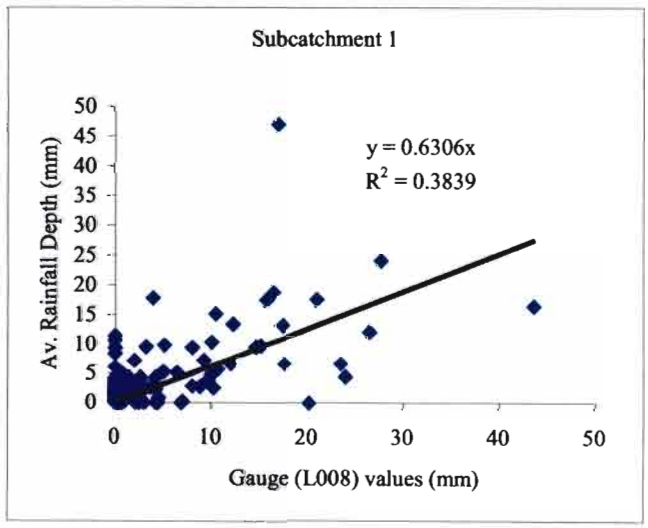

Figure B.1bMean areal rainfall in Subcatchment1 vs daily rainfall at tipping bucket Raingauge L008

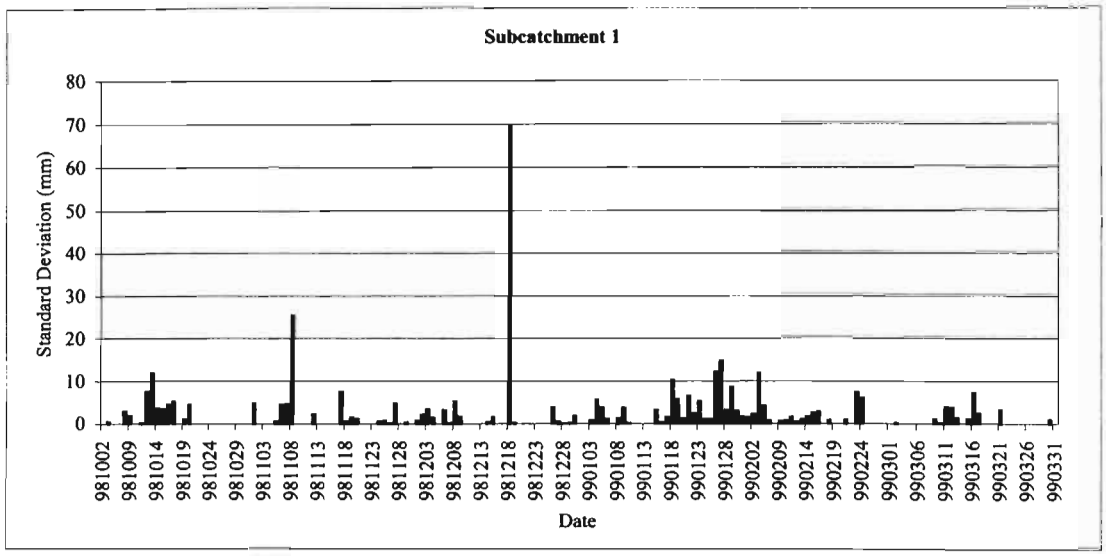

Figure B.1c Standard deviation of the spatial distribution of rainfall in Subcatchment 1

B.2. Subcatchment 2

The standard deviation of altitude in Subcatchment 2 is 39 m, as shown in Figure 5.2. Tipping buckets Raingauges L013 (1783 m) and L008 (1750 m) are located inside the subcatchment, as shown in Figure B.2a. Raingauge L013 and L008 represent the mean areal rainfall of the subcatchment reasonably well (Figure B.2b and B2.c). The variation in the spatial distribution of rainfall in the subcatchment does vary over the period considered, as shown in Figure B.2d, which is expected to affect the relationship between the mean areal rainfall of the subcatchment and the gauged daily rainfall.

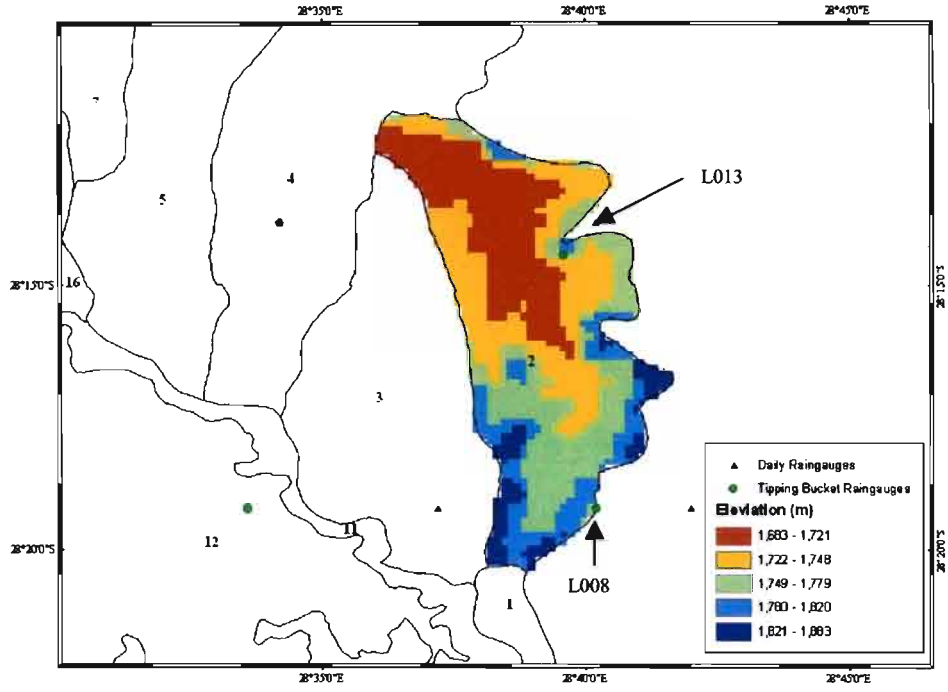

Figure B.2a Altitude map of Subcatchment 2

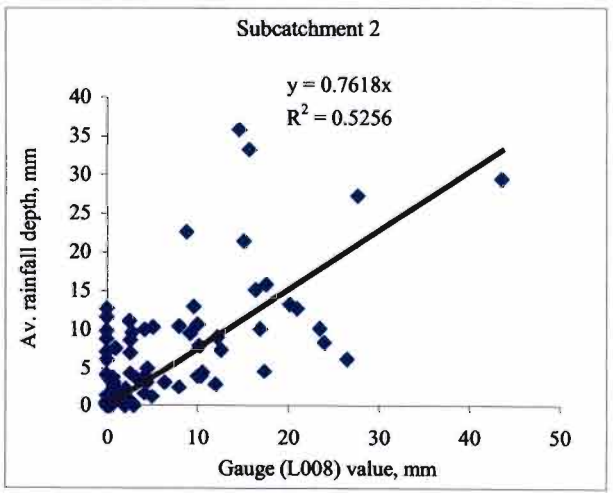

Figure B.2b Mean areal rainfall in Subcatchment2 vs daily rainfall at tipping bucket Raingauge L008

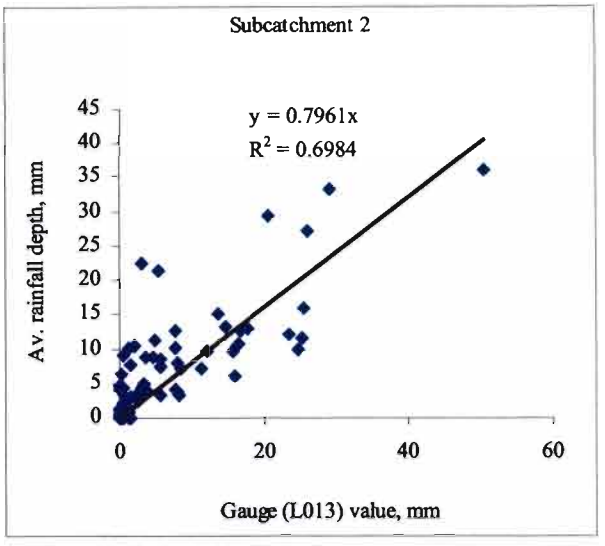

Figure B.2c Mean areal rainfall in Subcatchment 2 vs daily rainfall at tipping bucket Raingauge L003

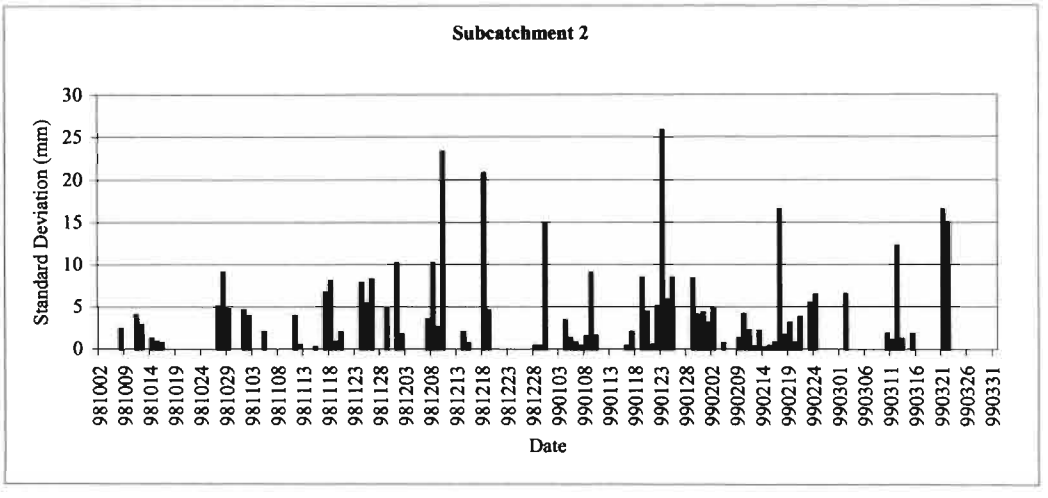

Figure B.2d Standard deviation of the spatial distribution of rainfall in Subcatchment 2

B.3. Subcatchment 3

The Standard deviation of altitude in Subcatchment 3 is 48.6 m, as shown in Figure 5.2. Figure B.3b shows that tipping bucket Raingauge L013 (1783 m) represents the areal rainfall of the subcatchment reasonably well, although it is located outside of the subcatchment as shown in Figure B.3a. Raingauge 0332119W (1810 m) is located inside Subcatchment 3 but it does not

have continuous data for the required period. The variability in the spatial distribution of rainfall in the subcatchment is shown in Figure B.3c.

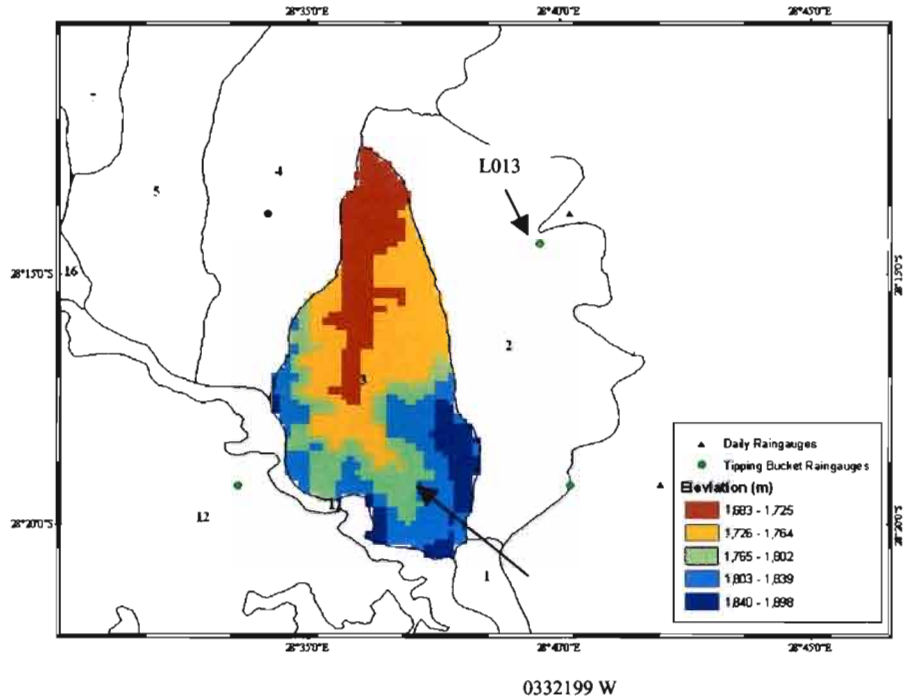

Figure B.3a Altitude map of Subcatchment 3

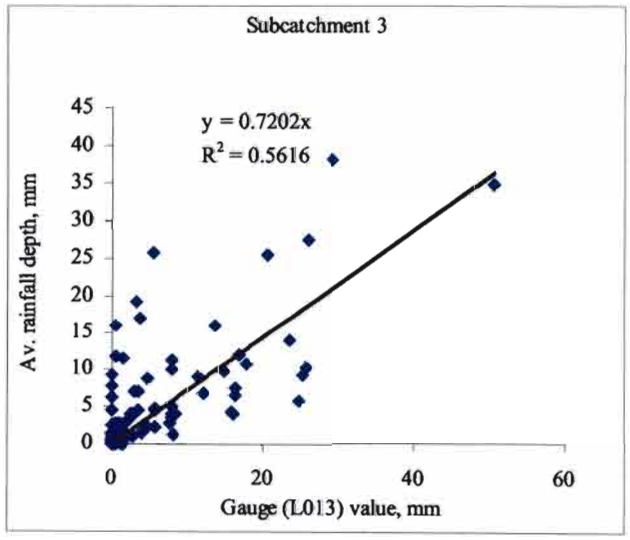

Figure B.3b Mean areal rainfall in Subcatchment 3 vs daily rainfall at tipping bucket Raingauge L013

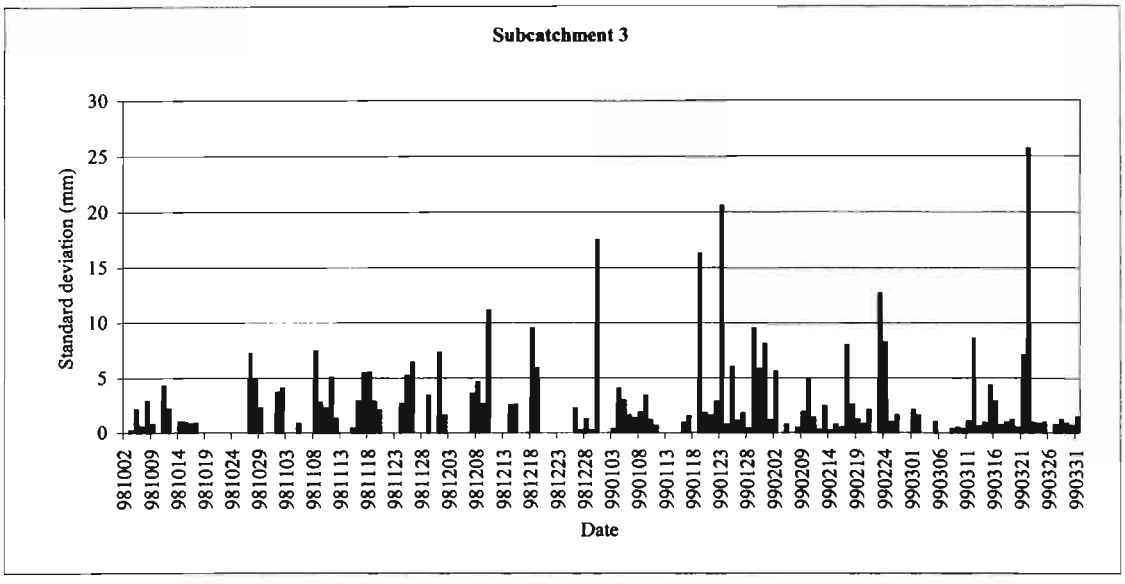

Figure B.3c Standard deviation of the spatial distribution of rainfall in Subcatchment 3

B.4. Subcatchment 4

The Standard deviation of altitude in Subcatchment 4 is 42 m, as shown in Figure 5.2. Tipping buckets Raingauge L012 (1709 m) and Raingauge 0332104 W (1709 m) are located at the same location inside the subcatchment as shown in Fgiure B.4a. There is a bias between the two data sets even though they are located at the same position. Tipping bucket Raingauge L012 estimates the areal rainfall of the subcatchment better than the Raingauge 0332104 W does (Figure B.4b & B.4c).

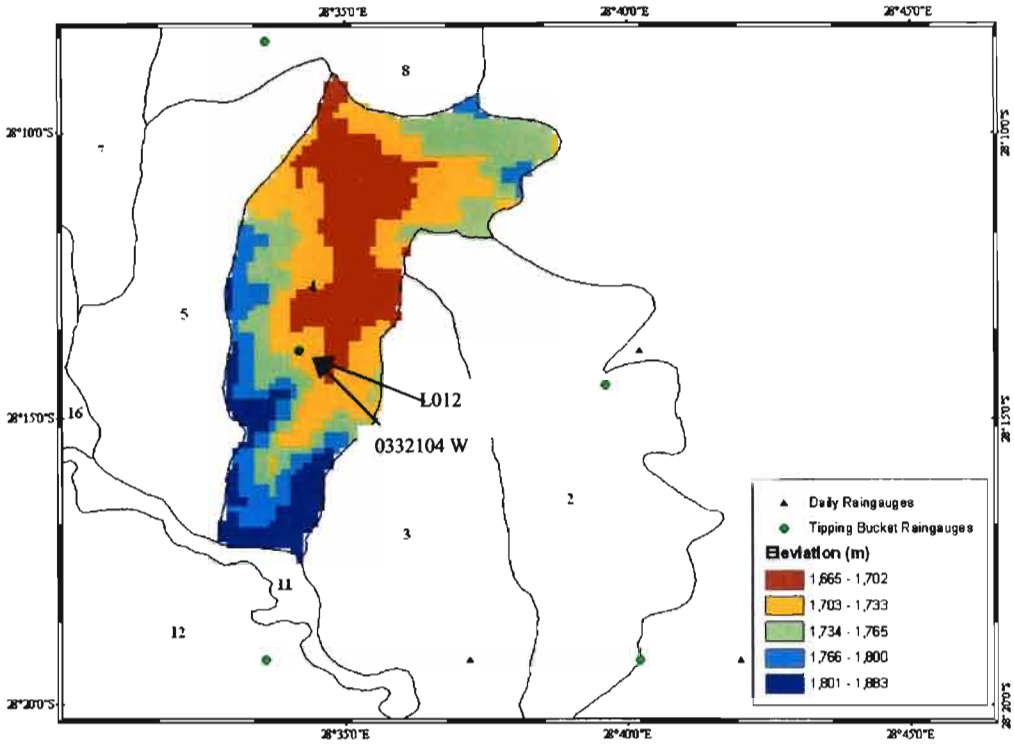

Figure B.4a Altitude map of Subcatchment 4

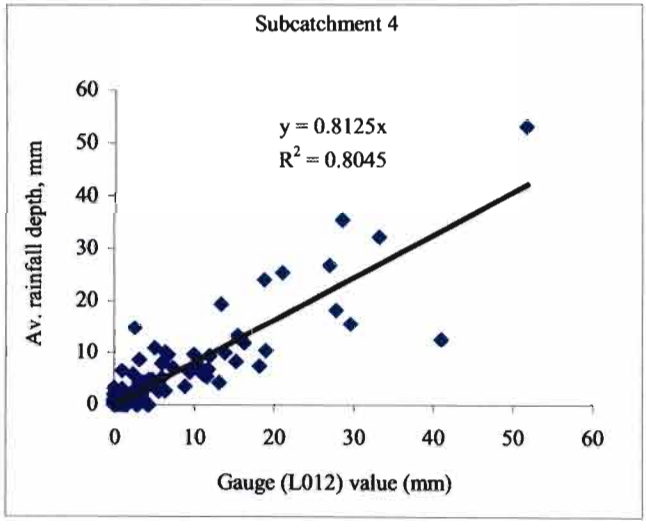

Figure B.4b Mean areal rainfall in Subcatchment 4 vs daily rainfall at tipping bucket Raingauge L012

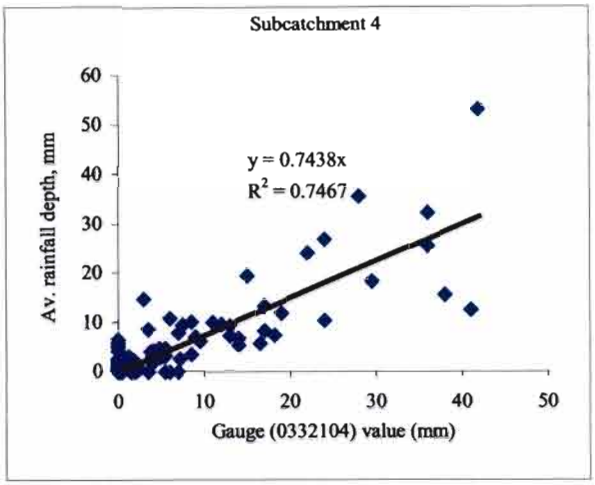

Figure B.4c Mean areal rainfall in Subcatchment 4 vs daily rainfall at Raingauge 03322104 W

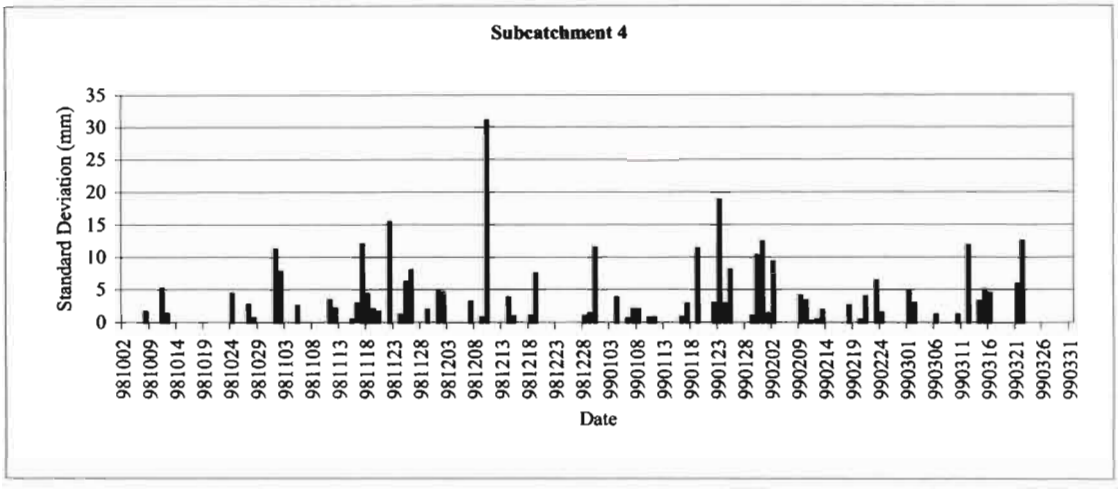

Figure B.4d Standard deviation of the spatial distribution of rainfall in Subcatchment 4

B.5. Subcatchment 5

The Standard deviation of altitude in Subcatchment 5 altitude is 53.6 m, as shown in Figure 5.2. Tipping bucket Raingauges L012 located at an altitude1709 m and Raingauge 0332104W located at an altitude 1709 m represent the areal rainfall of the subcatchment relatively well (Figure B.5b & B.5c), even though the raingauges are located outside the subcatchment (Figure B.5a). There is a consistent variation in the spatial rainfall distribution in the subcatchment on all the days as shown in Figure B.5d.

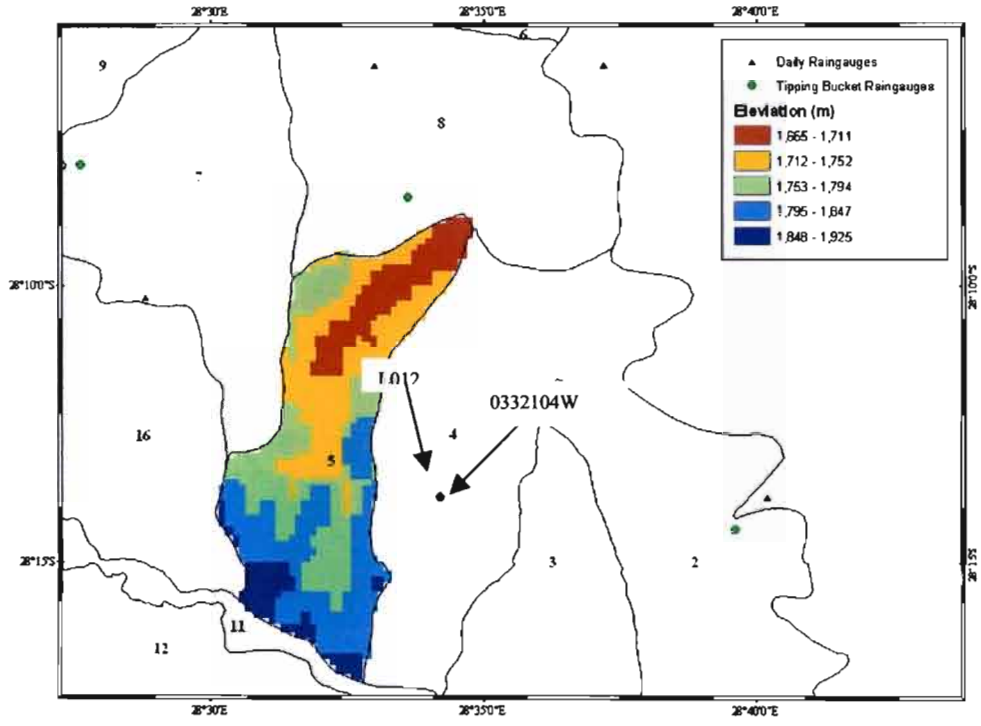

Figure B.5a Altitude map of Subcatchment 5

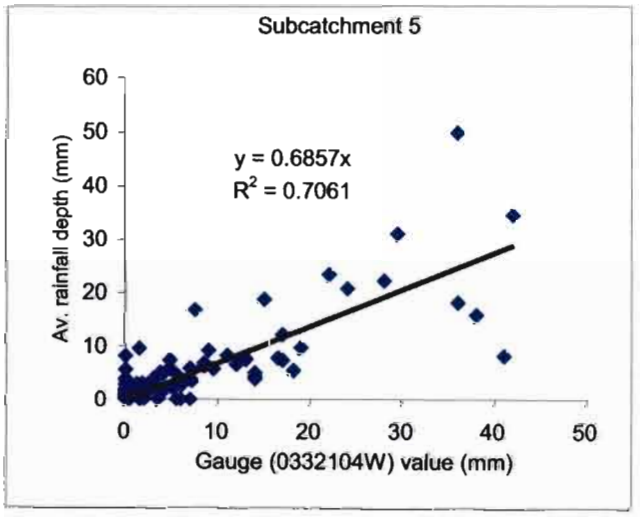

Figure B.5b Mean areal rainfall in Subcatchment 5 vs daily rainfall at Raingauge 0332104 W

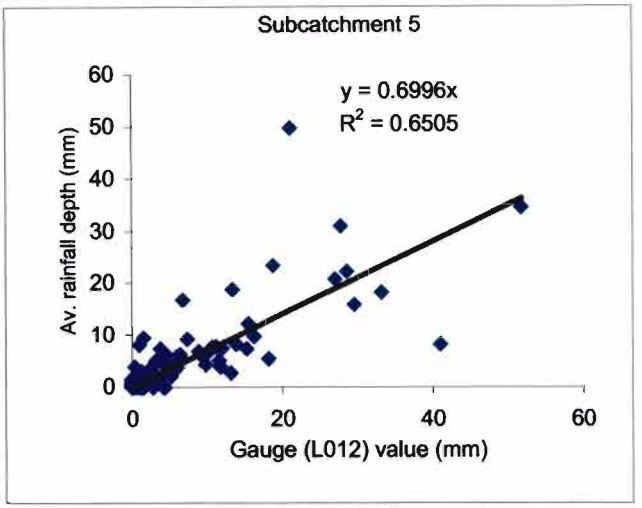

Figure B.5c Mean areal rainfall in Subcatchment 5 vs daily rainfall at tipping bucket Raingauge L012

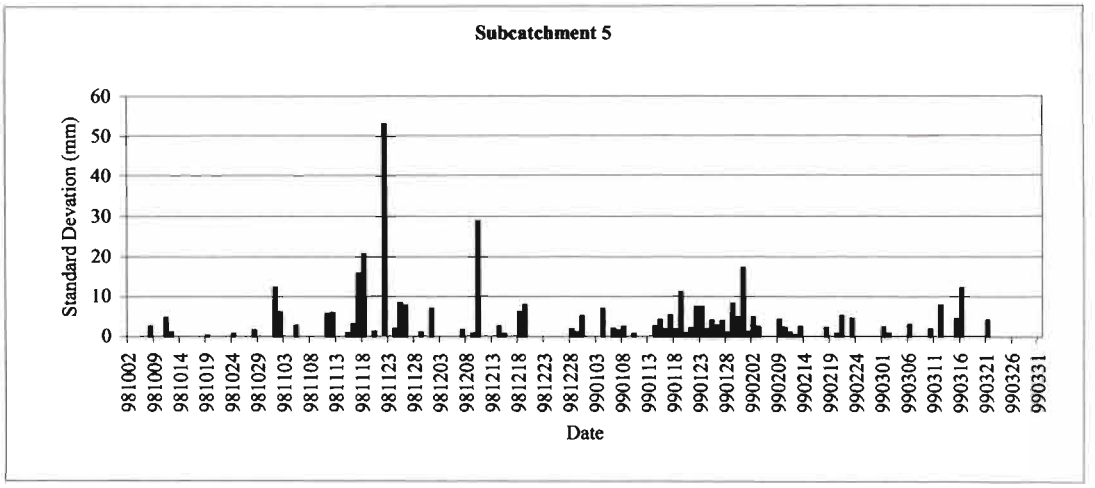

Figure B.5d Standard deviation of the spatial distribution of rainfall in Subcatchment 5

B.6. Subcatchment 6

The Standard deviation of altitude in Subcatchment 6 is 22 m, as shown in Figure 5.2 and tipping bucket Raingauge L021 (1686 m) is the only gauge located inside the subcatchment (Figure B.6a). Daily rainfall data from Raingauge L021 represents the mean areal rainfall of Subcatchment 6 reasonably well, as shown in Figure B.6b. A few days of the 6 months considered show a relatively higher variation in the spatial distribution of rainfall across the

subcatchment than the other days, as shown in Figure B.6c, and these have a negative effect on the relationship between the mean areal rainfall of the subcatchment and the daily rainfall data from Raingauge L021. The daily rainfall data from the Raingauge L021 thus underestimates the mean areal rainfall of the subcatchment on these days.

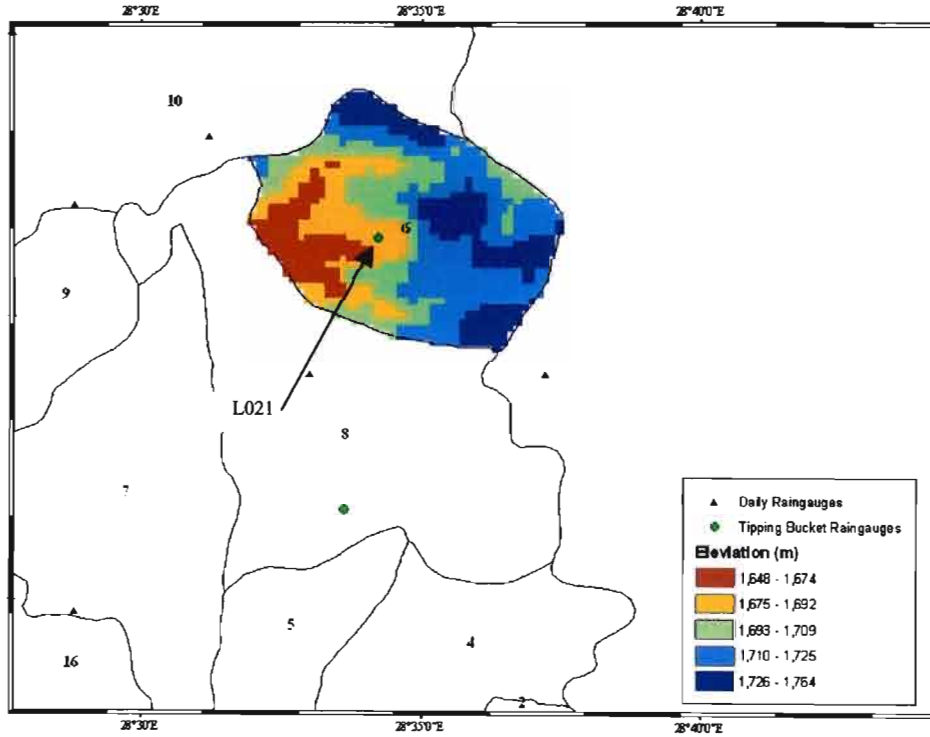

Figure B.6a Altitude map of Subcatchment 6

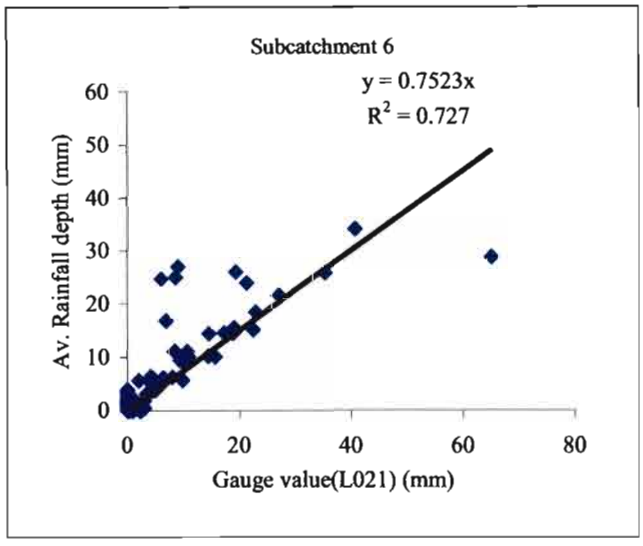

Figure B.6b Mean areal rainfall in Subcatchment 6 vs daily rainfall at tipping bucket Raingauge L021

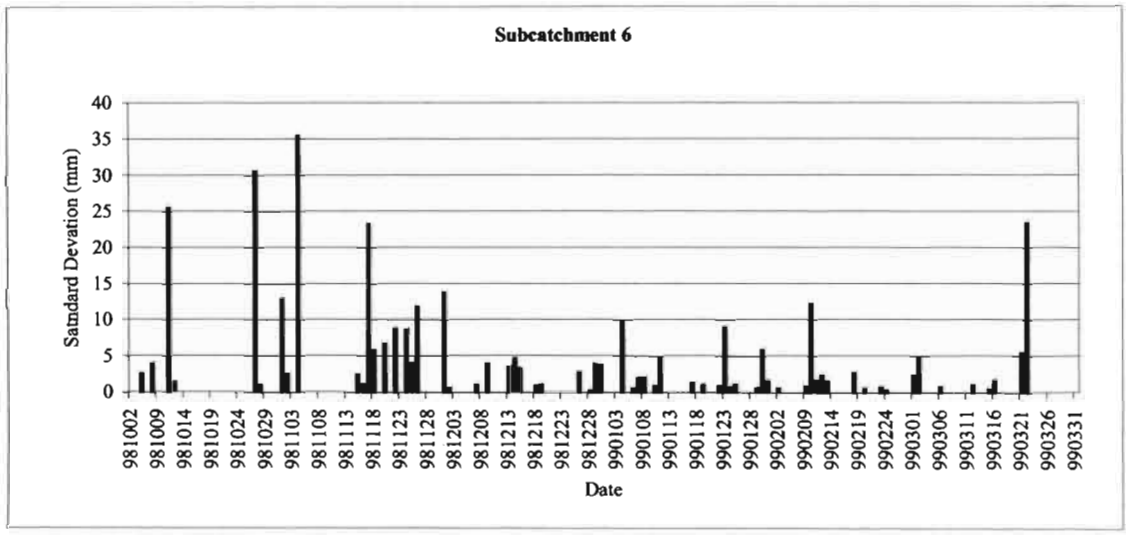

Figure B.6c Standard deviation of the spatial distribution of rainfall in Subcatchment 6

B.7. Subcatchment 7

The Standard deviation of altitude in Subcatchment 7 is 34 m, as shown in Figure 5.2. The daily rainfall at tipping bucket Raingauge L016 (1705 m), which is located inside the subcatchment (Figure B.7a), represents the areal rainfall of Subcatchment 7 reasonably well, as shown in Figure

B.7b. Raingauge 0331850W (1777 m) is located inside the subcatchment but the data for the required period are missing. The variation in the spatial rainfall distribution in the subcatchment is consistent throughout the period considered except for 28 November1998, as shown in Figure B.7c, where the standard deviation of the spatial rainfall distribution is 157 % (Figure B.7d). If the data for this day is removed from the relationship, the relationship improves significantly to $y = 1.2269x$ ($R^2 = 0.8845$).

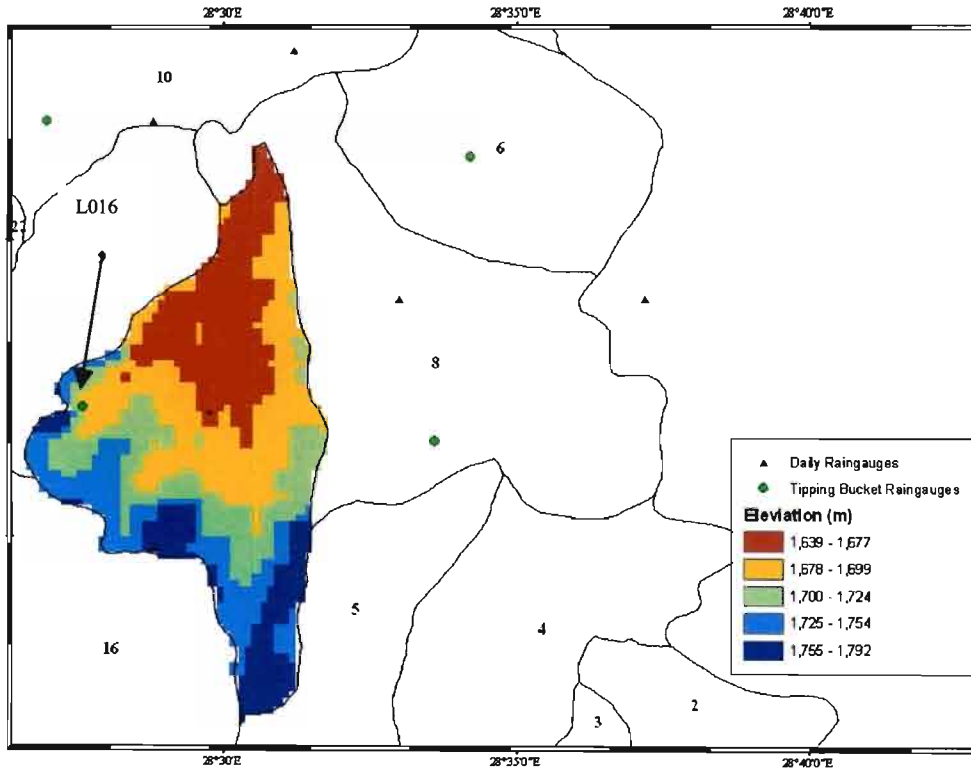

Figure B.7a Altitude map of Subcatchment 7

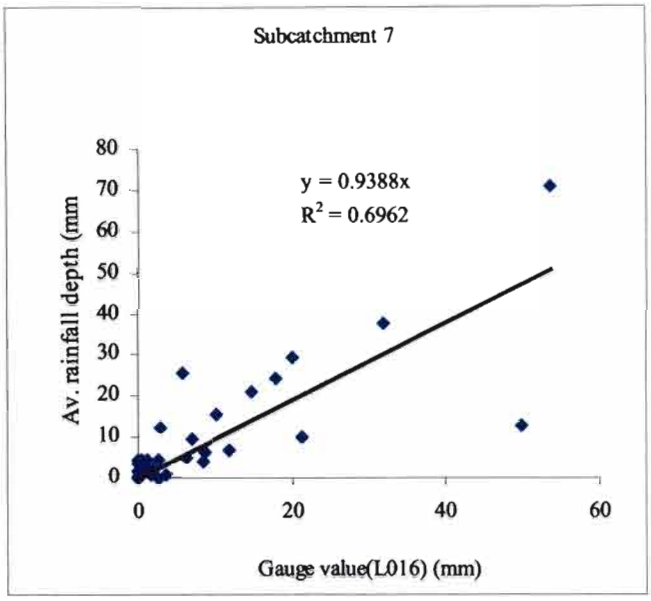

Figure B.7b Mean areal rainfall in Subcatchment 7 vs daily rainfall at tipping bucket Raingauge L016

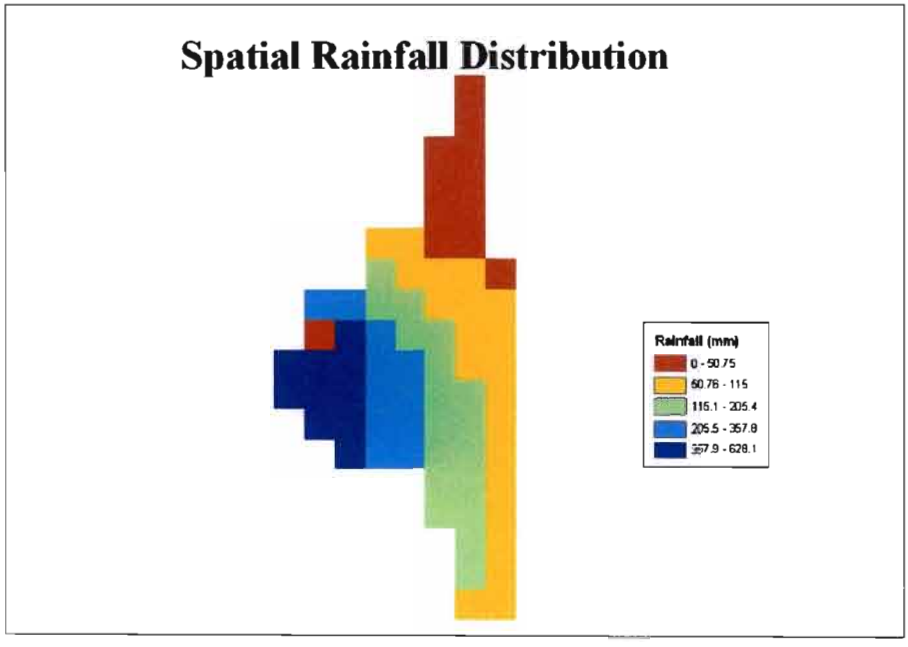

Figure B.7c Spatial rainfall distribution for 28 November 1998 in Subcatchment 7

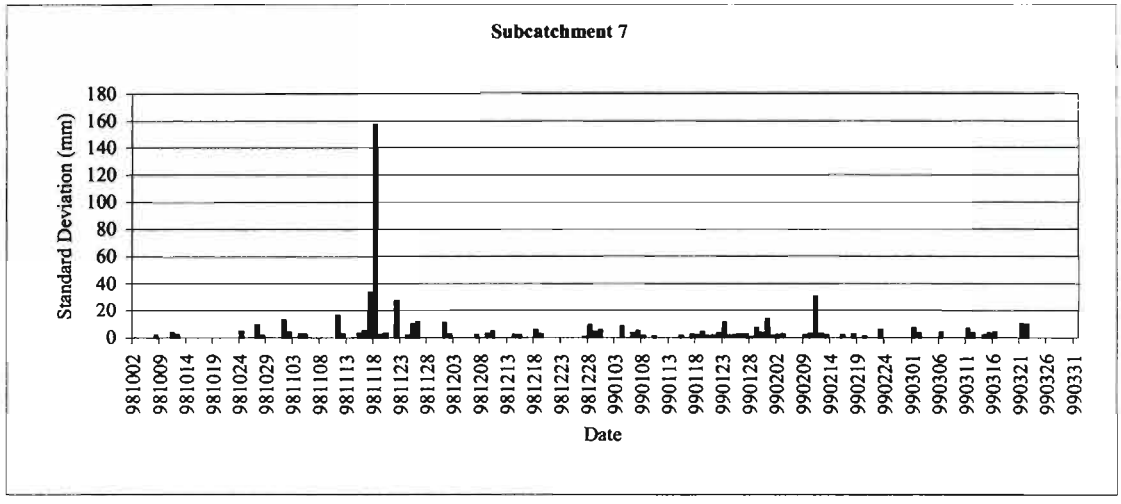

Figure B.7d Standard deviation of the spatial distribution of rainfall in Subcatchment 7

B.8. Subcatchment 8

The Standard deviation of altitude in Subcatchment 8 is 26 m, as shown in Figure 5.2. The relationship between Raingauge 0332066W (1667 m) and tipping bucket Raingauge L017 (1665m) daily rainfall data and the areal rainfall of the subcatchment is very strong as shown in Figure B.8b & B.8c. Both the gauges are located inside the subcatchment (Figure B.8a) and the spatial rainfall distribution of the subcatchment is relatively consistent compared to other subcatchments (Figure B.8d).

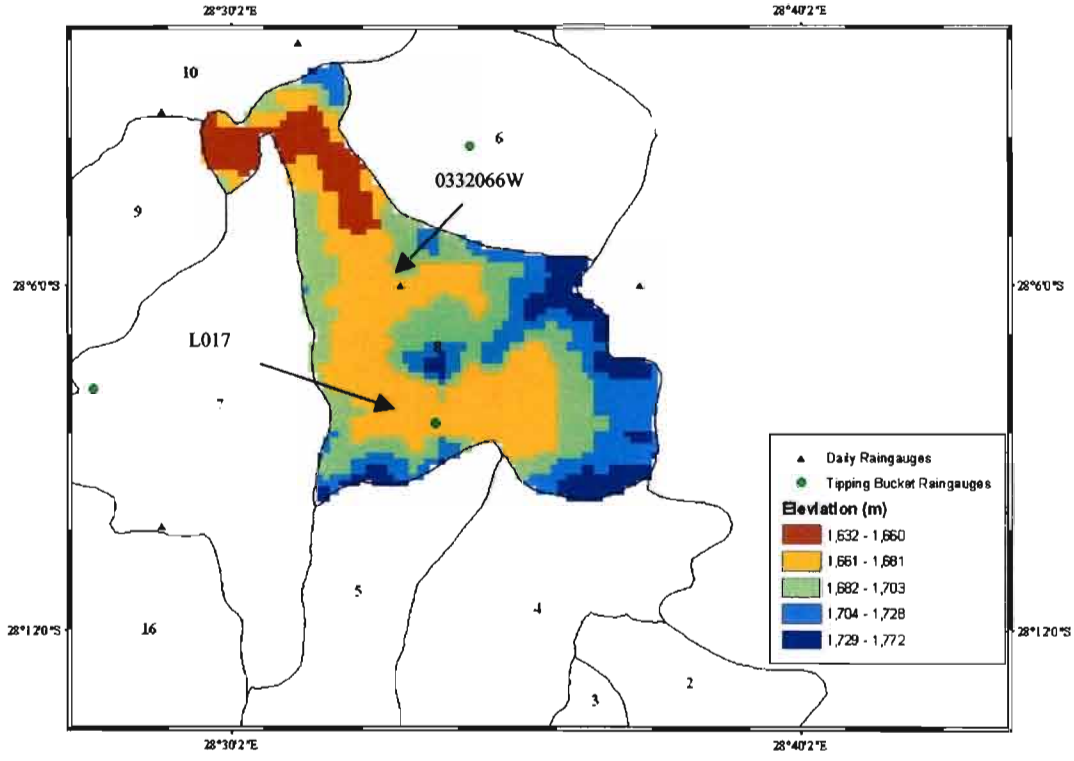

Figure B.8a Altitude map of Subcatchment 8

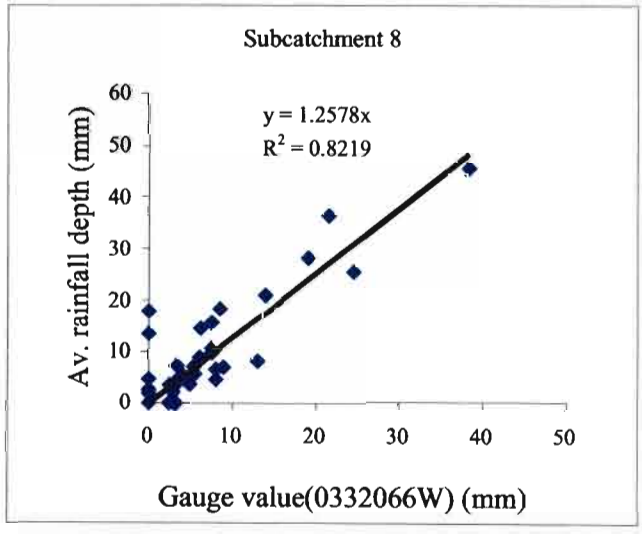

Figure B.8b Mean areal rainfall in Subcatchment 8 vs daily rainfall at Raingauge 0332066W

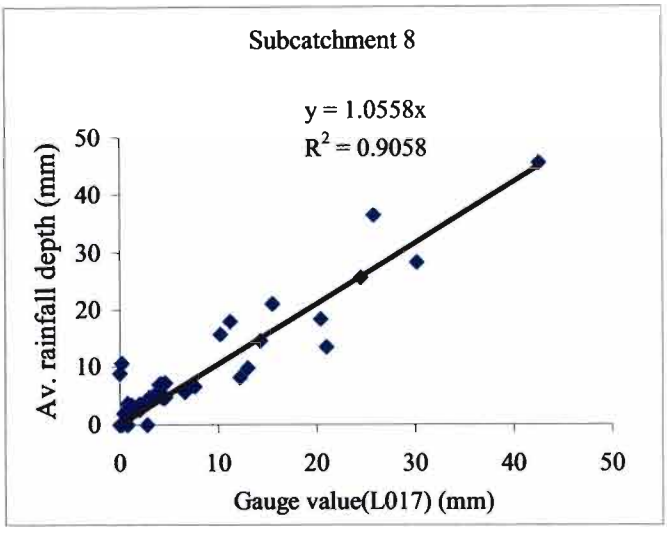

Figure B.8c Mean areal rainfall in Subcatchment 8 vs daily rainfall at tipping bucket Raingauge L017

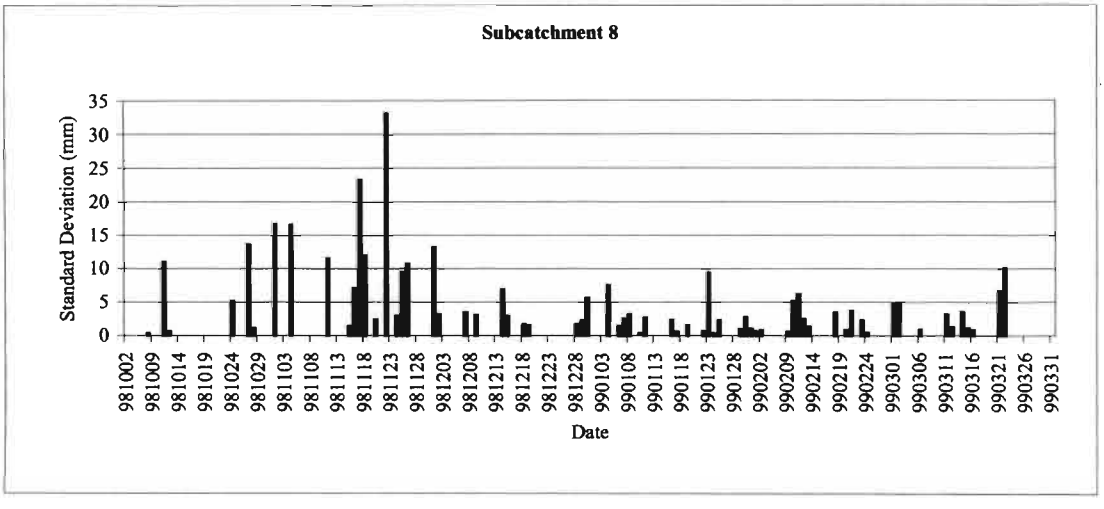

Figure B.8d Standard deviation of the spatial distribution of rainfall in Subcatchment 8

B.9. Subcatchment 9

The Standard deviation of altitude in Subcatchment 9 is 31.6 m, as shown in Figure 5.2. There is no raingauge which is located inside the subcatchment as shown in Figure B.9a, hence tipping

bucket Raingauge L016 (1705 m) was selected as the driver station to represent the areal rainfall of the subcatchment. However, Figure B.9b shows that the daily rainfall at Raingauge L016 significantly overestimates the areal rainfall of the subcatchment. This may be explained by the location of the raingauge at a relatively low altitude and on the perimeter of the subcatchment. L016 is located in Subcatchment 7 and the mean areal rainfall of the Subcatchment 7 is generally larger than the mean areal rainfall of the Subcatchment 9, as shown in Figure B.9c. Therefore, Subcatchment 7 and Raingauge L016 had more rainfall during the period considered than Subcatchment 9. The standard deviation of spatial rainfall distribution of the subcatchment is shown in Figure B.9d.

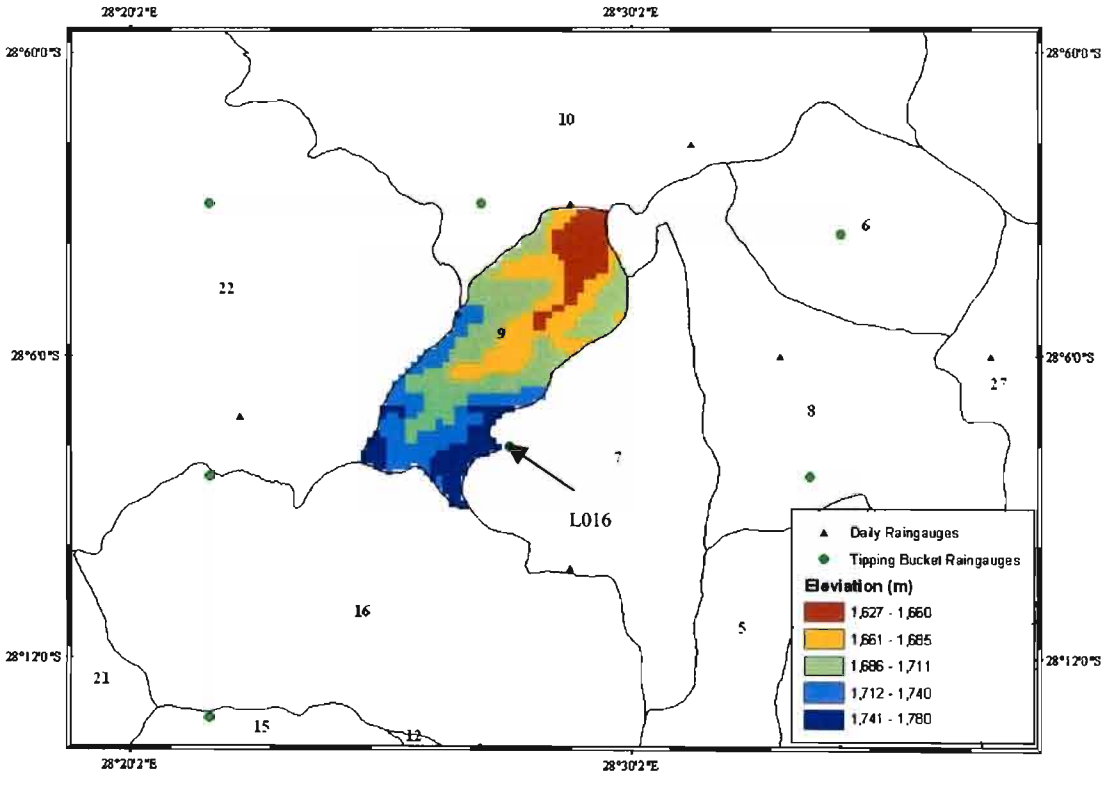

Figure B.9a Altitude map of Subcatchment 9

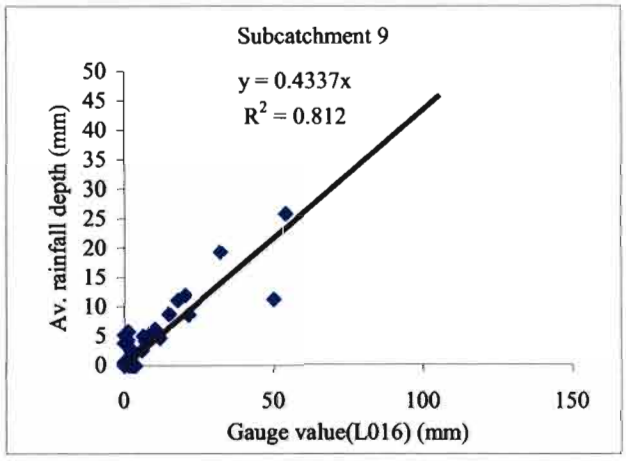

Figure B.9b Mean areal rainfall in Subcatchment 9 vs daily rainfall at tipping bucket Raingauge L016

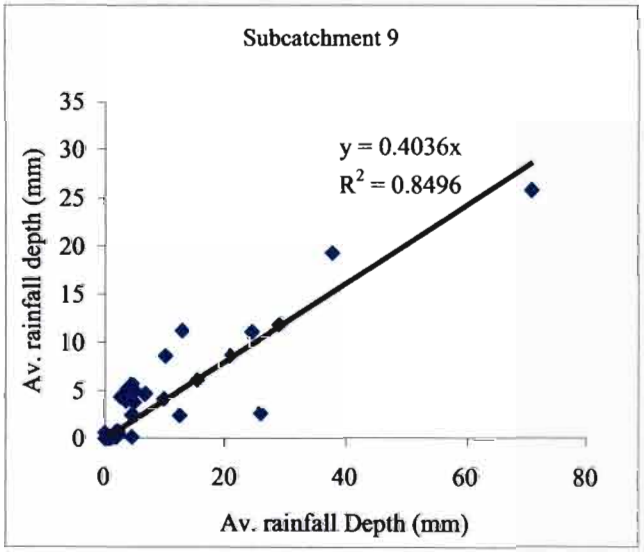

Figure B.9c Mean areal rainfall in Subcatchment 9 vs Mean areal rainfall in Subcatchment 7

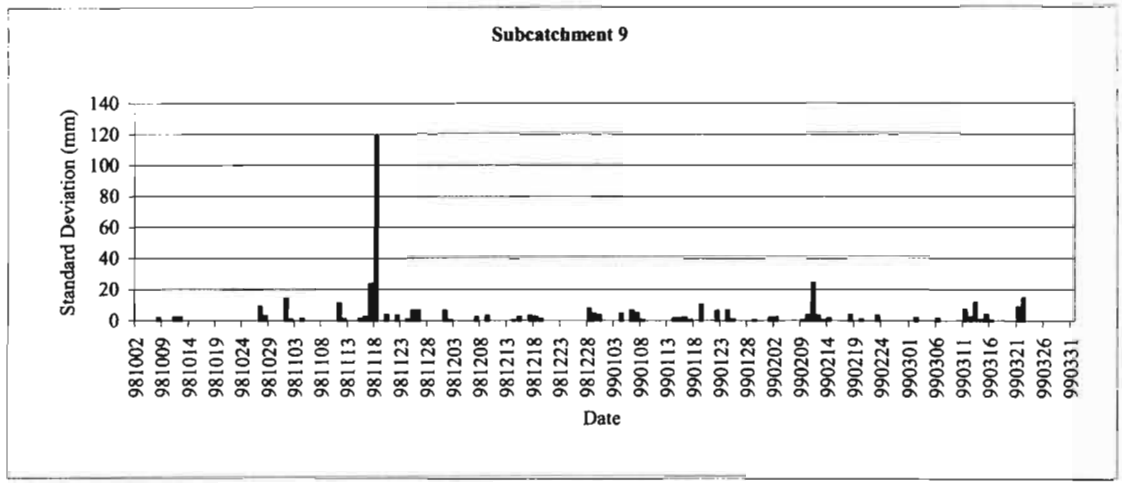

Figure B.9d Standard deviation of the spatial distribution of rainfall in Subcatchment 9

B.10. Subcatchment 10

The Standard deviation of altitude in Subcatchment 10 is 33.6 m, as shown in Figure 5.2. Subcatchment 10 has a relatively big area compared to other subcatchment and it has five tipping bucket raingauges and four daily gauges inside the perimeter (Figure B.10a). However, four of the tipping buckets do not have a continuous data for the periods considered and thus have a negative effect on the evaluation of the mean areal rainfall of the subcatchment, because they are used in the conditioning of the radar images. There is no strong relationship between the daily rainfall from Raingauge 0332002W and the mean areal rainfall of the subcatchment, as shown in Figure B.10b. These could be due to the missing tipping bucket rainfall data used in the conditioning of the radar images. The temporal variation in the spatial rainfall distribution of the subcatchment is shown in Figure B.10c.

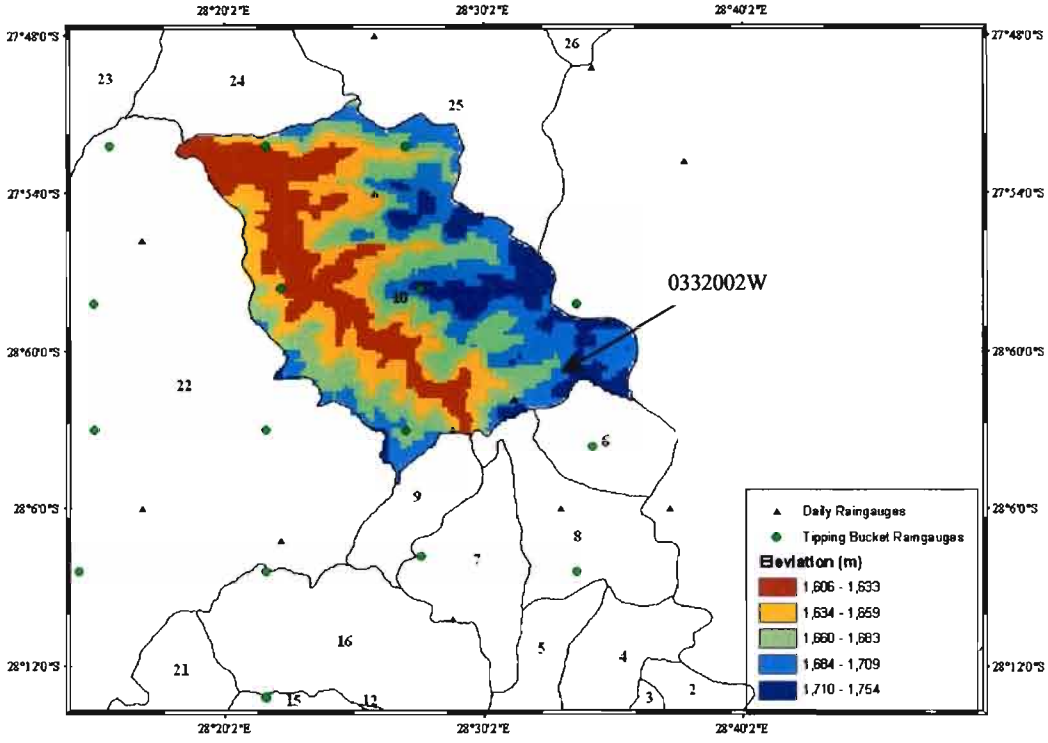

Figure B.10a Altitude map of Subcatchment 10

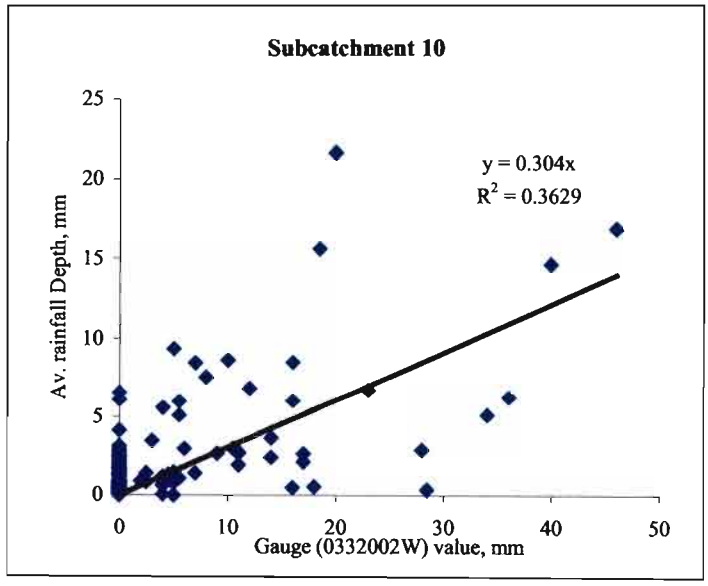

Figure B.10b Mean areal rainfall in Subcatchment 10 vs daily rainfall at Raingauge 0332002W

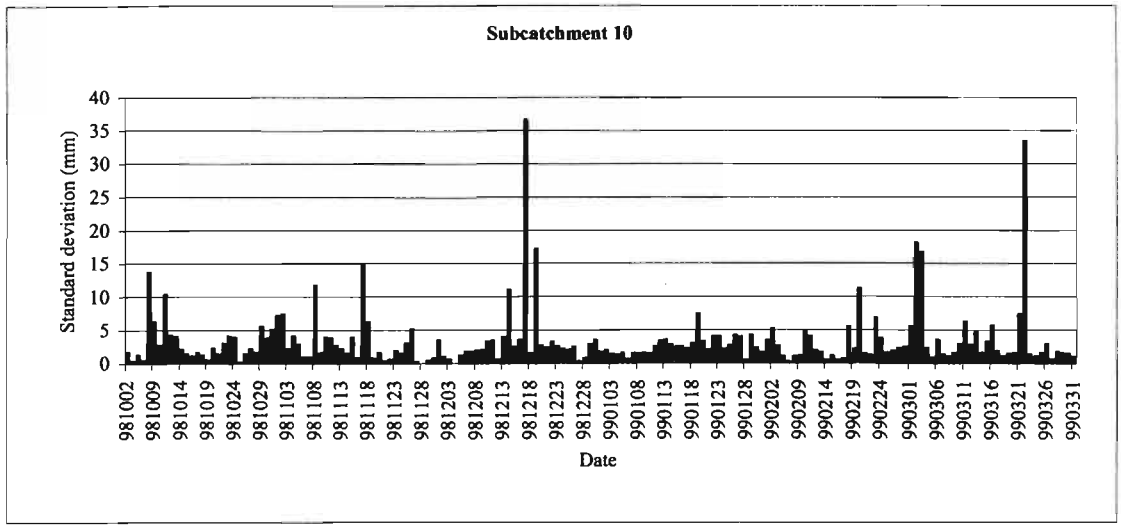

Figure B.10c Standard deviation of the spatial distribution of rainfall in Subcatchment 10

B.11. Subcatchment 11

The standard deviation of altitude Subcatchment 11 is 96 m, as shown in Figure 5.2. Subcatchment 11 is a mountainous area of the Liebenbergsvlei catchment and only tipping bucket Raingauge L003 is situated inside perimeter of the subcatchment (Figure B.11a). The radar images of the subcatchment are highly susceptible to a ground clutter due to the high altitude of the subcatchment. L003 tipping bucket doesn't have a continuous rainfall data for the considered period. The spatial rainfall distribution of the subcatchment is higher and more variable compared to other subcatchment, as shown in Figure B.11b.

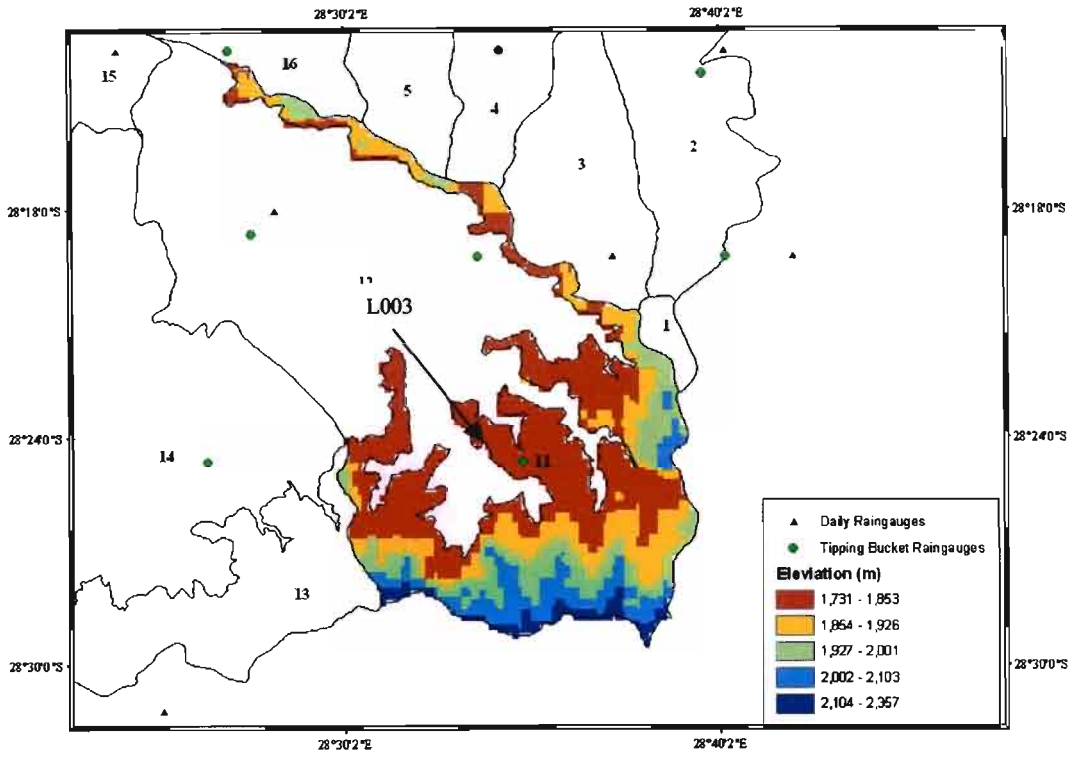

Figure B.11a Altitude map of Subcatchment 11

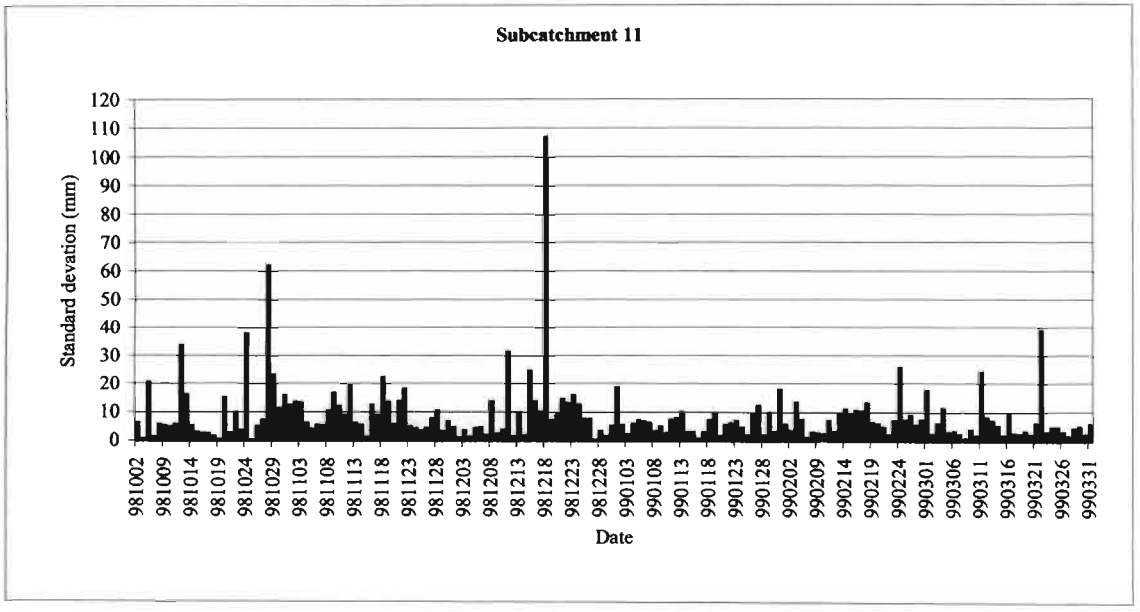

Figure B.11b Standard deviation of the spatial distribution of rainfall in Subcatchment 11

B.12. Subcatchment 12

The Standard deviation of altitude in Subcatchment 12 is 45.5 m, as shown in Figure 5.2. Tipping bucket Raingauges L006 and L007 and Raingauge0331828W are located inside the perimeter of the subcatchment (Figure B.12a). However, both Raingauges L007 and 0331828W do not have a continuous record for the considered period. The standard deviation of the spatial distribution of rainfall in the subcatchment is shown in Figure B.12b, and the values are relatively higher compared to the other subcatchment. The size of the subcatchment is also another factor that affects the relationship between the mean areal rainfall of the subcatchment and point rainfall and is postulated to be the main cause of the weak relationship between the point rainfall of L006 and the mean areal rainfall of the subcatchment.

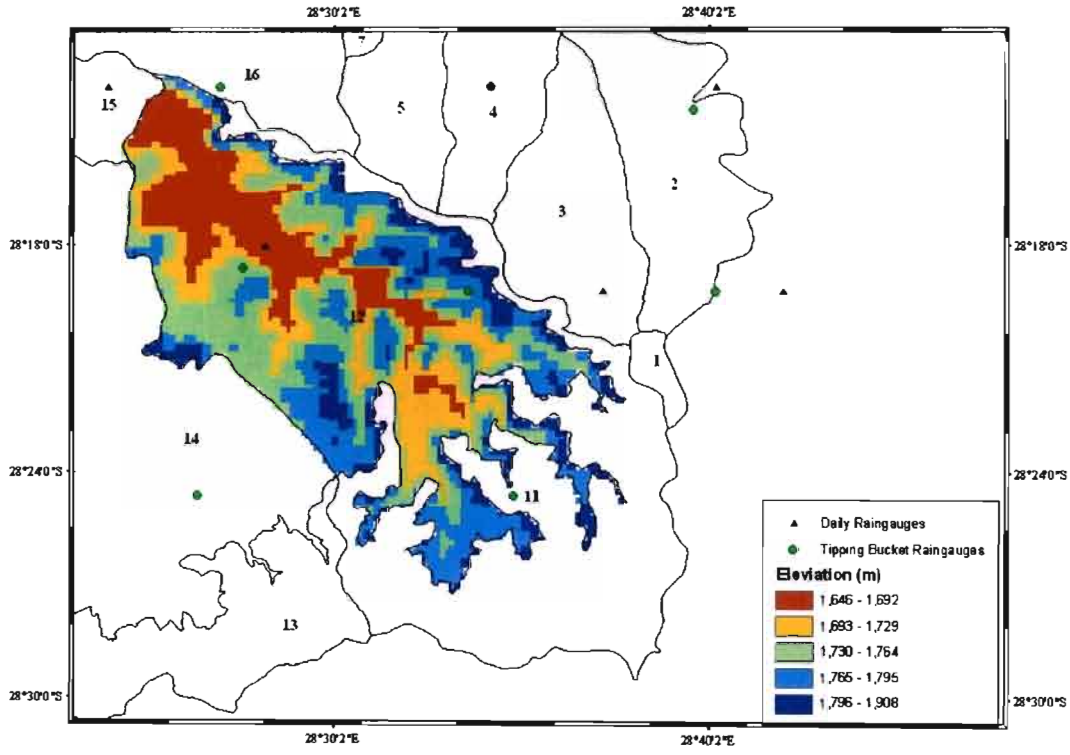

Figure B.12a Altitude map of Subcatchment 12

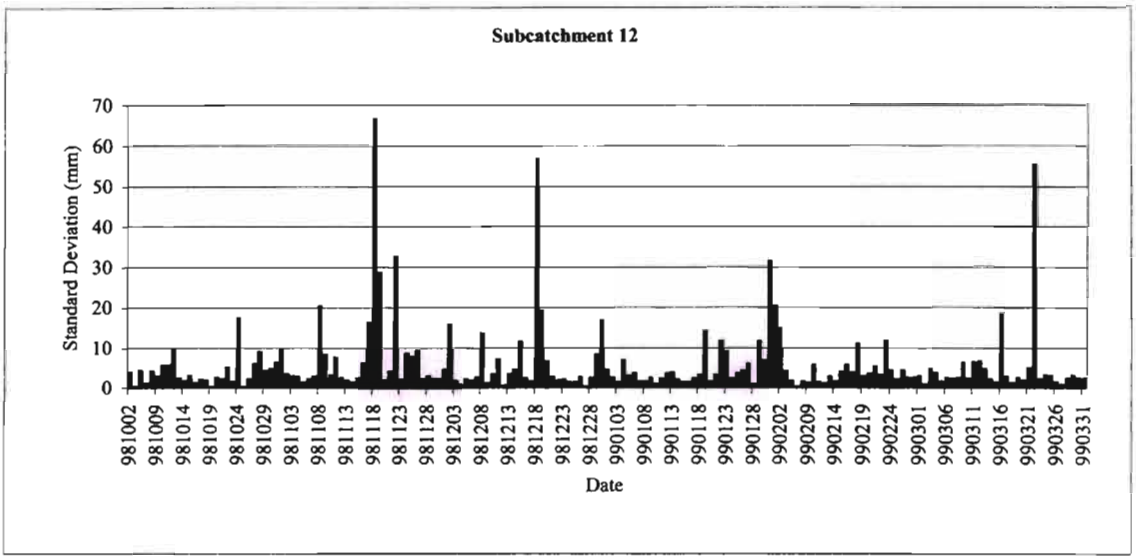

Figure B.12b Standard deviation of the spatial distribution of rainfall in Subcatchment 12

B.13. Subcatchment 13

The standard deviation of altitude in Subcatchment13 is 104 m, as shown in Figure 5.2. The subcatchment is located at a higher altitude relative to the other subcatchments in the Liebenbergsvlei catchment and the radar images for Subcatchment 13 are highly susceptible to ground cluttering as a result of the high elevation. There is no raingauge which is located inside the perimeter of the subcatchment as shown in Figure B.13a. Figure B.13b also shows high variability of spatial rainfall distribution of the subcatchment.

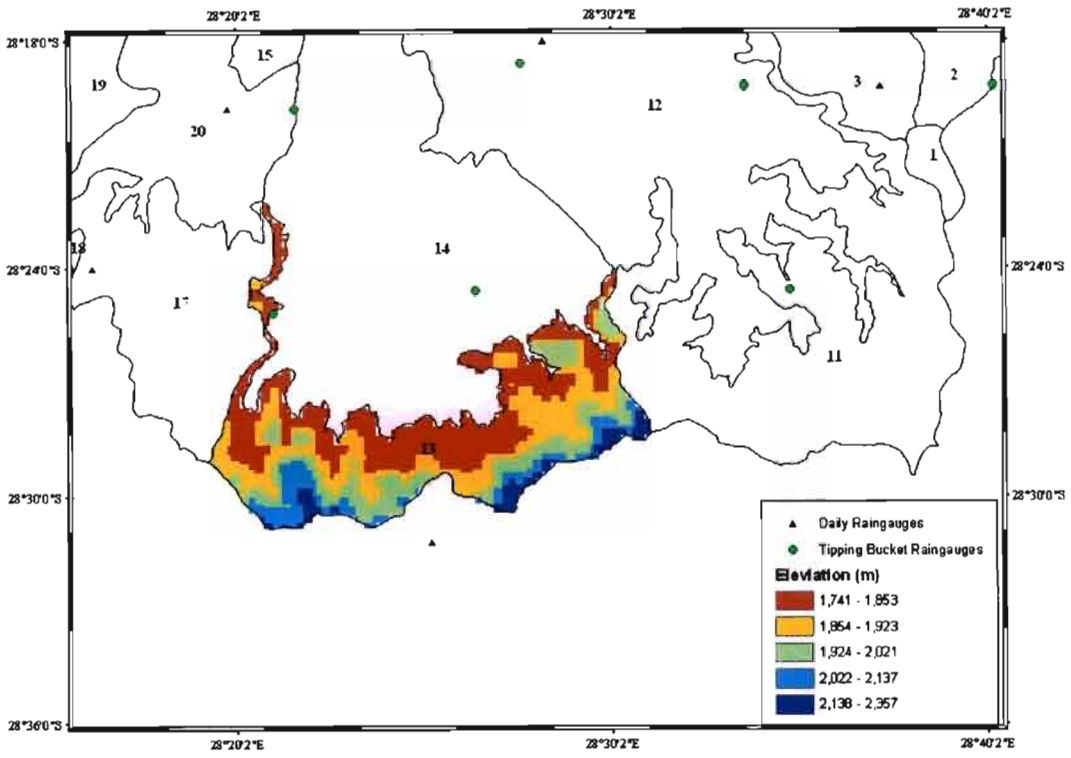

Figure B.13a Altitude map of Subcatchment 13

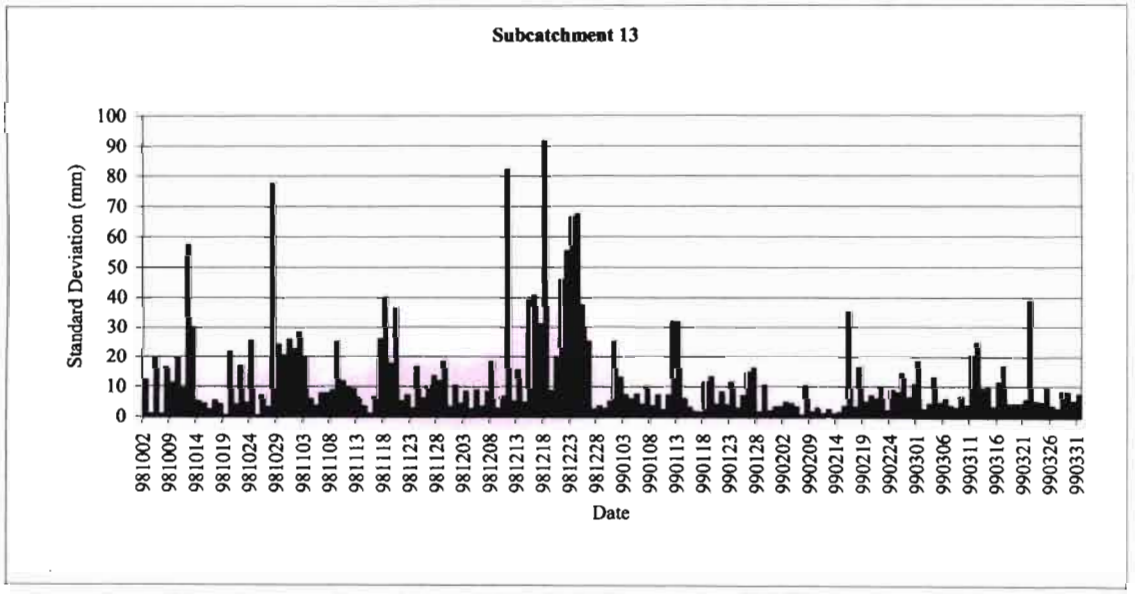

Figure B.13b Standard deviation of the spatial distribution of rainfall in Subcatchment 13

B.14. Subcatchment 14

The standard deviation of altitude in Subcatchment 14 is 43.9 m, as shown in Figure 5.2. Tipping bucket Raingauges L001 (1795 m) and L002 (1753 m) are located inside the subcatchment (Figure B.14a). Raingauge L002 does not have a continuous record for the required period; hence Raingauge L001 rainfall data was selected as the driver station to estimate the mean areal rainfall of the subcatchment. Figure B.14b shows that tipping bucket Raingauge L001 rainfall data represents the areal rainfall of the subcatchment reasonably well, though the spatial rainfall distribution of the subcatchment is relatively variable (Figure B.14c).

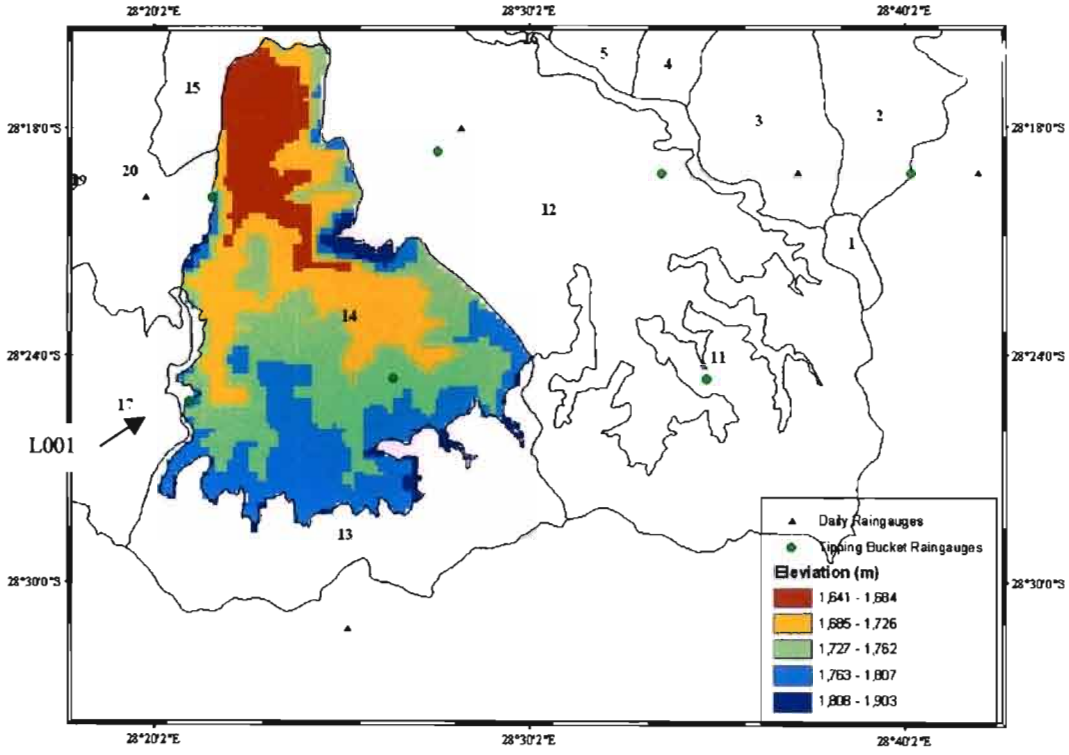

Figure B.14a Altitude map of Subcatchment 14

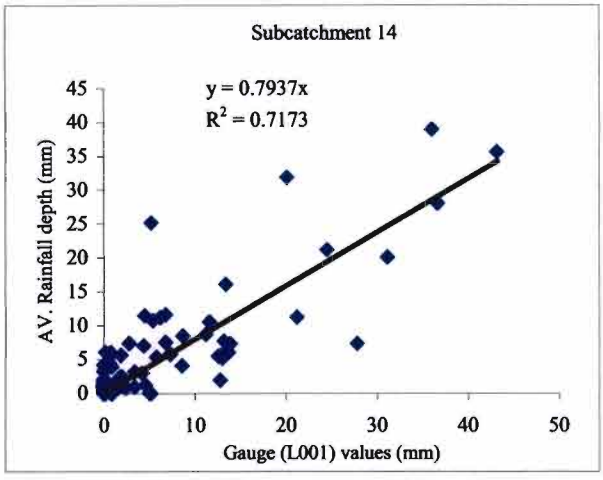

Figure B.14b Mean areal rainfall in Subcatchment 14 vs daily rainfall at tipping bucket Raingauge L001

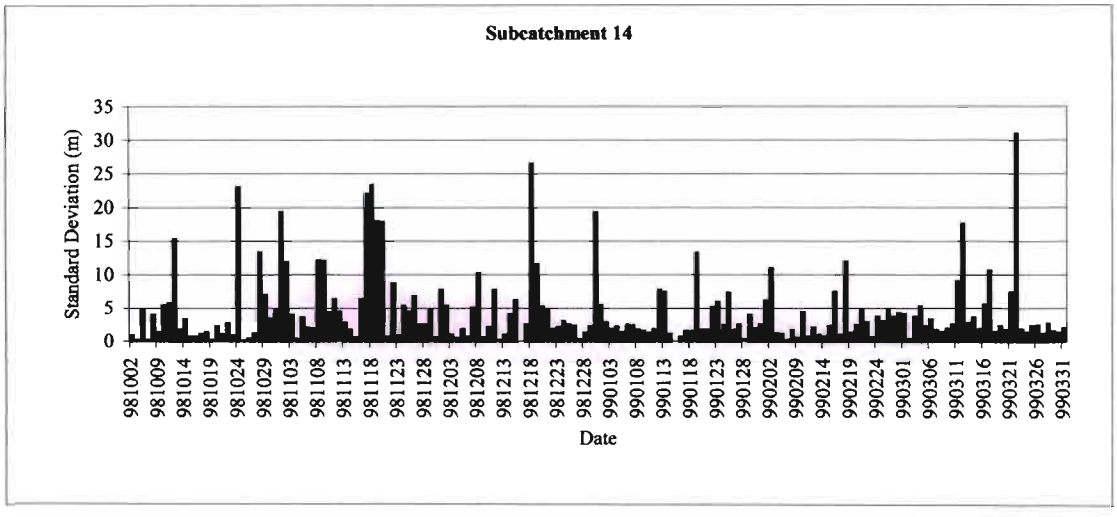

Figure B.14c Standard deviation of the spatial distribution of rainfall in Subcatchment 14

B.15. Subcatchment 15

The standard deviation of altitude in in Subcatchment 15 is 32.9 m, as shown in Figure 5.2. Tipping bucket Raingauge L010 (1662 m) and Raingauge 0331704W (1641 m) are located inside the subcatchment as shown in Figure B.15a. Tipping bucket L010 rainfall data represents the areal rainfall of the subcatchment reasonably well as shown in Figure B.15b, while rainfall data

from Raingauge 0331704W are missing for the required period. The spatial rainfall distribution of the subcatchment is reasonably uniform with low standard deviation (Figure B.15c).

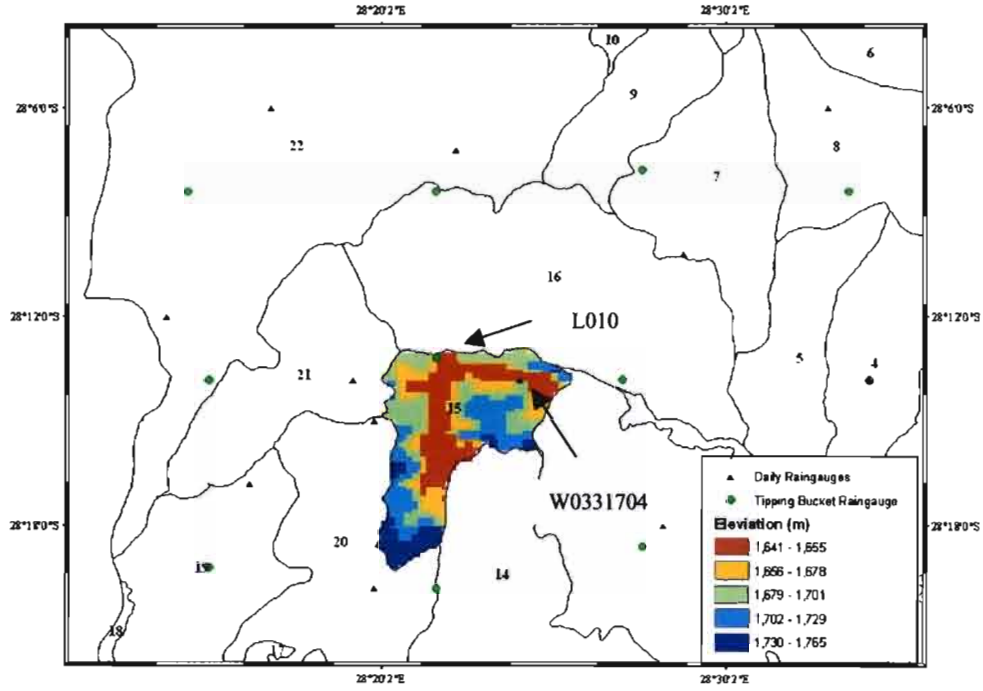

Figure B.15a Altitude map of Subcatchment 15

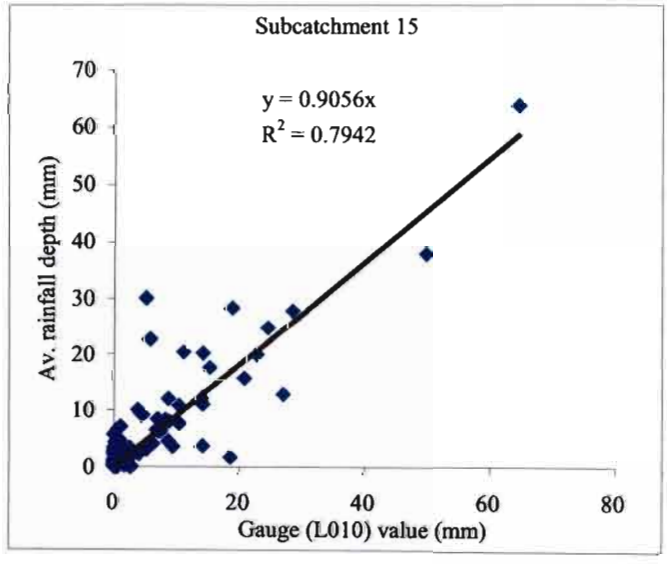

Figure B.15b Mean areal rainfall in Subcatchment 15 vs daily rainfall at tipping bucket Raingauge L010

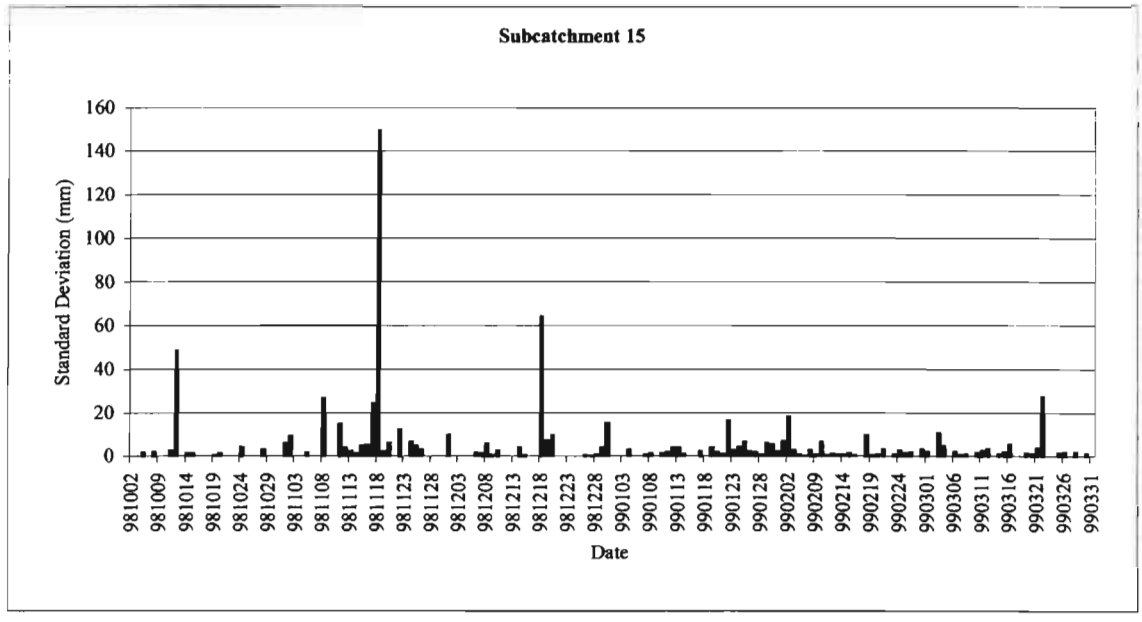

Figure B.15c Standard deviation of the spatial distribution of rainfall in Subcatchment 15

B.16. Subcatchment 16

The standard deviation of altitude in Subcatchment 16 is 60.4 m, as shown in Figure 5.2. Tipping bucket Raingauges L011 (1759 m) and L015 (1723 m) are located inside the subcatchment as shown in Figure B.16a. Tipping bucket Raingauge L015 rainfall data represents the areal rainfall of the subcatchment better than tipping bucket Raingauge L011 as shown in Figures B.16b and B.16c. The spatial rainfall distribution is relatively steady over the period considered, except for 18 November1998 (Figure B.16d). These could be due errors related with radar rainfall measurement quality.

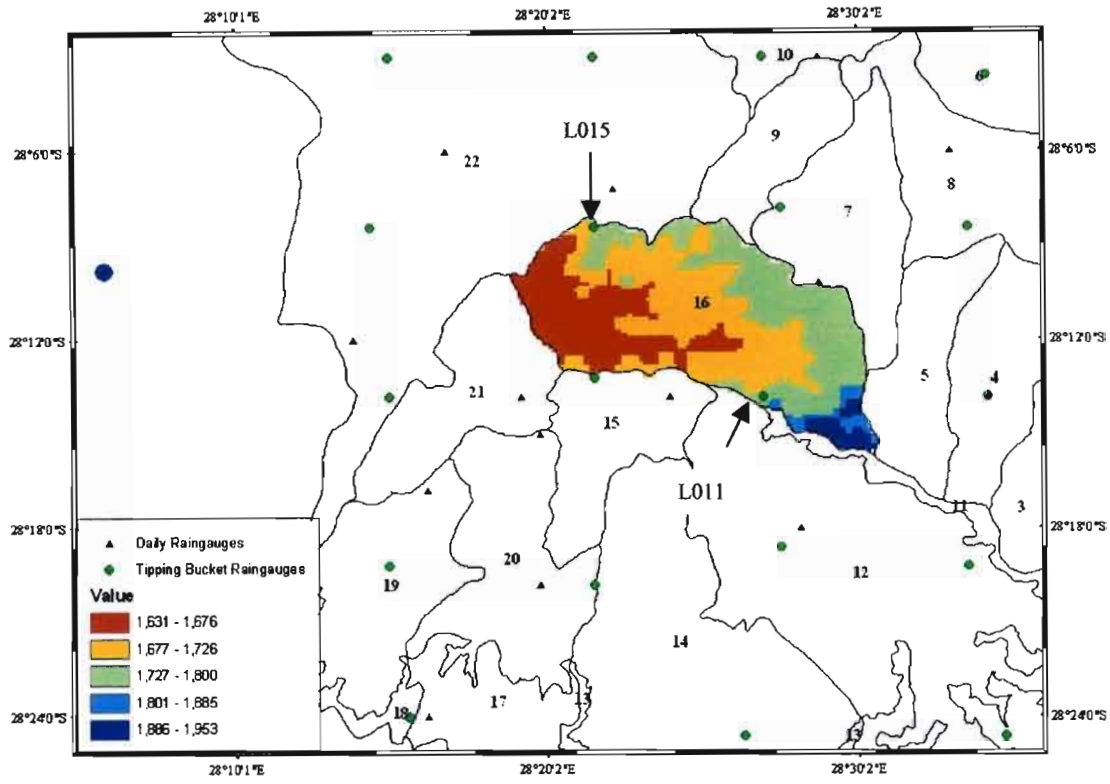

Figure B.16a Altitude map of Subcatchment 16

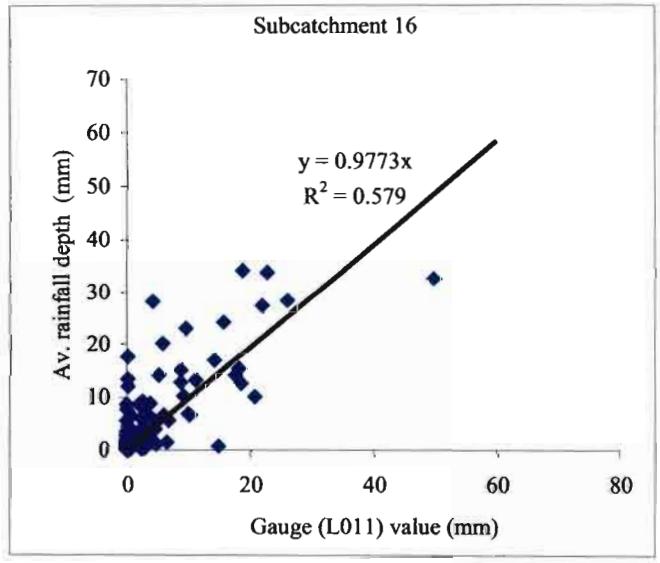

Figure B.16b Mean areal rainfall in Subcatchment 16 vs daily rainfall at tipping bucket Raingauge L011

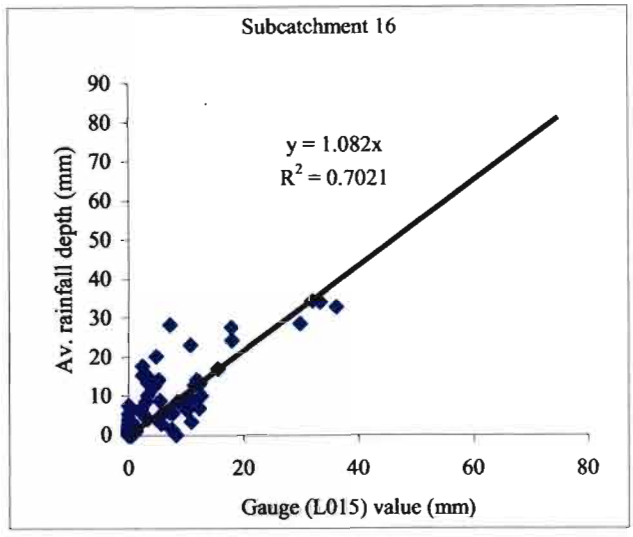

Figure B.16c Mean areal rainfall in Subcatchment 16 vs daily rainfall at tipping bucket Raingauge L015

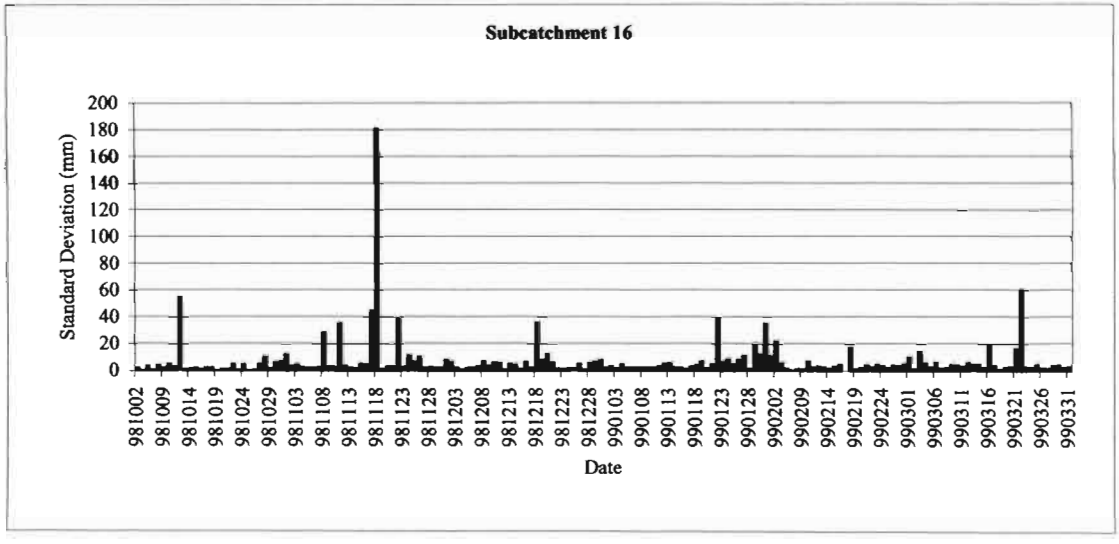

Figure B.16d Standard deviation of the spatial distribution of rainfall in Subcatchment 16

B.17. Subcatchment 17

The standard deviation of altitude in Subcatchment 17 is 41 m, as shown in Figure 5.2. Raingauge 0331474W is located inside the subcatchment, but daily rainfall data for this gauge the

required period is not reliable. While tipping bucket Raingauge L045 (1920 m) is just outside of the subcatchment as shown in Figure B.17a, data from Raingauge L045 represents the areal rainfall of the subcatchment reasonably, well as shown in Figure B.17b. The standard deviation of spatial rainfall in the subcatchment on a daily bases is shown in Figure B.17c and it is more variable compared to the other subcatchments.

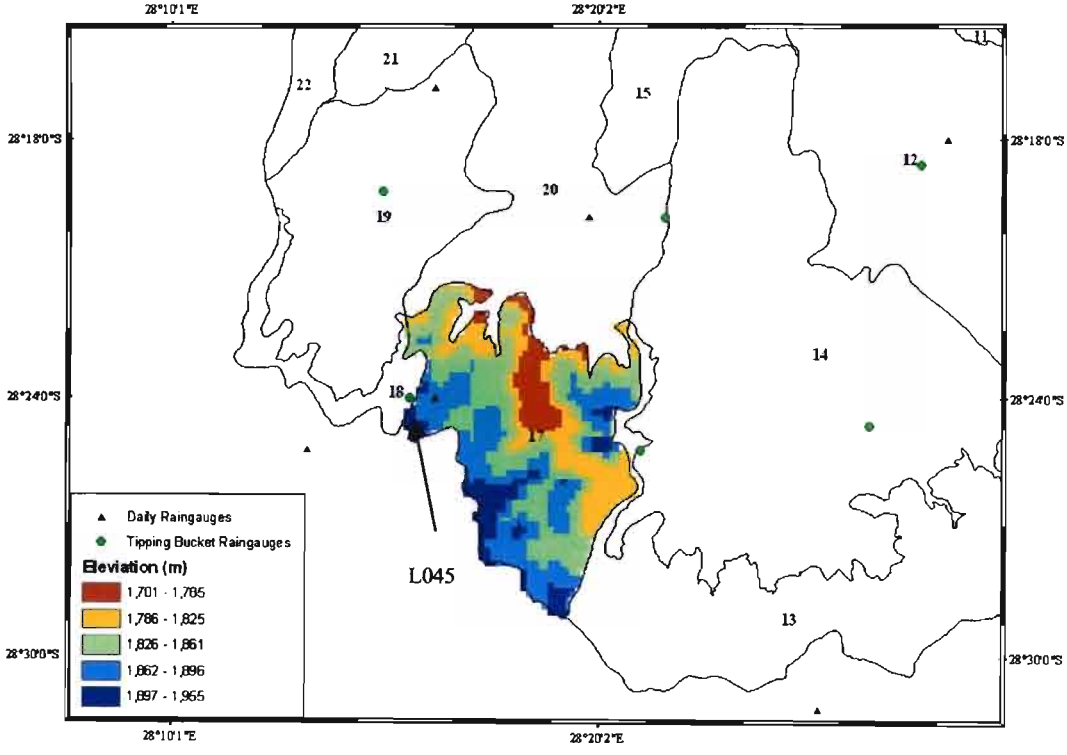

Figure B.17a Altitude map of Subcatchment 17

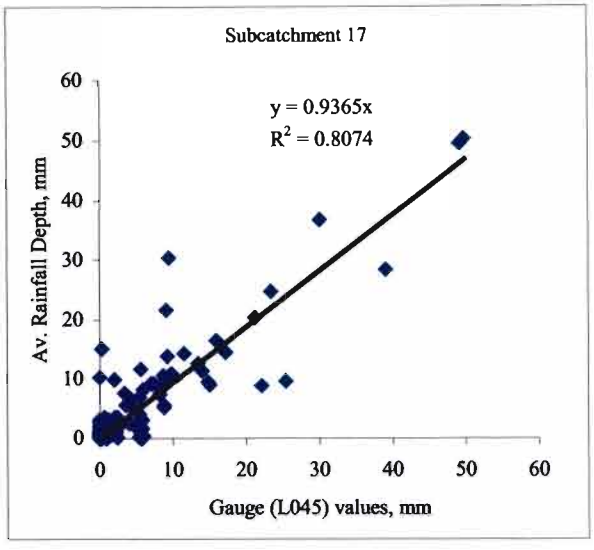

Figure B.17b Mean areal rainfall in Subcatchment 17 vs daily rainfall at tipping bucket Raingauge L045

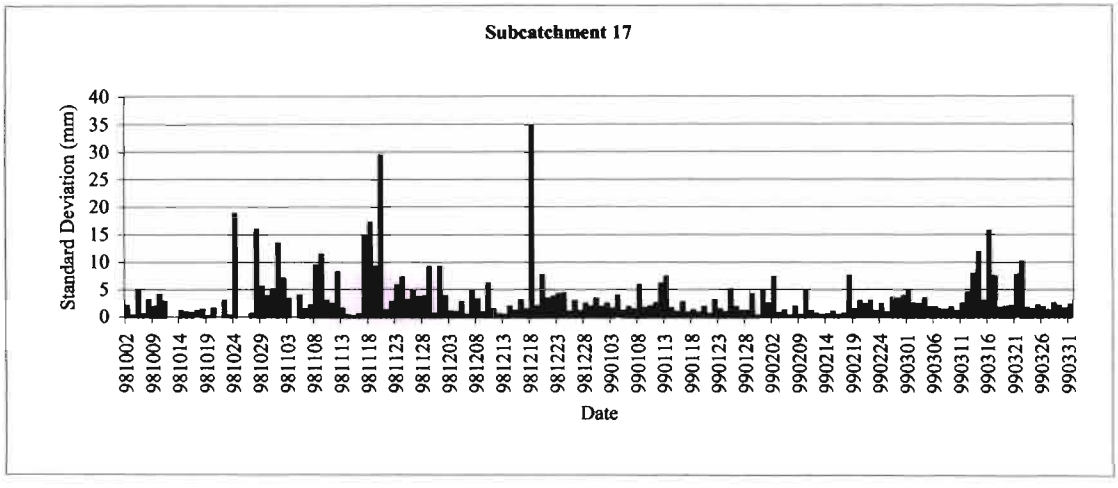

Figure B.17c Standard deviation of the spatial distribution of rainfall in Subcatchment 17

B.18. Subcatchment 18

The standard deviation of altitude in Subcatchment 18 is 45.6 m, as shown in Figure 5.2. Tipping bucket Raingauge L045 (1920 m) is the only raingauge located inside the perimeter of the subcatchment as shown in Figure B.18a, its rainfall data represents the areal rainfall of

Subcatchment reasonably well as shown in Figure B.18b. The standard deviation of the spatial rainfall of the subcatchment on a daily bases is shown in Figure B.18c.

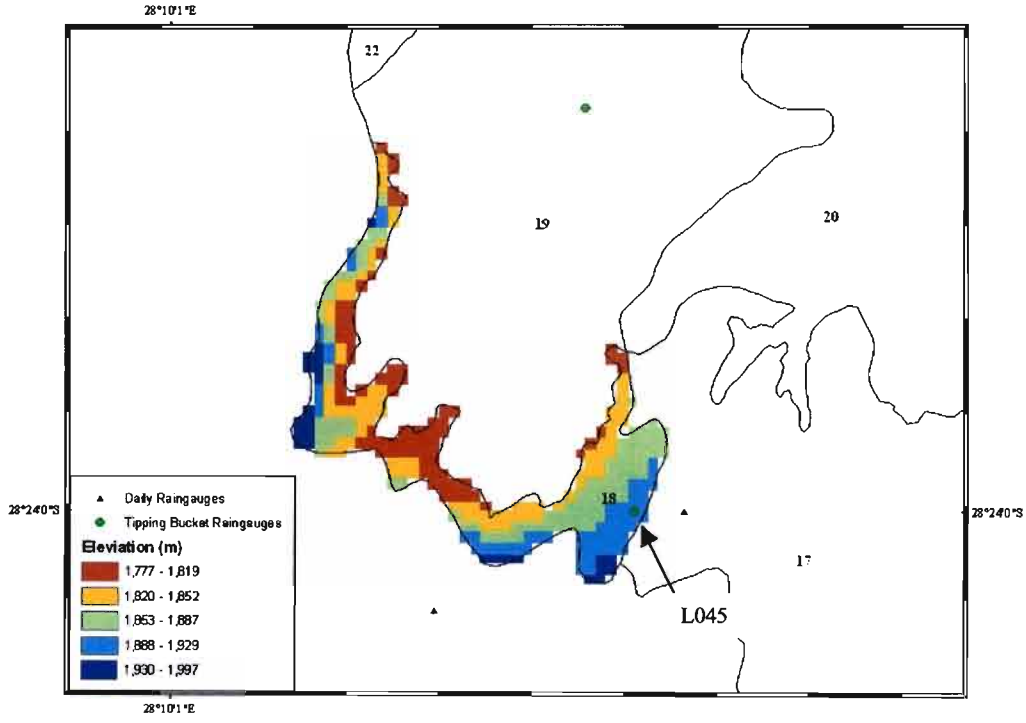

Figure B.18a Altitude map of Subcatchment 18

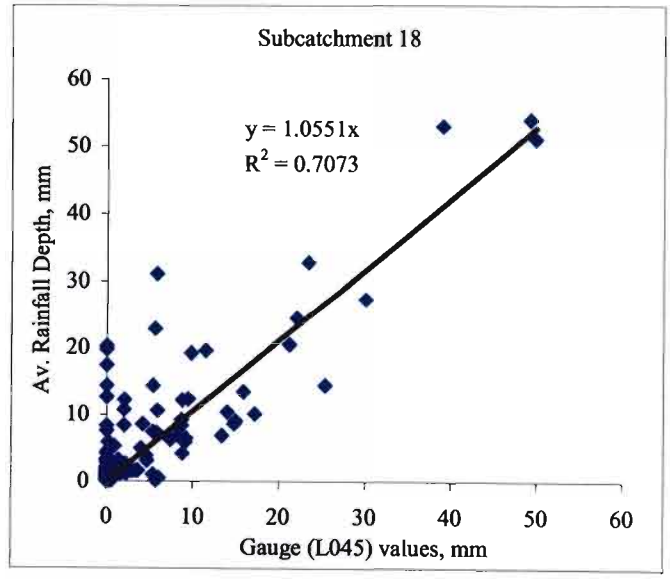

Figure B.18b Mean areal rainfall in Subcatchment 18 vs daily rainfall at tipping bucket Raingauge L045

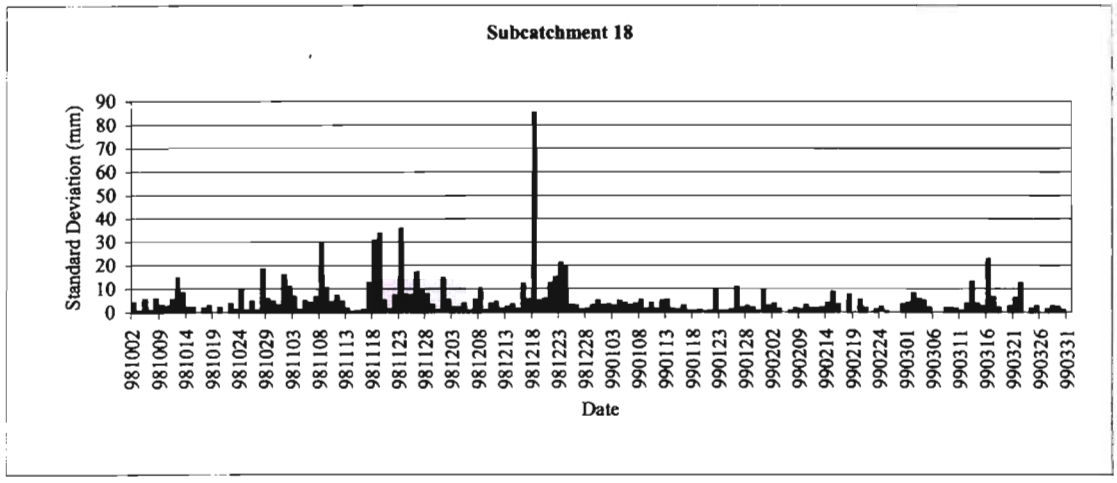

Figure B.18c Standard deviation of the spatial distribution of rainfall in Subcatchment 18

B.19. Subcatchment 19

The standard deviation of altitude in Subcatchment 19 is 31.7 m, as shown in Figure 5.2. Tipping bucket Raingauge L004 (1699 m) and Raingauge 0331467W (1716 m) are located inside the subcatchment as shown in Figure B.19a; however Raingauge 0331467W rainfall data is not reliable the required period. Daily rainfall data from Raingauge L004 represents the areal rainfall of the subcatchment satisfactorily, as shown in Figure B.19b. The standard deviation of spatial rainfall distribution of subcatchment is shown in Figure B.19c.

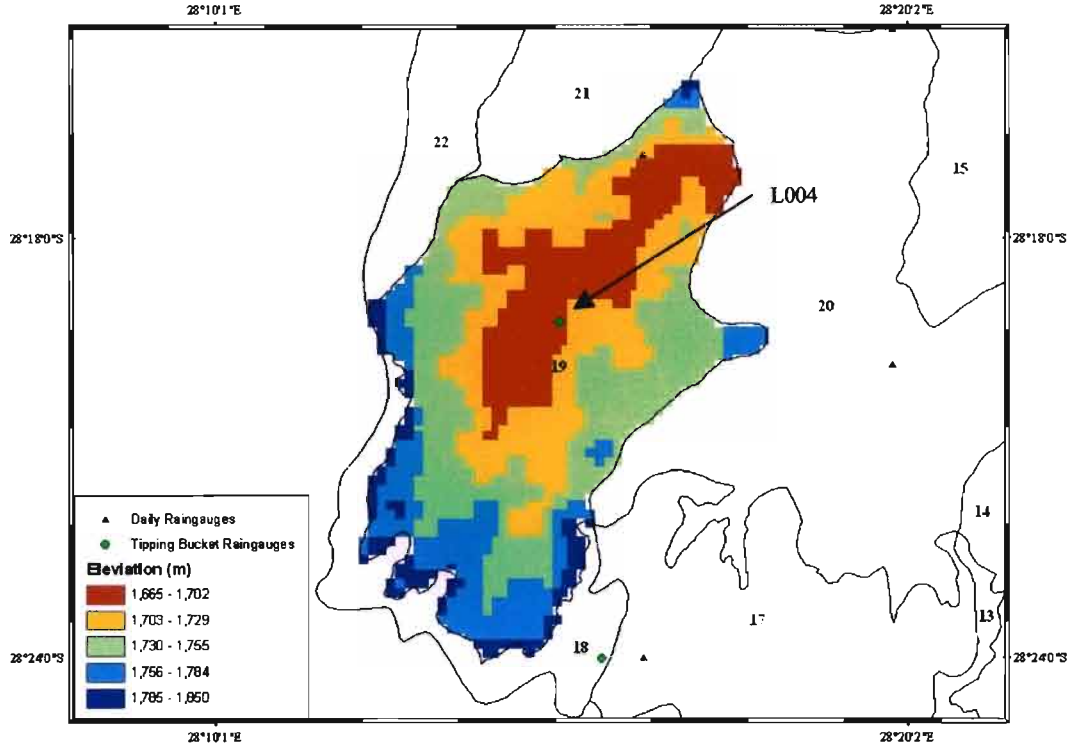

Figure B.19a Altitude map of Subcatchment 19

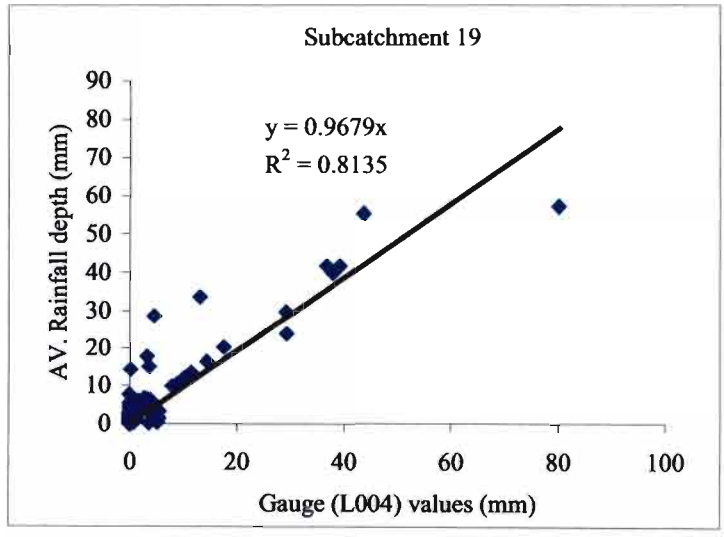

Figure B.19b Mean areal rainfall in Subcatchment 19 vs daily rainfall at tipping bucket Raingauge L004

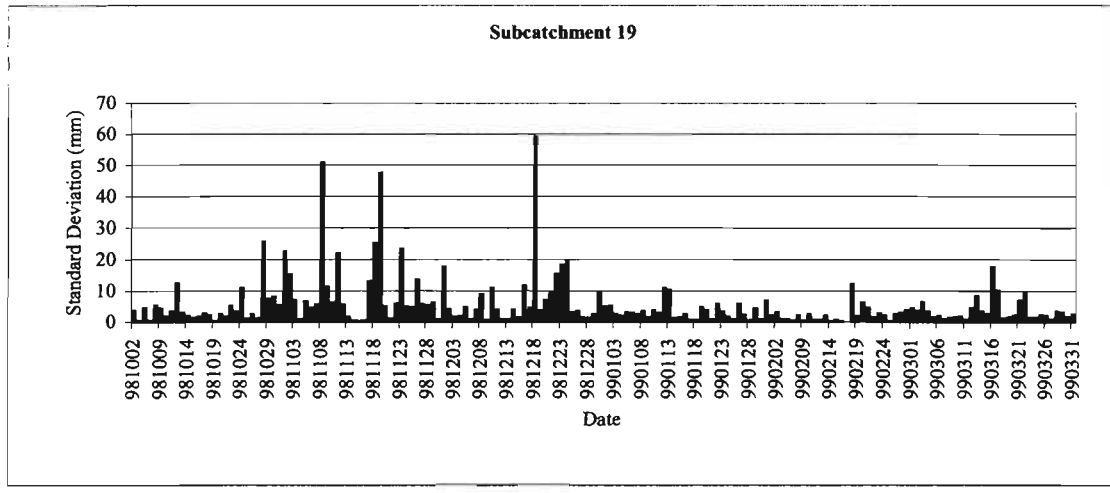

Figure B.19c Standard deviation of the spatial distribution of rainfall in Subcatchment 19

B.20. Subcatchmnet20

The standard deviation of altitude in Subcatchment 20 is 41.3 m, as shown in Figure 5.2. Tipping bucket Raingauge L005 (1779 m) and Raingauge 0331590W (1722 m) are located inside the subcatchment as shown in Figure B.20a and their daily rainfall data represent the areal rainfall of the subcatchment reasonably well as a shown in Figure B.20b and B.20c. Some of the days from considered have a high variation of spatial rainfall over the subcatchment, while the other days have a relatively uniform spatial distribution rainfall, as shown in Figure B.20d.

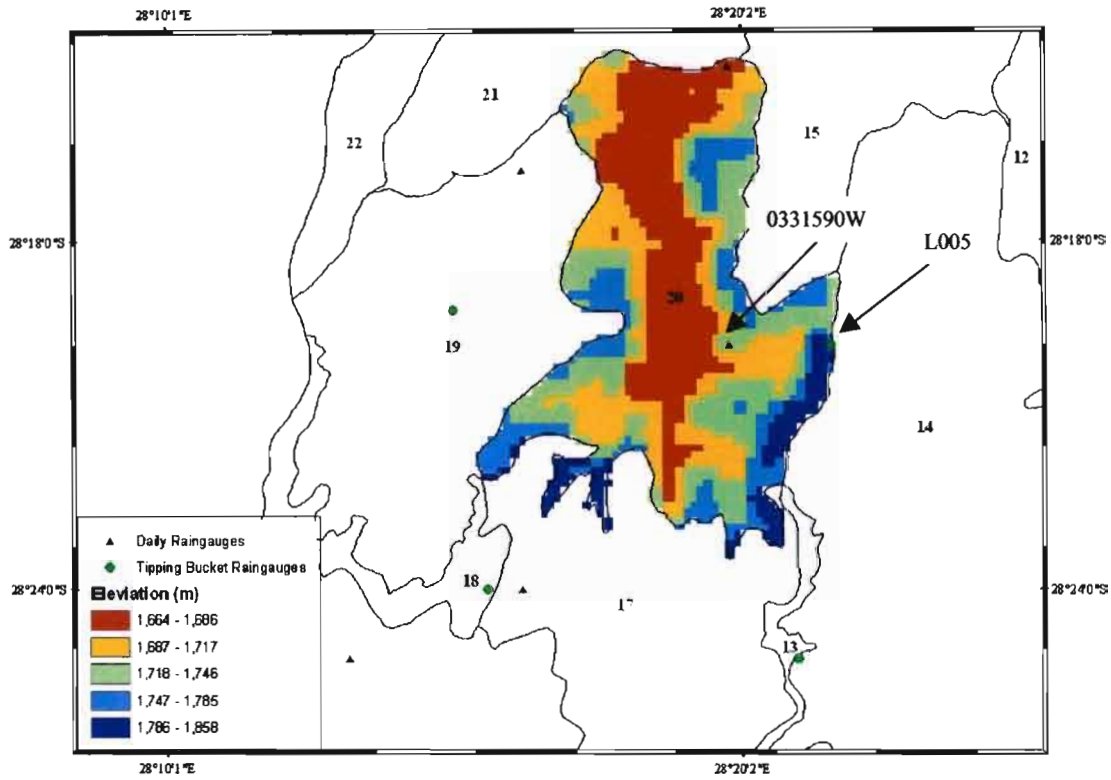

Figure B.20a Altitude map of Subcatchment 20

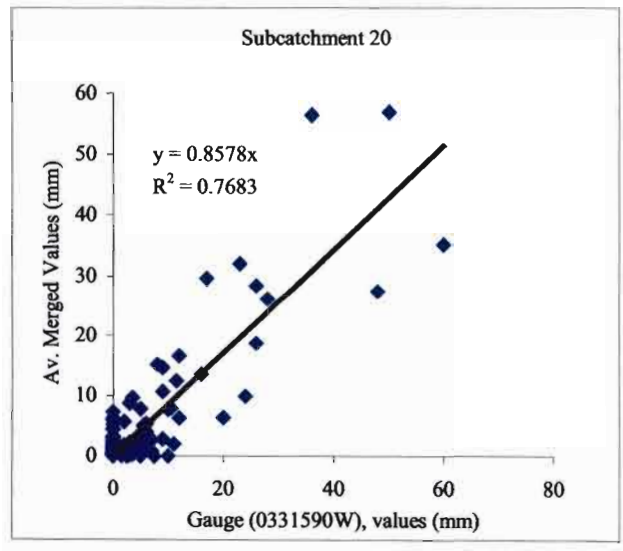

Figure B.20b Mean areal rainfall in Subcatchment 20 vs daily rainfall at Raingauge 0331590W

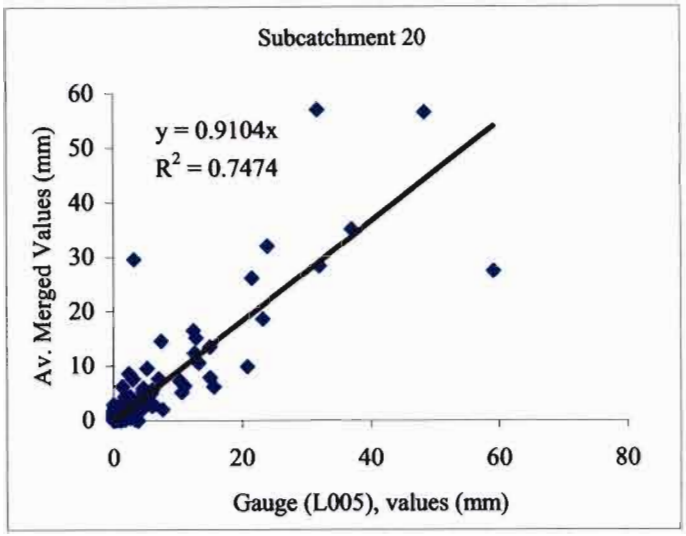

Figure B.20c Mean areal rainfall in Subcatchment 20 vs daily rainfall at tipping bucket Raingauge L005

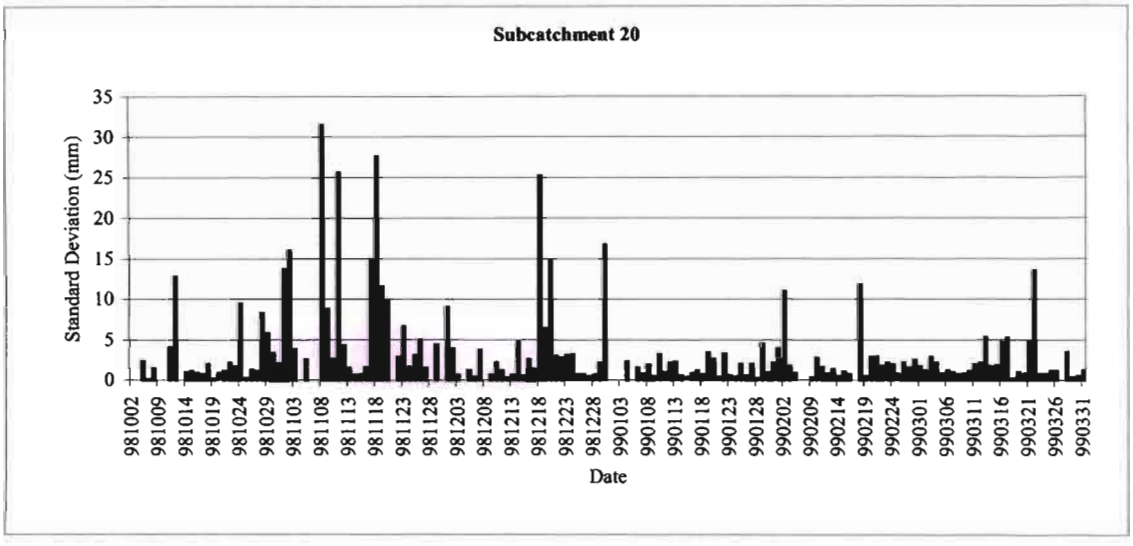

Figure B.20d Standard deviation of the spatial distribution of rainfall in Subcatchment 20

B.21. Subcatchment 21

The standard deviation of altitude in Subcatchment 21 is 35.2 m, as shown in Figure 5.2. Raingauge 0331554W is the only gauge located inside the perimeter of the subcatchment as shown in Figure B.21a; however rainfall data from Raingauge 0331554W for the required period is not reliable. Therefore, tipping bucket Raingauge L009 (1683 m) and Raingauge 0331585W (1711 m) were chosen to represent the areal of the subcatchment and their daily rainfall represents the areal rainfall of the subcatchment reasonably well, as shown in Figure B.21b (i) and B.21b(ii). The spatial rainfall of the subcatchment is relatively uniform for most of the days as shown in Figure B.21c.

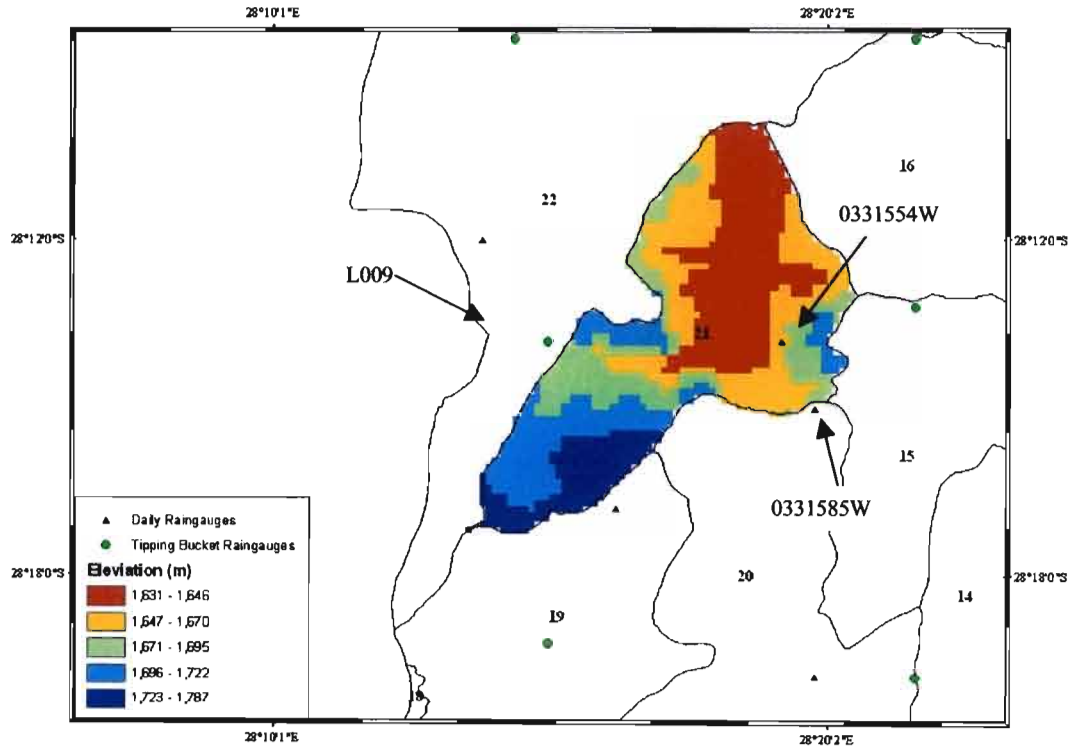

Figure B.21a Altitude map of Subcatchment 21

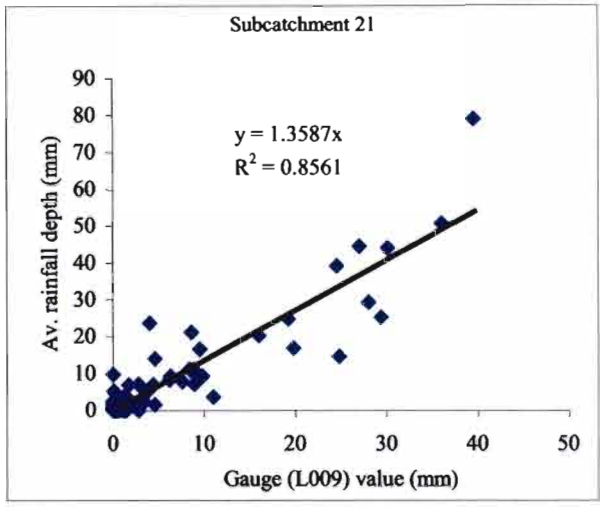

Figure B.21b(i) Mean areal rainfall in Subcatchment 21 vs daily rainfall at tipping bucket Raingauge L009

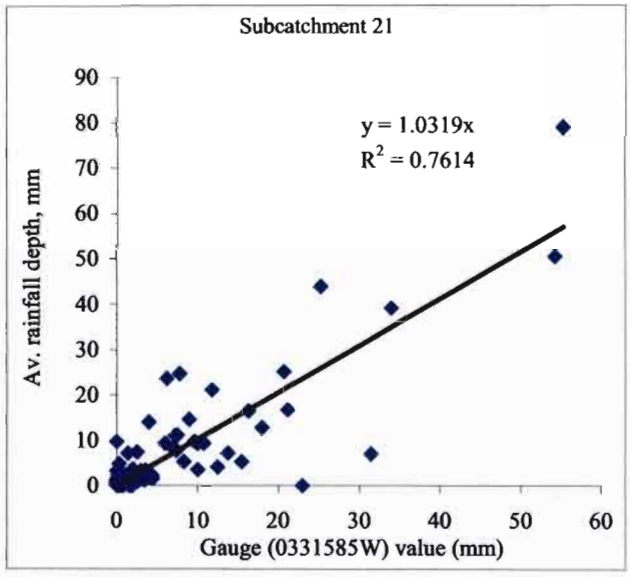

Figure B.21b(i) Mean areal rainfall in Subcatchment 21 vs daily rainfall at Raingauge 0331585W

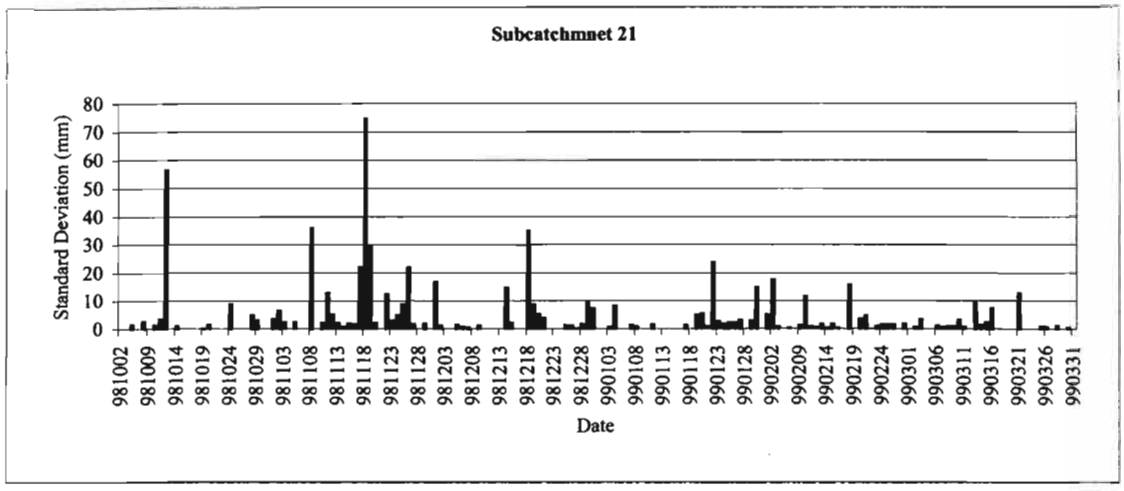

Figure B.21c Standard deviation of the spatial distribution of rainfall in Subcatchment 21

B.22. Subcatchment 22

The standard deviation of altitude in Subcatchment 22 is 33.0 m, as shown in Figure 5.2, and it is located in relatively flat part of Liebenbergsvlei catchment. There are four tipping bucket and three daily raingauges inside the subcatchment, as shown in Figure B.22a. Tipping bucket Raingauges L022, L019 and daily Raingauge 0331607W were selected to compare their daily rainfall data with the areal rainfall of the subcatchment. The subcatchment is also located close to the radar station and part of the subcatchment is masked out because it is outreach of the radar beam. The radar measures the reflectivity of the rain at 2 km above the ground to avoid ground cluttering. Figure B.22b shows that the relationship of the point rainfall from the three raingauges against the areal rainfall of the subcatchment, and there is a satisfactory relationship. Rainfall data from Raingauge 0331607W represents the areal rainfall of the subcatchment better than the two tipping bucket raingauges. There is relatively uniform spatial rainfall distribution of rainfall in the subcatchment, as shown in Figure B.22c, even though the size of the subcatchment is relatively big.

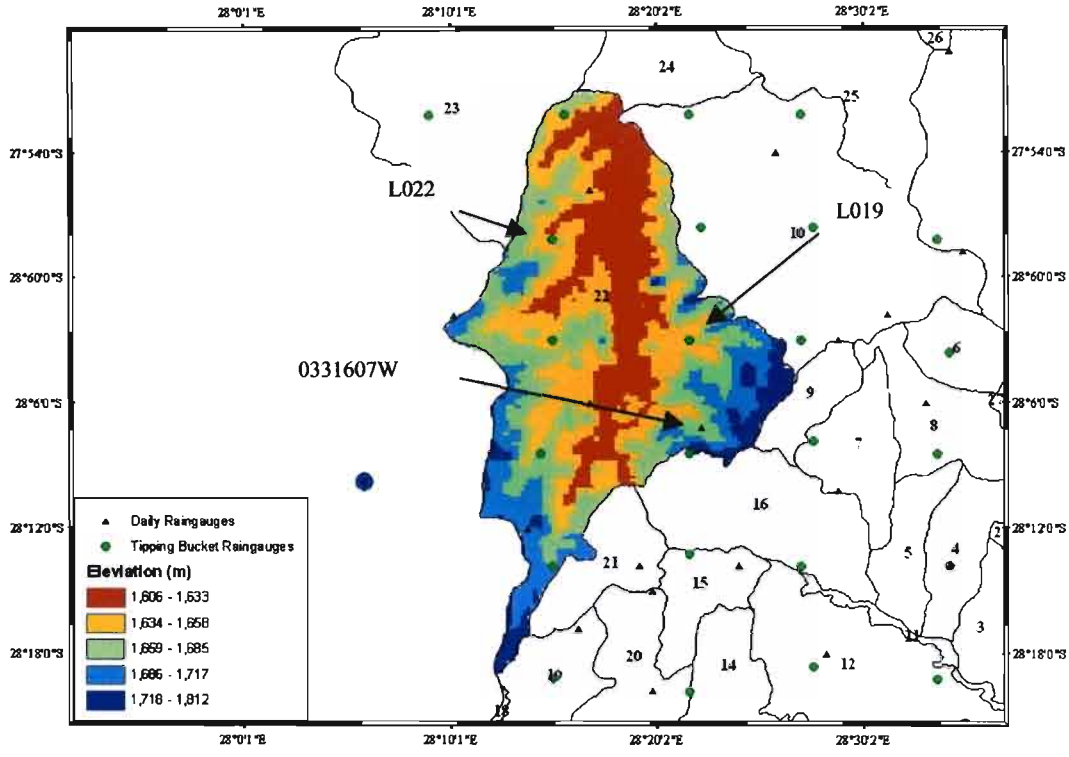

Figure B.22a Altitude map of Subcatchment 22

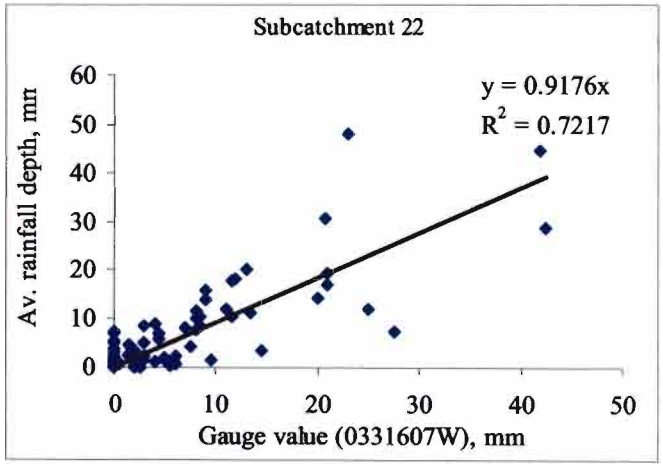

Figure B.22b(i) Mean areal rainfall in Subcatchment 22 vs daily rainfall at Raingauge 0331607W

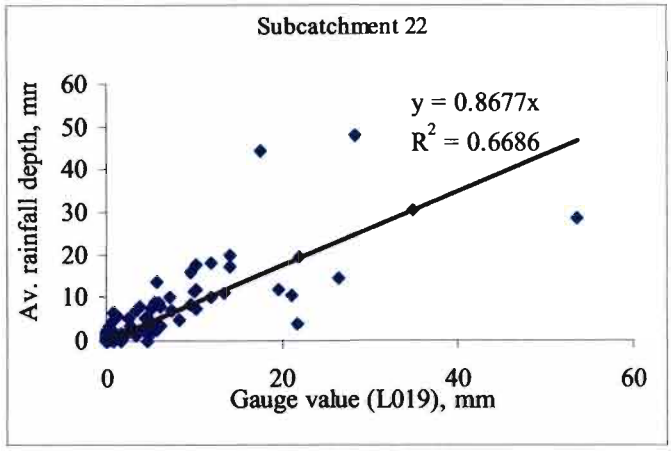

FigureB.22 b(ii) Mean areal rainfall in Subcatchment 22 vs daily rainfall at tipping bucket Raingauge L019

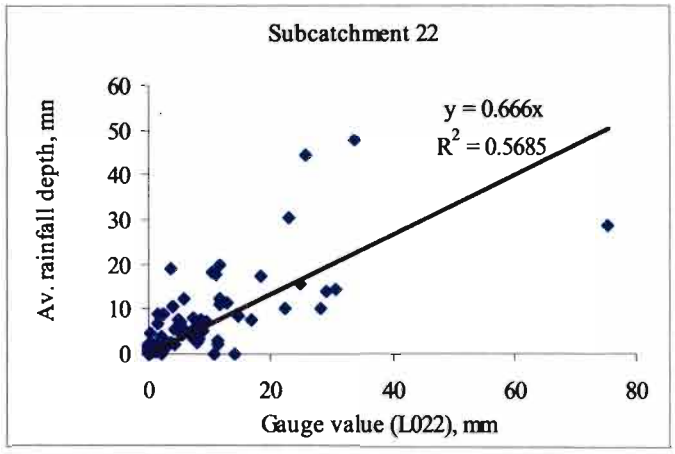

FigureB.22b(iii) Mean areal rainfall in Subcatchment 22 vs daily rainfall at tipping bucket Raingauge L022

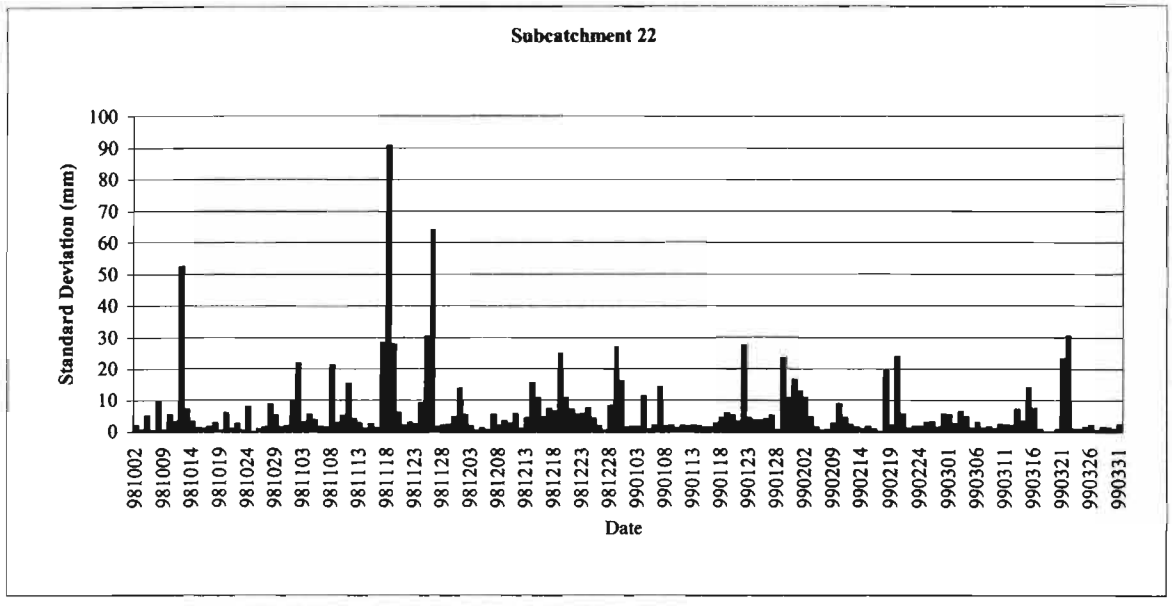

Figure B.22c Standard deviation of the spatial distribution of rainfall in Subcatchment 22

B.24. Subcatchment 24

The standard deviation of altitude in Subcatchment 24 is 42.9 m, as shown in Figure 5.2. There are three tipping buckets and two daily raingauges inside the subcatchment as shown in Figure B.24a. Tipping bucket Raingauge L035 and the two daily raingauges do not have a continuous record for the required period. Therefore tipping bucket Raingauge L031 (1603 m) and L038 (1640 m) are used to compare point rainfall data with the mean areal rainfall of the subcatchment, as shown in Figure B.24b. Both the tipping bucket and daily raingauge data represent the areal rainfall of the subcatchment reasonably well. The spatial rainfall distribution of the subcatchment on a daily bases is shown in Figure B.24c and it is relatively uniform for most of the days.

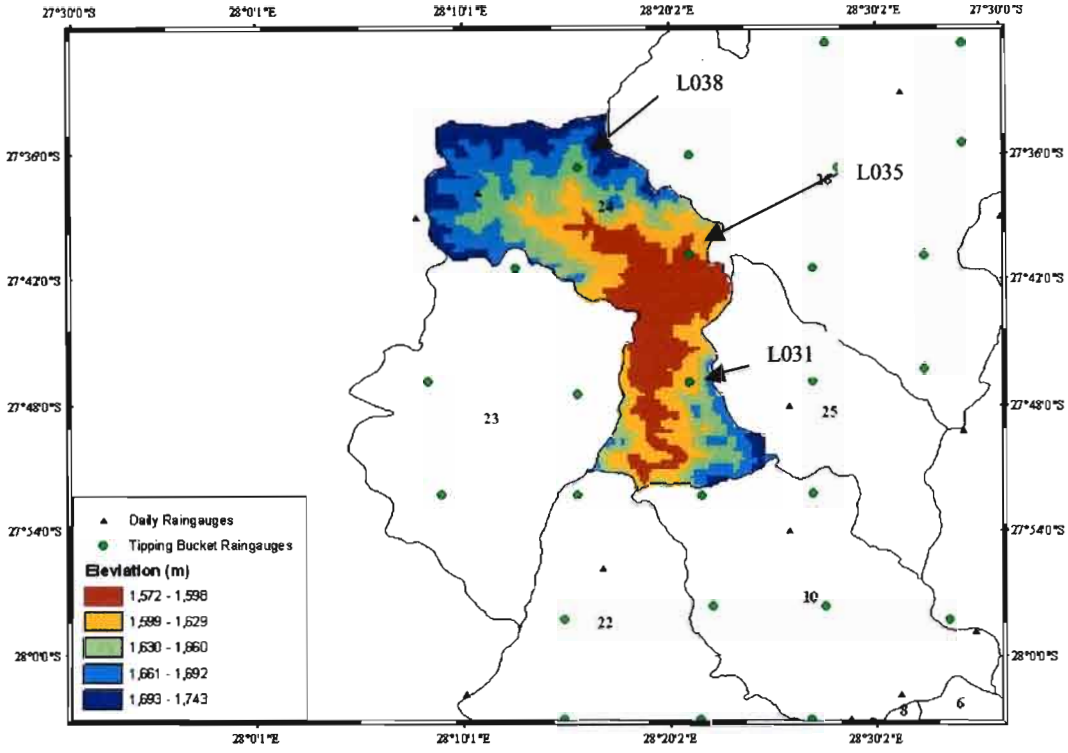

Figure B.24a Altitude map of Subcatchment 24

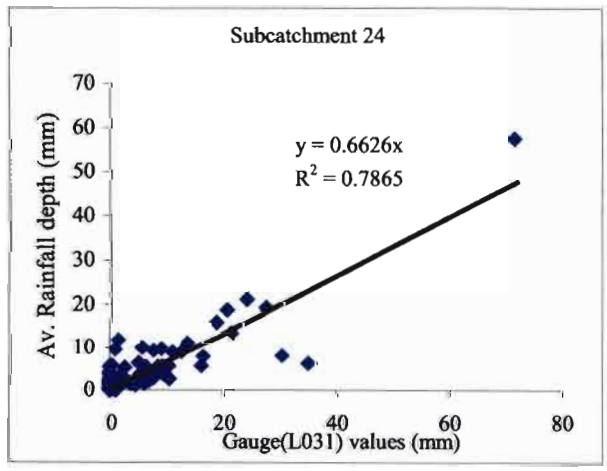

Figure B.24b(i) Mean areal rainfall in Subcatchment 24 vs daily rainfall at tipping bucket Raingauge L031

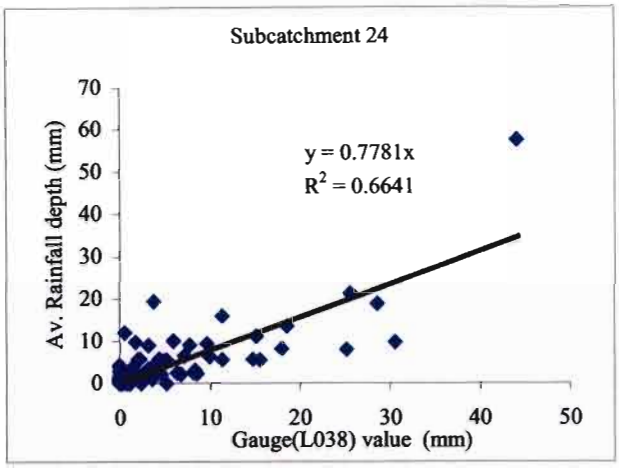

Figure B.24b(ii) Mean areal rainfall in Subcatchment 24 vs daily rainfall at tipping bucket Raingauge L038

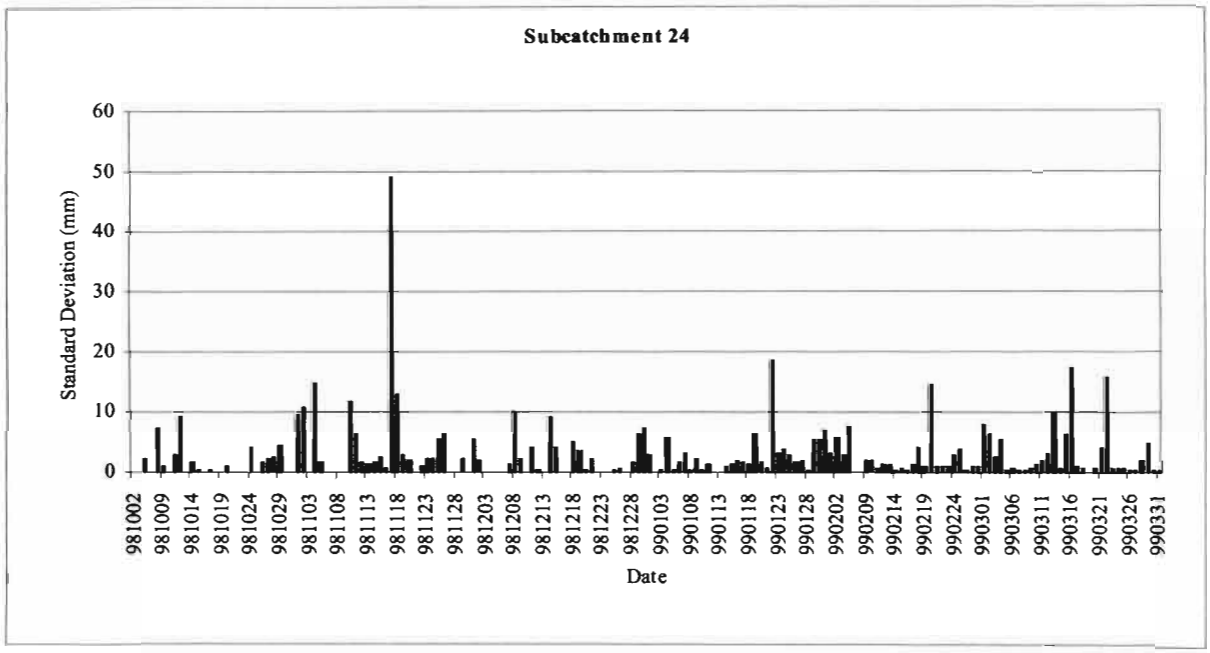

Figure B.24c Standard deviation of the spatial distribution of rainfall in Subcatchment 24

B.25. Subcatchment 25

The standard deviation of altitude in Subcatchment 25 is 39.7 m, as shown in Figure 5.2. Tipping bucket Raingauge L032 and Raingauge 0367768W are located inside the subcatchment as shown in Figure B.25a and both are used for comparison as shown in Figure B.25b and B.25c. Both

point rainfall data represent the areal rainfall of the subcatchment reasonably well, with x-coefficient and R^2 greater than 0.5. The spatial rainfall distribution of the subcatchment is shown in Figure B.25d.

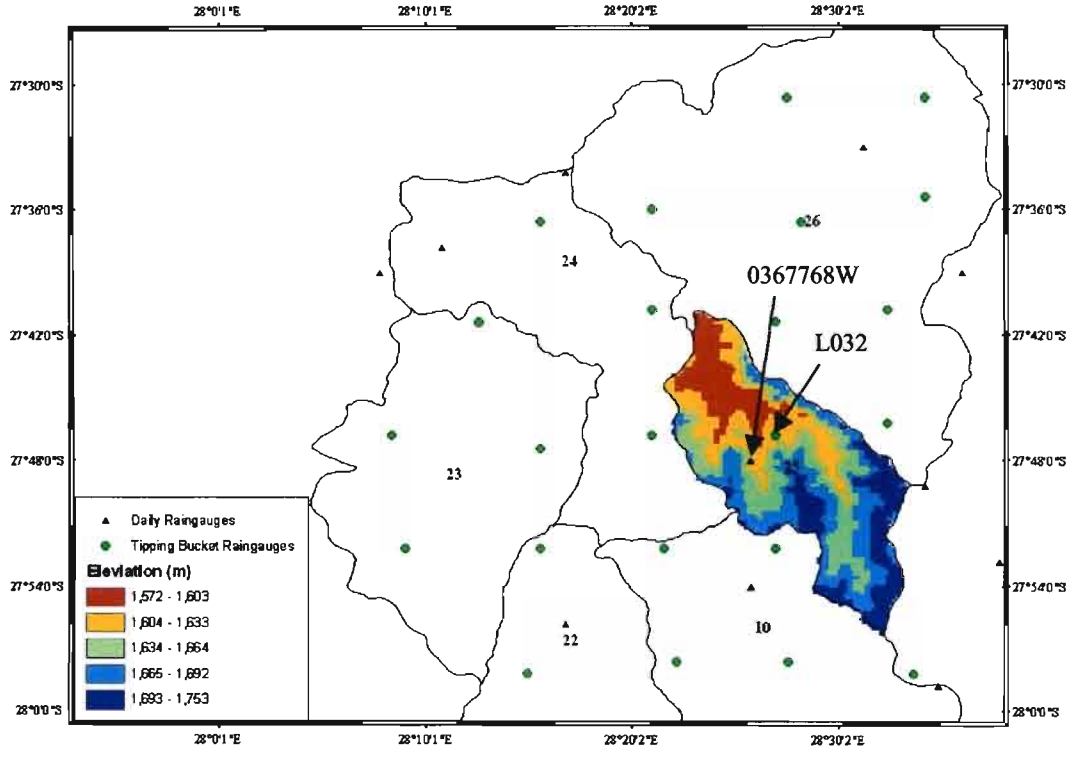

Figure B.25a Altitude map of Subcatchment 25

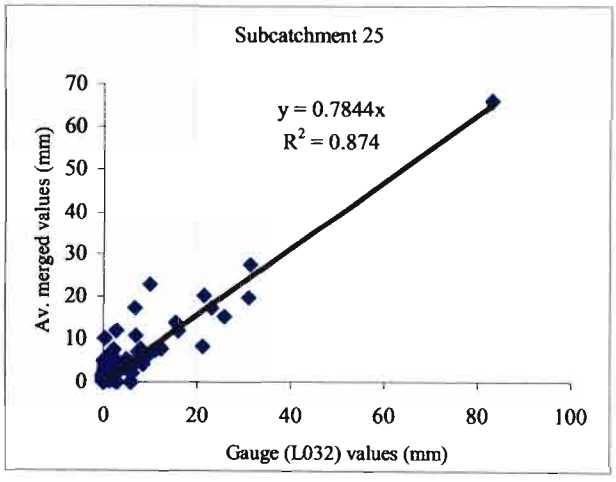

Figure B.25b Mean areal rainfall in Subcatchment 25 vs daily rainfall at tipping bucket Raingauge L032

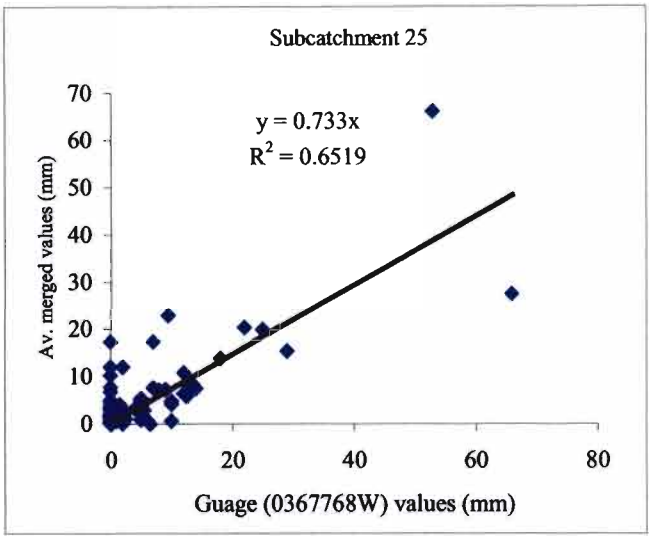

Figure B.25c Mean areal rainfall in Subcatchment 24 vs daily rainfall at Raingauge 0367768W

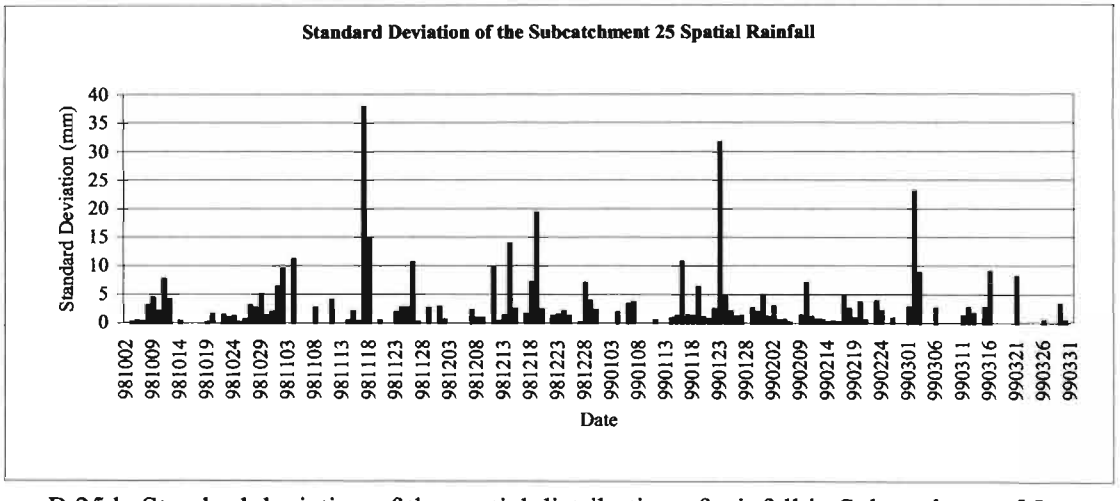

Figure B.25d Standard deviation of the spatial distribution of rainfall in Subcatchment 25